Mathematical Problems in Engineering

Computational Intelligence Techniques for Realization of Power Electronic Converters for Next Generation Grids 2022

Lead Guest Editor: Ravi Samikannu
Guest Editors: Abu Zaharin Ahmad and Albert Alexander Stonier

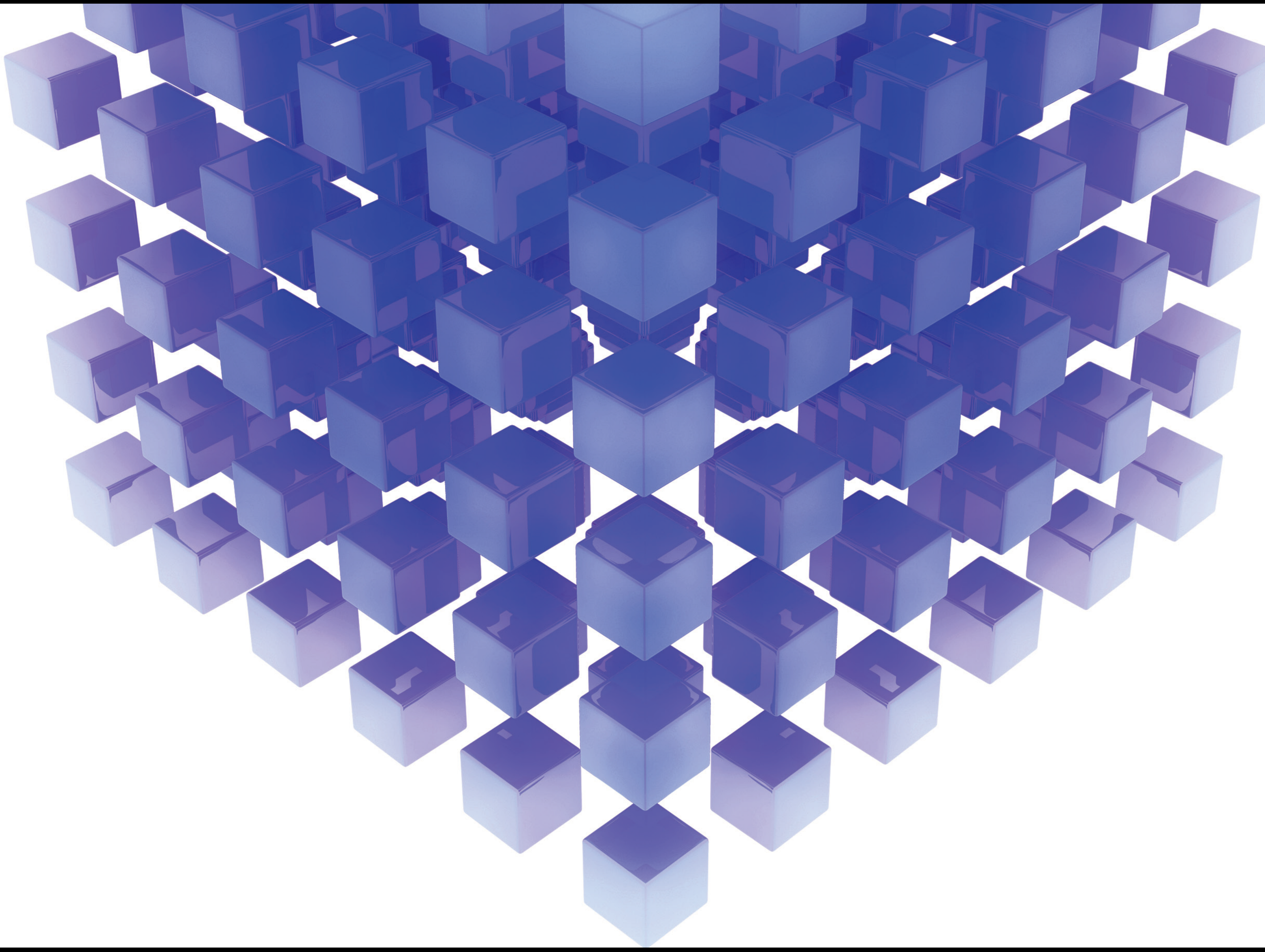

Computational Intelligence Techniques for Realization of Power Electronic Converters for Next Generation Grids 2022

Mathematical Problems in Engineering

Computational Intelligence Techniques for Realization of Power Electronic Converters for Next Generation Grids 2022

Lead Guest Editor: Ravi Samikannu
Guest Editors: Abu Zaharin Ahmad and Albert Alexander Stonier

Paolo Boscariol, Italy
Daniela Boso, Italy
Guillermo Botella-Juan, Spain
Abdesselem Boulkroune, Algeria
Boulaïd Boulkroune, Belgium
Fabio Bovenga, Italy
Francesco Braghin, Italy
Ricardo Branco, Portugal
Julien Bruchon, France
Matteo Bruggi, Italy
Michele Brun, Italy
Maria Elena Bruni, Italy
Maria Angela Butturi, Italy
Bartłomiej Błachowski, Poland
Dhanamjayulu C, India
Raquel Caballero-Águila, Spain
Filippo Cacace, Italy
Salvatore Caddemi, Italy
Zuowei Cai, China
Roberto Caldelli, Italy
Francesco Cannizzaro, Italy
Maosen Cao, China
Ana Carpio, Spain
Rodrigo Carvajal, Chile
Caterina Casavola, Italy
Sara Casciati, Italy
Federica Caselli, Italy
Carmen Castillo, Spain
Inmaculada T. Castro, Spain
Miguel Castro, Portugal
Giuseppe Catalanotti, United Kingdom
Alberto Cavallo, Italy
Gabriele Cazzulani, Italy
Fatih Vehbi Celebi, Turkey
Miguel Cerrolaza, Venezuela
Gregory Chagnon, France
Ching-Ter Chang, Taiwan
Kuei-Lun Chang, Taiwan
Qing Chang, USA
Xiaoheng Chang, China
Prasenjit Chatterjee, Lithuania
Kacem Chehdi, France
Peter N. Cheimets, USA
Chih-Chiang Chen, Taiwan
He Chen, China
Kebing Chen, China
Mengxin Chen, China
Shyi-Ming Chen, Taiwan
Xizhong Chen, Ireland
Xue-Bo Chen, China
Zhiwen Chen, China
Qiang Cheng, USA
Zeyang Cheng, China
Luca Chiapponi, Italy
Francisco Chicano, Spain
Tirivanhu Chinyoka, South Africa
Adrian Chmielewski, Poland
Seongim Choi, USA
Gautam Choubey, India
Hung-Yuan Chung, Taiwan
Yusheng Ci, China
Simone Cinquemani, Italy
Roberto G. Citarella, Italy
Joaquim Ciurana, Spain
John D. Clayton, USA
Piero Colajanni, Italy
Giuseppina Colicchio, Italy
Vassilios Constantoudis, Greece
Enrico Conte, Italy
Alessandro Contento, USA
Mario Cools, Belgium
Gino Cortellessa, Italy
Carlo Cosentino, Italy
Paolo Crippa, Italy
Erik Cuevas, Mexico
Guozeng Cui, China
Mehmet Cunkas, Turkey
Giuseppe D'Aniello, Italy
Peter Dabnichki, Australia
Weizhong Dai, USA
Zhifeng Dai, China
Purushothaman Damodaran, USA
Sergey Dashkovskiy, Germany
Adiel T. De Almeida-Filho, Brazil
Fabio De Angelis, Italy
Samuele De Bartolo, Italy
Stefano De Miranda, Italy
Filippo De Monte, Italy

José António Fonseca De Oliveira Correia, Portugal
Jose Renato De Sousa, Brazil
Michael Defoort, France
Alessandro Della Corte, Italy
Laurent Dewasme, Belgium
Sanku Dey, India
Gianpaolo Di Bona, Italy
Roberta Di Pace, Italy
Francesca Di Puccio, Italy
Ramón I. Diego, Spain
Yannis Dimakopoulos, Greece
Hasan Dinçer, Turkey
José M. Domínguez, Spain
Georgios Dounias, Greece
Bo Du, China
Emil Dumic, Croatia
Madalina Dumitriu, United Kingdom
Premraj Durairaj, India
Saeed Eftekhar Azam, USA
Said El Kafhali, Morocco
Antonio Elipe, Spain
R. Emre Erkmen, Canada
John Escobar, Colombia
Leandro F. F. Miguel, Brazil
FRANCESCO FOTI, Italy
Andrea L. Facci, Italy
Shahla Faisal, Pakistan
Giovanni Falsone, Italy
Hua Fan, China
Jianguang Fang, Australia
Nicholas Fantuzzi, Italy
Muhammad Shahid Farid, Pakistan
Hamed Faroqi, Iran
Yann Favennec, France
Fiorenzo A. Fazzolari, United Kingdom
Giuseppe Fedele, Italy
Roberto Fedele, Italy
Baowei Feng, China
Mohammad Ferdows, Bangladesh
Arturo J. Fernández, Spain
Jesus M. Fernandez Oro, Spain
Francesco Ferrise, Italy
Eric Feulvarch, France
Thierry Floquet, France
Eric Florentin, France
Gerardo Flores, Mexico
Antonio Forcina, Italy
Alessandro Formisano, Italy
Francesco Franco, Italy
Elisa Francomano, Italy
Juan Frausto-Solis, Mexico
Shujun Fu, China
Juan C. G. Prada, Spain
HECTOR GOMEZ, Chile
Matteo Gaeta, Italy
Mauro Gaggero, Italy
Zoran Gajic, USA
Jaime Gallardo-Alvarado, Mexico
Mosè Gallo, Italy
Akemi Gálvez, Spain
Maria L. Gandarias, Spain
Hao Gao, Hong Kong
Xingbao Gao, China
Yan Gao, China
Zhiwei Gao, United Kingdom
Giovanni Garcea, Italy
José García, Chile
Harish Garg, India
Alessandro Gasparetto, Italy
Stylianos Georgantzinos, Greece
Fotios Georgiades, India
Parviz Ghadimi, Iran
Ştefan Cristian Gherghina, Romania
Georgios I. Giannopoulos, Greece
Agathoklis Giaralis, United Kingdom
Anna M. Gil-Lafuente, Spain
Ivan Giorgio, Italy
Gaetano Giunta, Luxembourg
Jefferson L.M.A. Gomes, United Kingdom
Emilio Gómez-Déniz, Spain
Antonio M. Gonçalves de Lima, Brazil
Qunxi Gong, China
Chris Goodrich, USA
Rama S. R. Gorla, USA
Veena Goswami, India
Xunjie Gou, Spain
Jakub Grabski, Poland

Francisco J. Martos, Spain
Elio Masciari, Italy
Paolo Massioni, France
Alessandro Mauro, Italy
Jonathan Mayo-Maldonado, Mexico
Pier Luigi Mazzeo, Italy
Laura Mazzola, Italy
Driss Mehdi, France
Zahid Mehmood, Pakistan
Roderick Melnik, Canada
Xiangyu Meng, USA
Jose Merodio, Spain
Alessio Merola, Italy
Mahmoud Mesbah, Iran
Luciano Mescia, Italy
Laurent Mevel, France
Constantine Michailides, Cyprus
Mariusz Michta, Poland
Prankul Middha, Norway
Aki Mikkola, Finland
Giovanni Minafò, Italy
Edmondo Minisci, United Kingdom
Hiroyuki Mino, Japan
Dimitrios Mitsotakis, New Zealand
Ardashir Mohammadzadeh, Iran
Francisco J. Montáns, Spain
Francesco Montefusco, Italy
Gisele Mophou, France
Rafael Morales, Spain
Marco Morandini, Italy
Javier Moreno-Valenzuela, Mexico
Simone Morganti, Italy
Caroline Mota, Brazil
Aziz Moukrim, France
Shen Mouquan, China
Dimitris Mourtzis, Greece
Emiliano Mucchi, Italy
Taseer Muhammad, Saudi Arabia
Ghulam Muhiuddin, Saudi Arabia
Amitava Mukherjee, India
Josefa Mula, Spain
Jose J. Muñoz, Spain
Giuseppe Muscolino, Italy
Marco Mussetta, Italy
Hariharan Muthusamy, India
Alessandro Naddeo, Italy
Raj Nandkeolyar, India
Keivan Navaie, United Kingdom
Soumya Nayak, India
Adrian Neagu, USA
Erivelton Geraldo Nepomuceno, Brazil
AMA Neves, Portugal
Ha Quang Thinh Ngo, Vietnam
Nhon Nguyen-Thanh, Singapore
Papakostas Nikolaos, Ireland
Jelena Nikolic, Serbia
Tatsushi Nishi, Japan
Shanzhou Niu, China
Ben T. Nohara, Japan
Mohammed Nouari, France
Mustapha Nourelfath, Canada
Kazem Nouri, Iran
Ciro Núñez-Gutiérrez, Mexico
Wlodzimierz Ogryczak, Poland
Roger Ohayon, France
Krzysztof Okarma, Poland
Mitsuhiro Okayasu, Japan
Murat Olgun, Turkey
Diego Oliva, Mexico
Alberto Olivares, Spain
Enrique Onieva, Spain
Calogero Orlando, Italy
Susana Ortega-Cisneros, Mexico
Sergio Ortobelli, Italy
Naohisa Otsuka, Japan
Sid Ahmed Ould Ahmed Mahmoud, Saudi Arabia
Taoreed Owolabi, Nigeria
EUGENIA PETROPOULOU, Greece
Arturo Pagano, Italy
Madhumangal Pal, India
Pasquale Palumbo, Italy
Dragan Pamučar, Serbia
Weifeng Pan, China
Chandan Pandey, India
Rui Pang, United Kingdom
Jürgen Pannek, Germany
Elena Panteley, France
Achille Paolone, Italy

George A. Papakostas, Greece
Xosé M. Pardo, Spain
You-Jin Park, Taiwan
Manuel Pastor, Spain
Pubudu N. Pathirana, Australia
Surajit Kumar Paul, India
Luis Payá, Spain
Igor Pažanin, Croatia
Libor Pekař, Czech Republic
Francesco Pellicano, Italy
Marcello Pellicciari, Italy
Jian Peng, China
Mingshu Peng, China
Xiang Peng, China
Xindong Peng, China
Yuexing Peng, China
Marzio Pennisi, Italy
Maria Patrizia Pera, Italy
Matjaz Perc, Slovenia
A. M. Bastos Pereira, Portugal
Wesley Peres, Brazil
F. Javier Pérez-Pinal, Mexico
Michele Perrella, Italy
Francesco Pesavento, Italy
Francesco Petrini, Italy
Hoang Vu Phan, Republic of Korea
Lukasz Pieczonka, Poland
Dario Piga, Switzerland
Marco Pizzarelli, Italy
Javier Plaza, Spain
Goutam Pohit, India
Dragan Poljak, Croatia
Jorge Pomares, Spain
Hiram Ponce, Mexico
Sébastien Poncet, Canada
Volodymyr Ponomaryov, Mexico
Jean-Christophe Ponsart, France
Mauro Pontani, Italy
Sivakumar Poruran, India
Francesc Pozo, Spain
Aditya Rio Prabowo, Indonesia
Anchasa Pramuanjaroenkij, Thailand
Leonardo Primavera, Italy
B Rajanarayan Prusty, India
Krzysztof Puszynski, Poland
Chuan Qin, China
Dongdong Qin, China
Jianlong Qiu, China
Giuseppe Quaranta, Italy
DR. RITU RAJ, India
Vitomir Racic, Italy
Carlo Rainieri, Italy
Kumbakonam Ramamani Rajagopal, USA
Ali Ramazani, USA
Angel Manuel Ramos, Spain
Higinio Ramos, Spain
Muhammad Afzal Rana, Pakistan
Muhammad Rashid, Saudi Arabia
Manoj Rastogi, India
Alessandro Rasulo, Italy
S.S. Ravindran, USA
Abdolrahman Razani, Iran
Alessandro Reali, Italy
Jose A. Reinoso, Spain
Oscar Reinoso, Spain
Haijun Ren, China
Carlo Renno, Italy
Fabrizio Renno, Italy
Shahram Rezapour, Iran
Ricardo Riaza, Spain
Francesco Riganti-Fulginei, Italy
Gerasimos Rigatos, Greece
Francesco Ripamonti, Italy
Jorge Rivera, Mexico
Eugenio Roanes-Lozano, Spain
Ana Maria A. C. Rocha, Portugal
Luigi Rodino, Italy
Francisco Rodríguez, Spain
Rosana Rodríguez López, Spain
Francisco Rossomando, Argentina
Jose de Jesus Rubio, Mexico
Weiguo Rui, China
Rubén Ruiz, Spain
Ivan D. Rukhlenko, Australia
Dr. Eswaramoorthi S., India
Weichao SHI, United Kingdom
Chaman Lal Sabharwal, USA
Andrés Sáez, Spain

Yong (Aaron) Tan, United Kingdom
Marco Antonio Taneco-Hernández, Mexico
Lu Tang, China
Tianyou Tao, China
Hafez Tari, USA
Alessandro Tasora, Italy
Sergio Teggi, Italy
Adriana del Carmen Téllez-Anguiano, Mexico
Ana C. Teodoro, Portugal
Efstathios E. Theotokoglou, Greece
Jing-Feng Tian, China
Alexander Timokha, Norway
Stefania Tomasiello, Italy
Gisella Tomasini, Italy
Isabella Torcicollo, Italy
Francesco Tornabene, Italy
Mariano Torrisi, Italy
Thang nguyen Trung, Vietnam
George Tsiatas, Greece
Le Anh Tuan, Vietnam
Nerio Tullini, Italy
Emilio Turco, Italy
Ilhan Tuzcu, USA
Efstratios Tzirtzilakis, Greece
FRANCISCO UREÑA, Spain
Filippo Ubertini, Italy
Mohammad Uddin, Australia
Mohammad Safi Ullah, Bangladesh
Serdar Ulubeyli, Turkey
Mati Ur Rahman, Pakistan
Panayiotis Vafeas, Greece
Giuseppe Vairo, Italy
Jesus Valdez-Resendiz, Mexico
Eusebio Valero, Spain
Stefano Valvano, Italy
Carlos-Renato Vázquez, Mexico
Martin Velasco Villa, Mexico
Franck J. Vernerey, USA
Georgios Veronis, USA
Vincenzo Vespri, Italy
Renato Vidoni, Italy
Venkatesh Vijayaraghavan, Australia
Anna Vila, Spain
Francisco R. Villatoro, Spain
Francesca Vipiana, Italy
Stanislav Vítek, Czech Republic
Jan Vorel, Czech Republic
Michael Vynnycky, Sweden
Mohammad W. Alomari, Jordan
Roman Wan-Wendner, Austria
Bingchang Wang, China
C. H. Wang, Taiwan
Dagang Wang, China
Guoqiang Wang, China
Huaiyu Wang, China
Hui Wang, China
J.G. Wang, China
Ji Wang, China
Kang-Jia Wang, China
Lei Wang, China
Qiang Wang, China
Qingling Wang, China
Weiwei Wang, China
Xinyu Wang, China
Yong Wang, China
Yung-Chung Wang, Taiwan
Zhenbo Wang, USA
Zhibo Wang, China
Waldemar T. Wójcik, Poland
Chi Wu, Australia
Qiuhong Wu, China
Yuqiang Wu, China
Zhibin Wu, China
Zhizheng Wu, China
Michalis Xenos, Greece
Hao Xiao, China
Xiao Ping Xie, China
Qingzheng Xu, China
Binghan Xue, China
Yi Xue, China
Joseph J. Yame, France
Chuanliang Yan, China
Xinggang Yan, United Kingdom
Hongtai Yang, China
Jixiang Yang, China
Mijia Yang, USA
Ray-Yeng Yang, Taiwan

Contents

Hindawi
Mathematical Problems in Engineering
Volume 2023, Article ID 1264345, 8 pages
https://doi.org/10.1155/2023/1264345

Research Article

Abnormal Health Monitoring and Assessment of a Three-Phase Induction Motor Using a Supervised CNN-RNN-Based Machine Learning Algorithm

Abhinav Saxena ,[1] Rajat Kumar ,[2] Arun Kumar Rawat ,[1] Mohd Majid ,[3] Jay Singh ,[4] S. Devakirubakaran ,[5] and Gyanendra Kumar Singh [6]

[1]*Department of Electrical Engineering, JSS Academy of Technical Education, Noida, Uttar Pradesh, India*
[2]*Department of Electrical Engineering, Dayalbagh Educational Institute, Dayalbagh, Uttar Pradesh, Agra, India*
[3]*Department of Mechanical Engineering, Sant Longowal Institute of Engineering and Technology, Longowal, Sangrur, Punjab, India*
[4]*Department of Electrical and Electronics Engineering, GL Bajaj Institute of Technology and Management, Noida, Uttar Pradesh, India*
[5]*Dapartment of Electrical and Electronics Engineering, QIS College of Engineering and Technology, Ongole, Andhra Pradesh, India*
[6]*School of Mechanical, Chemical and Materials Engineering, Adama Science and Technology University, Adama, Ethiopia*

Correspondence should be addressed to Gyanendra Kumar Singh; gksinghgu@yahoo.com

Received 30 September 2022; Revised 18 October 2022; Accepted 24 November 2022; Published 30 January 2023

Academic Editor: Ravi Samikannu

This paper shows the health monitoring and assessment of a three-phase induction motor in abnormal conditions using a machine learning algorithm. The convolutional neural network (CNN) and recurrent neural network (RNN) algorithms are the prominent methods used in machine learning algorithms, and the combined method is known as the CRNN method. The abnormal conditions of a three phase-induction motor are represented by three-phase faults, line-to-ground faults, etc. The pattern of fault current is traced, and key features are extracted by the CRNN algorithm. The performance parameters like THD (%), accuracy, and reliability of abnormal conditions are measured with the CRNN algorithm. The assessment of abnormal conditions is being realized at the terminals of a three-phase induction motor. A fuzzy logic controller (FLC) is also used to assess such abnormalities. It is observed that performance parameters are found to be better with the CRNN method in comparison to CNN, RNN, ANN, and other methods. Such a realization makes the system more compatible with abnormality recognition.

1. Introduction

Induction motors are one of the most versatile and frequently used variable-speed drives for industrial and domestic applications. Normally, the three-phase supply-based induction motor is used to drive heavy loads. The major challenge with the induction motor is maintaining the normal supply. The changing loads, fault conditions, and overspeeding affect the supply and create abnormalities that can be assessed using the machine learning algorithm. The monitoring aspect of machine failure diagnostics is important, and for recognizing a failure in mechanical systems, classifying the error, and recognizing group faults, numerous sensors are installed to gather information from thermal imaging or vibration. Afterward, these data are analyzed to see whether a defect has occurred or not, and if so, what kind of fault it is.

Traditionally, to identify a machine's malfunction, a sensor is required for signal acquisition, feature selection, and fault categorization, as well as extraction. Sensing data acquisition entails gathering sensor data while the device in use is active. Conventional extracted features include original sensor data from time data in both the temporal and frequency domains. A new framework for deep learning is proposed to achieve very accurate machine fault detection and to understand how to facilitate and expedite deep neural network training networks. In comparison to current techniques, the suggested technique is more accurate and quicker to train. The initial sensor data are utilized using wavelet transformation to turn the data into pictures, followed by assembling the time-frequency distributions. Then, a trained network is applied to extract more fundamental features, including the time-frequency label [1–5]. The higher tiers of the algorithm are then fine-tuned using photographs and neural network design. The document causes a bug in the system, in which experiments and a diagnosis pathway are used to confirm the pipeline's efficiency and applicability in general on three fundamental mechanical data sets containing gearboxes, induction motors, and bearings with three-time series samples of different sizes [6–11].

The proposed method can be used to diagnose faults in rotary machine systems' exterior bearings and uses deep learning and information fusion. The suggested method takes as its direct input raw signals from various phases of the motor current, from which features are then retrieved. Afterward, CNN classifies each feature set separately for the network of neurons. An innovative decision-level information fusion strategy is presented to combine data from all of the used convolutional neural networks in order to improve classification accuracy. CNN provides higher accuracy in its image recognition pattern and a better approach to automatically detecting important features without any human supervision. On the contrary, RNN produces the sequential output, which depends on time-sequence events. Decision-level data processing has difficulty because of straightforward pattern categorization problems that can be efficiently solved by well-known supervised learning algorithms. The suggested fault diagnosis product's efficacy is validated by tests that used genuine bearing fault signals [12–14]. This work describes a technique for identifying bearing defects and tracking bearing deterioration in electric motors. The method collects fault features that reflect various faults based on signal kurtosis and cross-correlation, and the characteristics are then integrated to create a health index using hierarchical clustering and a semisupervised k-nearest neighbour distance measure. Experiments with a computer cooling fan motor bearing and a simulator for machinery faults were used to validate the method. The technique can locate defects under masking noise and diagnose faults in their early stages. Additionally, it offers a health index that monitors fault degeneration while excluding intermittent defects. Furthermore, inaccurate reference data are not necessary [15–18]. In theory, sophisticated artificial intelligence-based systems provide early fault identification, but their complexity conflicts with instant messaging are fundamental characteristics.

This manuscript utilizes the motor current signature, which is already present in standard drives, and proposes a combination of simulations and upsampling to practice the neural network effectively without any need for numerous broken prototypes, which is the main obstacle to industrial viability [19–22]. Deep conviction systems for biomedical applications using intuitive procedures with a cross-point approach are analyzed. The mechanism of the Internet of things (IoT) integrated with radio frequency identification (RFID) technology for healthcare systems gives fruitful information. Biomedical signals for healthcare using Hadoop infrastructure with artificial intelligence and fuzzy logic interpretation show the health analysis [23–25]. An induction motor driven by an inverter and its diagnosis using a machine learning algorithm are well analyzed. With the help of growing curvilinear component analysis, the stator of an induction motor helps to track the fault at the grid terminal. A diagnosis of the IGBT converter and current sensor fault for the inverter-driven induction motor using the online Simulink method is well explained in [26–28].

2. Mathematical Modeling of Three-phase Induction Motor

The mathematical modeling of a three-phase induction motor is designed in the d-q reference frame coordinates. The conversion of three-phase coordinates to (d–q) coordinates is assessed using the Clarke and Park transformation. In the Clarke transformation, three-phase (a, b, and c) coordinates are converted into stationary reference coordinates (α–β). A further Park transformation is used to convert the stationary reference coordinates (α–β) into synchronous reference frame coordinates (d–q). The mathematical modeling of a three-phase induction motor is represented as

$$
\begin{aligned}
V_{sd} &= R_s i_{sd} + \frac{d}{dt}\phi_{sd} - \omega_s \phi_{sq} \\
V_{sq} &= R_s i_{sq} + \frac{d}{dt}\phi_{sq} + \omega_s \phi_{sq} \\
V_{rd} &= R_r i_{rd} + \frac{d}{dt}\phi_{rd} - \omega_r \phi_{rq} \\
V_{rq} &= R_r i_{rq} + \frac{d}{dt}\phi_{rq} + \omega_r \phi_{rd}, \\
\phi_{sd} &= L_s i_{sd} + L_m i_{rd} \\
\phi_{sq} &= L_s i_{sq} + L_m i_{rq} \\
\phi_{rd} &= L_s i_{rd} + L_m i_{sd} \\
\phi_{rq} &= L_s i_{rq} + L_m i_{sq}
\end{aligned}
\tag{1}
$$

where V_{sd} and i_{sd} are d-axis stator voltage and stator current, respectively. V_{rd} and i_{rd} are d-axis rotor voltage and rotor current, respectively. V_{sq} and i_{sq} are q-axis stator voltage and stator current, respectively. V_{rq} and i_{rq} are q-axis rotor voltage and rotor current, respectively.

The torque equation is given by

$$T_e - T_L = J\frac{d(\omega_r)}{dt}. \tag{2}$$

Electromagnetic torque is given by

$$T_e = p\left(\phi_{sd} i_{sq} - \phi_{sq} i_{sd}\right), \tag{3}$$

where p is the pole pair.

The general structure of a grid-connected three-phase induction motor is shown in Figure 1.

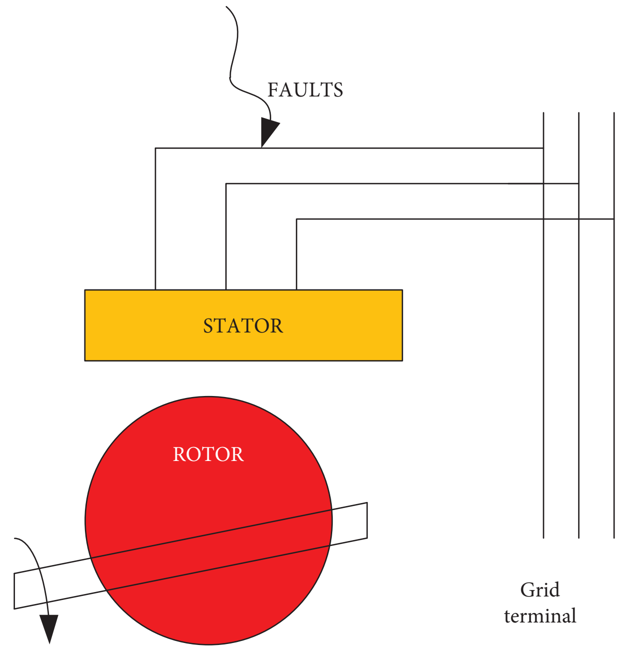

Figure 1: Structure of a grid-connected three-phase induction motor [6].

3. Design of the Convolution Neural Network (CNN)

CNN is defined as a product of the two inputs in the real-time domain. A particular kind of feedforward neural network is the convolutional neural network (CNN). It can be used for target recognition, segmentation, and image classification, among other things. The CNN model is different from other neural networks in that it has convolutional and pooling layers. The feedforward network can be illustrated as a function, as given in the following equation:

$$Y = f(X, f). \tag{4}$$

where $X = [x)_1, x_2, x_3, ...x_n]$ are inputs vectors. $Y = [y)_1, y_2, y_3, ... y_n]$ are output vectors. f is the faulty current at the different level.

The convolution layer's goal is to derive local characteristics from input data, as shown in the following equation:

$$Y_F = \text{conv}(Y, f). \tag{5}$$

$$Y_F = \text{conv}(Y, \text{convf}). \tag{6}$$

Conv is a convolution layer, Y_F is a set of extracted features, and extraction of the convolution layer from X. Y_f is the set of extracted features after the pooling layer. CNN has Softmax layers to integrate and categorize features as part of a classification model. The compressed features of the output are given as Y_{ff} , as shown in the following equation:

$$\begin{aligned} Y_F &= \text{pool}(Y_F, \text{poolf}), \\ Y_{\text{FF}} &= \text{Soft max}\,(FC, (Y_F, \text{poolf})). \end{aligned} \tag{7}$$

The architecture of CNN with a pooling layer is shown in Figure 2, and data extraction from Table 1 process is shown in Figure 3.

4. Design of the Recurrent Neural Network (RNN)

RNNs are a variety of feedforward neural networks . RNN is most often used for data that has a sequence, for example in speech recognition and translation software. A popular RNN model was the LSTM LSTM-RNN, which uses memory cells to retain long-term data to address the issue of vanishing gradients. As a classification algorithm, LSTM-RNN additionally includes Softmax layers as well as full levels [22]. The architecture of the RNN is shown in Figure 4. The normalized output of the RNN is represented mathematically, as shown in the following equation:

$$Y_{\text{FF}} = \text{Soft max}\,(F)C\,(LSTM\,(Y_F, \text{poolf})). \tag{8}$$

5. Design of the Convolution Recurrent Neural Network (CRNN)

CRNN is a combination of CNN and RNN. The effectiveness of CNN-based models in utilizing geographic information characteristics, such as those seen in photographs, is good. CNN, unfortunately, is unable to handle sequential data. RNN-based models, on the other hand, excel at modeling sequential data, such as texts. A novel model called CRNN is suggested, which combines CNN and RNN and is influenced by their traits. The characteristics of the inputs are extracted by the CNN, and the retrieved features are further processed by the RNN to lessen the dependence on variables under various variable situations. By eliminating the ambiguity and boundary conditions of the images, it investigates the options one at a time [22]. The general equations of CRNN are listed in the following equations:

$$\mathrm{i_t} = \sigma\,(\mathrm{W})_{\mathrm{iw}}\mathrm{x_t} + \mathrm{U_{ih}}\mathrm{h_{t-1}} + \mathrm{b_i}), \tag{9}$$

$$\mathrm{f_t} = \sigma\,(\mathrm{W})_{\mathrm{fw}}\mathrm{x_t} + \mathrm{U_{fh}}\mathrm{h_{t-1}} + \mathrm{b_f}), \tag{10}$$

$$o_{\mathrm{t}} = \sigma\,(\mathrm{W})_{\mathrm{ow}}\mathrm{x_t} + \mathrm{U_{oh}}\mathrm{h_{t-1}} + \mathrm{b_o}), \tag{11}$$

$$g_{\mathrm{t}} = \tanh\,(\mathrm{W})_{\mathrm{gw}}\mathrm{x_t} + \mathrm{U_{gh}}\mathrm{h_{t-1}} + \mathrm{b}_g), \tag{12}$$

$$c_{\mathrm{t}} = \mathrm{f_t} \circ c_{\mathrm{t-1}} + \mathrm{i_t} \circ g_{\mathrm{t}}, \tag{13}$$

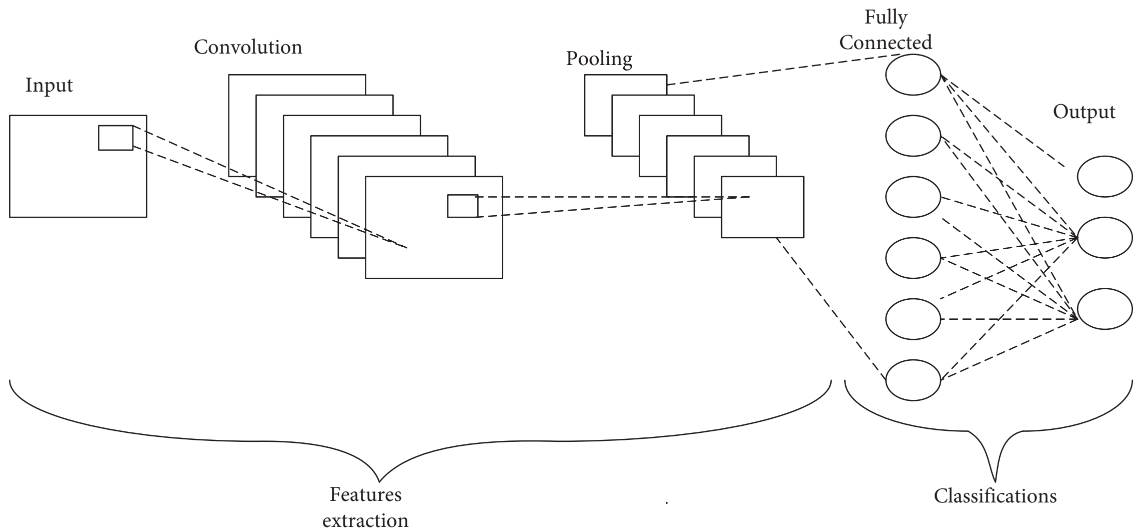

Figure 2: Architecture of the CNN [1].

Table 1: Fault level at various conditions.

Level (f)	L1	L2	L3	L4	L5	L6	L7	L8	L9
Three-phase fault	1	0	1	0	1	1	1	0	0
Line to ground fault	0	1	1	1	0	0	1	1	0
Line to line fault	1	1	0	0	0	1	1	1	0

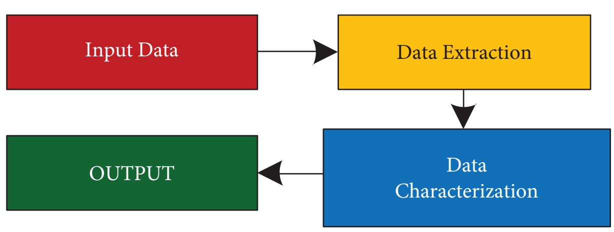

Figure 3: Data extraction of the CNN [2].

$$h_t = o_t \circ \tanh c_t, \quad (14)$$

where t is the LSTM step. xt is the input data. ht is the hidden data. ct is the cell state. it, ft, and ot are the input gate, forget gate, and output gate, respectively. Ws, Us, and bs are the weights and bias. σ, tanh, $\circ$ are sigmoid functions, hyperbolic tangents, and multiplicators, respectively. The mixed solution of CNN and RNN in mathematical form for evaluating the various fault conditions of a three-phase induction motor is shown as

$$\begin{aligned} Y_{\text{FF}} = \text{Soft max}\big(FC\big(\text{LSTM}\big(Y_F, \text{poolf}\big), \\ \text{conv}\big(Y, \text{convf}\big), \text{pool}\big(Y_F, \text{poolf}\big). \end{aligned} \quad (15)$$

The architecture of the problem solution of CRNN is shown in Figure 5. The forget gate is mathematically represented by $c_t{}^f = f_t o c_{t-1}$, which means that it is the dot product of the convolution of two inputs. While taking the dot product of two inputs, a few elements are removed from the output, which can be forgotten. LSTM is a long short-term memory that is an extended part of an RNN, and it occurs when gradient failure.

6. Result and Performance Analysis of the Abnormal Condition

In previous sections, the designs of CNN, RNN, and CRNN have been discussed in detail. Now, the performance parameters like THD (%), accuracy, and reliability will be estimated for the performance analysis of the single and multilabeling data. The comparison of THD (%) of fault current for single and multilabeling data is shown in Table 2. Such a graphic comparison is also depicted in Figure 6. In the same way, a comparison of the accuracy of fault current for single and multilabeling data is shown in Table 3 for the precision of 1.2% and 1.9%. Such a graphic comparison is also depicted in Figure 7.

In the same way, a comparison of the reliability of fault current for single and multilabeling data is shown in Table 4 for the precisions of 1.2% and 1.9%. Such a graphic comparison is also depicted in Figure 8.

It is observed that in Figures 6–8, the least and improved values of THD (%), accuracy, and reliability are attained with CRNN in comparison to CNN, RNN, and ANN [19]. THD is defined as total harmonic distortion, which is represented as

$$\text{THD} = \sqrt{\frac{1}{g^2} - 1}, \quad (16)$$

where g is the distortion factor, which is given in the following equation:

$$g = \frac{(X_{01})_{\text{rms}}}{(X)_{\text{rms}}}, \quad (17)$$

where X_{01} is the fundamental harmonic component, and $X1$ is the rms input value.

7. Conclusion

This study uses a machine learning method to monitor and evaluate a three-phase induction motor's health when it is in an aberrant state. The CRNN approach, which combines the well-

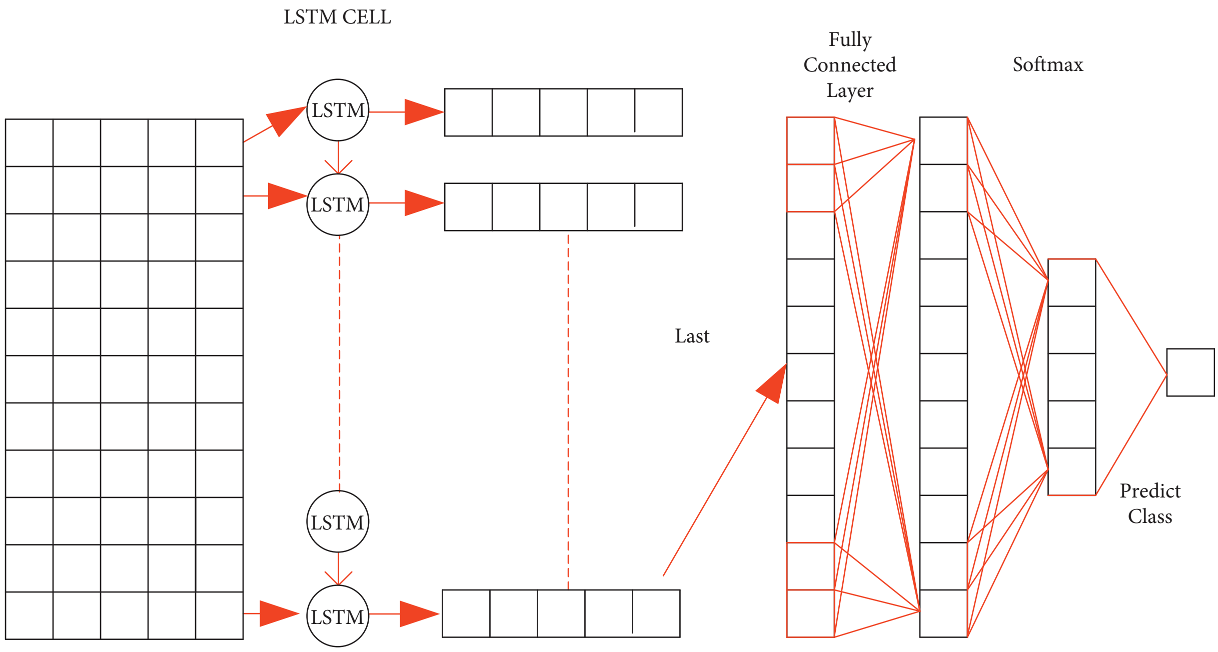

Figure 4: Architecture of the RNN [22].

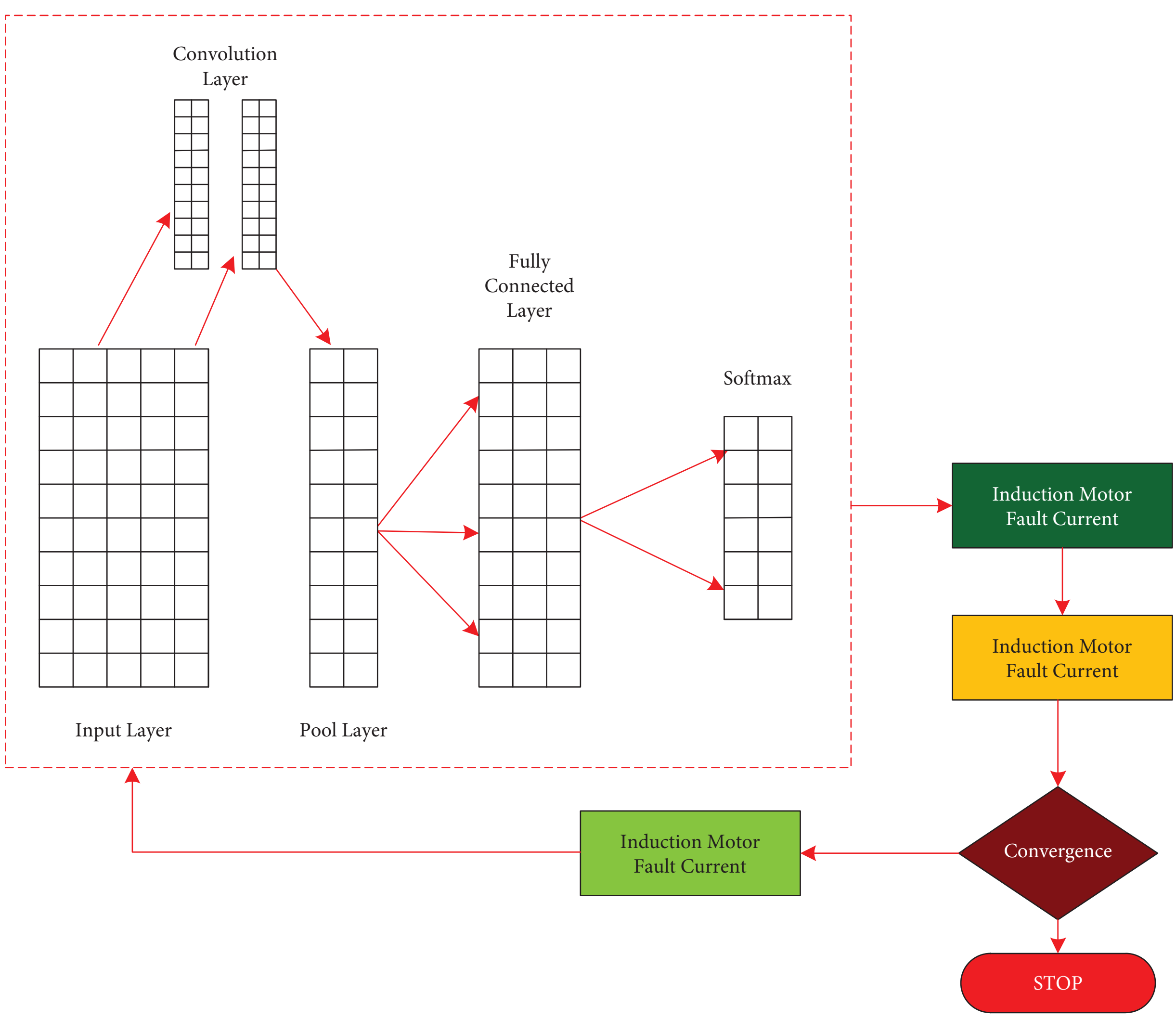

Figure 5: Architecture of the CRNN.

Table 2: Comparison of THD (%) of fault current with various methods.

Data	CRNN	CNN	RNN	ANN [19]
Single label	5.66	7.98	8.98	10.33
Multilabel	6.12	8.97	9.98	11.22

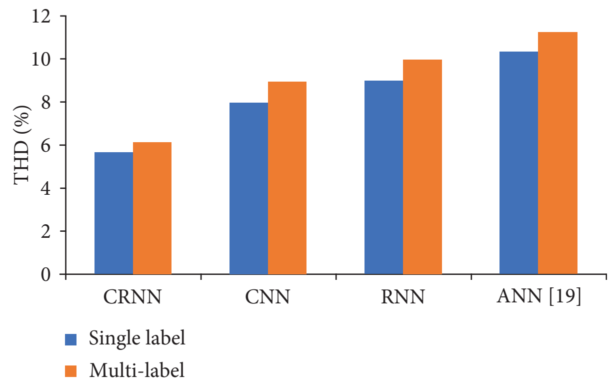

Figure 6: Graphical comparison of THD (%) with various methods.

Table 3: Comparison of the accuracy of fault current with various methods.

Data	1.2% precision				1.9% precision			
	CRNN	CNN	RNN	ANN [19]	CRNN	CNN	RNN	ANN [19]
Single label	1.36	2.36	2.66	3.69	1.56	2.98	3.78	4.65
Multilabel	1.45	2.89	3.21	4.23	1.61	2.91	3.06	4.02

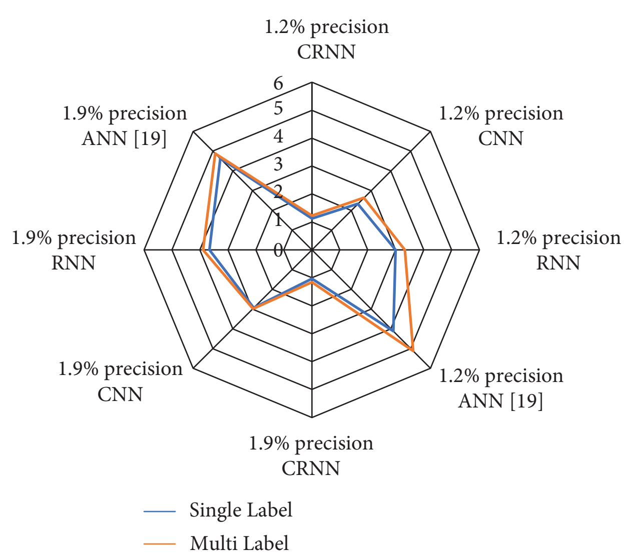

Figure 7: Graphical comparison of reliability with various methods for different precision values.

Table 4: Comparison of reliability of fault current with various methods.

Data	1.2% precision				1.9% precision			
	CRNN	CNN	RNN	ANN [19]	CRNN	CNN	RNN	ANN [19]
Single label	1.12	2.33	2.99	4.12	1.03	2.94	3.66	4.63
Multilabel	1.23	2.64	3.33	5.12	1.16	2.98	3.89	4.88

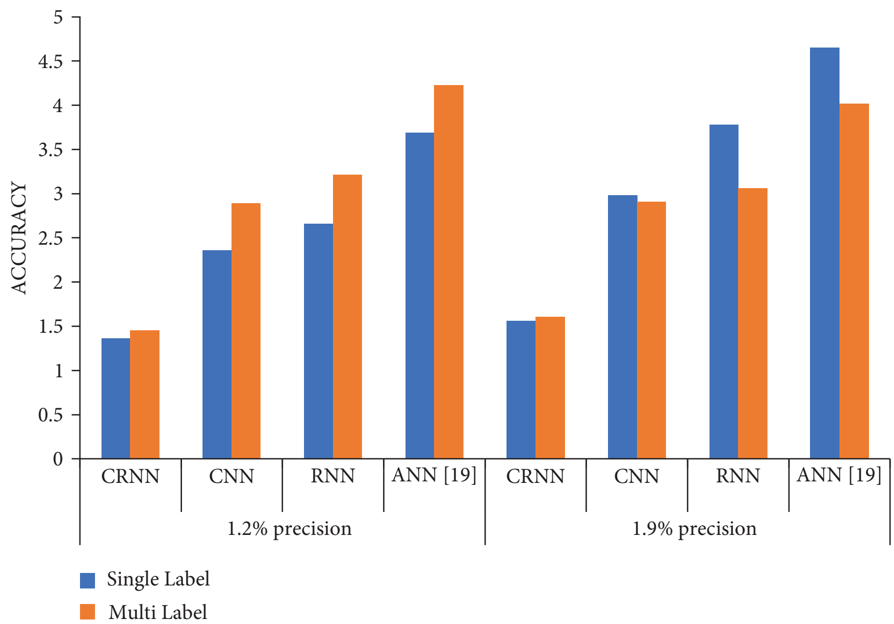

Figure 8: Graphical comparison of accuracy with various methods for different precision values.

known CNN and RNN algorithms, is one of the main machine learning algorithms. Three-phase faults and line-to-ground faults, are some of the abnormal conditions of a three-phase induction motor. By using the CRNN technique, the fault current's pattern is tracked and its main features are retrieved. With the CRNN algorithm, performance metrics including THD (%), accuracy, and reliability of abnormal conditions are measured. Also, the performance metrics including THD (%), accuracy, and reliability of abnormal conditions are measured. This abnormal condition assessment is realized at the terminals of a three-phase induction motor. An artificial neural network (ANN) is also used to evaluate this irregularity. When compared to ANN, RNN, CNN, and other approaches, the CRNN method is proven to have better performance metrics. This realization improves the system's ability to detect abnormalities.

8. Future Scope

It is also a possibility that performance parameters like THD (%), accuracy, and reliability of abnormal conditions can be improved by using other advanced methods for the perfect recognition of abnormal conditions in induction motors.

Data Availability

No data were used to support the study.

Conflicts of Interest

The authors declare that they have no conflicts of interest.

References

[1] S. Shao, S. McAleer, R. Yan, and P. Baldi, "Highly-accurate machine fault diagnosis using deep transfer learning," *IEEE Transactions on Industrial Informatics*, vol. 15, no. 4, pp. 2446–2455, 2019.

[2] C. Shimmin, P. Sadowski, P. Baldi et al., "Decorrelated jet substructure tagging using adversarial neural networks," *Physical Review D*, vol. 96, no. 7, Article ID 074034, 2017.

[3] D. Fooshee, A. Mood, E. Gutman et al., "Deep learning for chemical reaction prediction," *Molecular Systems Design & Engineering*, vol. 3, no. 3, pp. 442–452, 2018.

[4] C. N. Magnan and P. Baldi, "SSpro/ACCpro 5: almost perfect prediction of protein secondary structure and relative solvent accessibility using profiles, machine learning, and structural similarity," *Bioinformatics*, vol. 30, no. 18, pp. 2592–2597, 2014.

[5] P. Baldi, "Deep learning in biomedical data science," *Annual Review of Biomedical Data Science*, vol. 1, pp. 181–205, 2018.

[6] W. Sun, S. Shao, R. Zhao, R. Yan, X. Zhang, and X. Chen, "A sparse auto-encoder based deep neural network approach for induction motor faults classification," *Measurement*, vol. 89, pp. 171–178, 2016.

[7] X. Ding and Q. He, "Energy-fluctuated multiscale feature learning with deep convnet for intelligent spindle bearing fault diagnosis," *IEEE Transactions on Instrumentation and Measurement*, vol. 66, no. 8, pp. 1926–1935, 2017.

[8] R. Zhao, D. Wang, R. Yan, K. Mao, F. Shen, and J. Wang, "Machine health monitoring using local feature-based gated recurrent unit networks," *IEEE Transactions on Industrial Electronics*, vol. 65, no. 2, pp. 1539–1548, 2018.

[9] S. J. Pan and Q. Yang, "A survey on transfer learning," *IEEE Transactions on Knowledge and Data Engineering*, vol. 22, no. 10, pp. 1345–1359, 2010.

[10] L. Wen, L. Gao, and X. Li, "A new deep transfer learning based on sparse autoencoder for fault diagnosis," *IEEE Transactions on Systems, Man, and Cybernetics: Systems*, vol. 49, no. 1, pp. 136–144, 2019.

[11] F. Shen, C. Chen, R. Yan, and R. X. Gao, "Bearing fault diagnosis based on SVD feature extraction and transfer learning classification," in *Proceedings of the 2015 Prognostics and System Health Management Conference (PHM)*, pp. 1–6, IEEE, Beijing, October 2015.

[12] D. T. Hoang and H. J. Kang, "A Motor current signal based bearing fault diagnosis using deep learning and information

fusion," *IEEE Transactions on Instrumentation and Measurement*, vol. 69, no. 6, pp. 3325–3333, 2020.
[13] V. C. M. N. Leite, J. G. B. da Silva, G. L. Torres et al., *Bearing Fault Detection in Induction Machine Using Squared Envelope Analysis of Stator Current," Bearing Technology*, Springer, Berlin, Germany, 2017.
[14] E. Elbouchikhi, V. Choqueuse, F. Auger, and M. E. H. Benbouzid, "Motor current signal analysis based on a matched subspace detector," *IEEE Transactions on Instrumentation and Measurement*, vol. 66, no. 12, pp. 3260–3270, 2017.
[15] B. R. Nayana and P. Geethanjali, "Analysis of statistical time-domain features effectiveness in identification of bearing faults from vibration signal," *IEEE Sensors Journal*, vol. 17, no. 17, pp. 5618–5625, 2017.
[16] G. Maruthi and V. Hegde, "Application of mems accelerometer for detection and diagnosis of multiple faults in the roller element bearings of three phase induction motor," *IEEE Sensors Journal*, vol. 16, no. 1, pp. 145–152, 2016.
[17] J. Tian, C. Morillo, M. H. Azarian, and M. Pecht, "Motor bearing fault detection using spectral kurtosis-based feature extraction coupled with k-nearest neighbor distance analysis," *IEEE Transactions on Industrial Electronics*, vol. 63, no. 3, pp. 1793–1803, 2016.
[18] C. P. Mbo'o and K. Hameyer, "Fault diagnosis of bearing damage by means of the linear discriminant analysis of stator current features from the frequency selection," *IEEE Transactions on Industry Applications*, vol. 52, no. 5, pp. 3861–3868, 2016.
[19] D. Pasqualotto and M. Zigliotto, "Increasing feasibility of neural network-based early fault detection in induction motor drives," *IEEE Journal of Emerging and Selected Topics in Power Electronics*, vol. 10, no. 2, pp. 2042–2051, 2022.
[20] J. Pons-Llinares, J. A. Antonino-Daviu, M. Riera-Guasp, S. Bin Lee, T.-J. Kang, and C. Yang, "Advanced induction motor rotor fault diagnosis via continuous and discrete time–frequency tools," *IEEE Transactions on Industrial Electronics*, vol. 62, no. 3, pp. 1791–1802, 2015.
[21] K. N. Gyftakis, J. A. Antonino-Daviu, R. Garcia-Hernandez, M. D. McCulloch, D. A. Howey, and A. J. M. Cardoso, "Comparative experimental investigation of broken bar fault detectability in induction motors," *IEEE Transactions on Industry Applications*, vol. 52, no. 2, pp. 1452–1459, 2016.
[22] D. Pasqualotto and M. Zigliotto, "A comprehensive approach to convolutional neural networks-based condition monitoring of permanent magnet synchronous motor drives," *IET Electric Power Applications*, vol. 15, no. 7, pp. 1–16, 2021.
[23] S. Selvarajan, H. Manoharan, T. Hasanin et al., "Biomedical signals for healthcare using hadoop infrastructure with artificial intelligence and fuzzy logic interpretation," *Applied Sciences*, vol. 12, no. 10, p. 5097, 2022.
[24] H. Manoharan, S. Selvarajan, A. Yafoz et al., "Deep conviction systems for biomedical applications using intuiting procedures with cross point approach," *Frontiers in Public Health*, vol. 10, p. 909628, 2022.
[25] G. B. Mohammad, S. Shitharth, S. A. Syed et al., "Mechanism of internet of things (IoT) integrated with radio frequency identification (RFID) technology for healthcare system," *Mathematical Problems in Engineering*, vol. 2022, pp. 1–8, Article ID 4167700, 2022.
[26] B. D. E. Cherif, M. Chouai, S. Seninete, and A. Bendiabdellah, "Machine-learning-based diagnosis of an inverter-fed induction motor," *IEEE Latin America Transactions*, vol. 20, no. 6, pp. 901–911, 2022.
[27] R. R. Kumar, V. Randazzo, G. Cirrincione et al., "Induction machine stator fault tracking using the growing curvilinear component analysis," *IEEE Access*, vol. 9, pp. 2201–2212, 2021.
[28] B. Gou, Y. Xu, Y. Xia, Q. Deng, and X. Ge, "An online data-driven method for simultaneous diagnosis of igbt and current sensor fault of three-phase pwm inverter in induction motor drives," *IEEE Transactions on Power Electronics*, vol. 35, no. 12, pp. 13281–13294, 2020.

Hindawi
Mathematical Problems in Engineering
Volume 2022, Article ID 6389132, 43 pages
https://doi.org/10.1155/2022/6389132

Review Article

A Review of Control Techniques and Energy Storage for Inverter-Based Dynamic Voltage Restorer in Grid-Integrated Renewable Sources

Devalraju Prasad and C. Dhanamjayulu

School of Electrical Engineering, Vellore Institute of Technology, Vellore, Tamil Nadu, India

Correspondence should be addressed to C. Dhanamjayulu; dhanamjayulu.c@vit.ac.in

Received 19 August 2022; Accepted 12 September 2022; Published 29 September 2022

Academic Editor: Albert Alexander Stonier

Power quality (PQ) is a key issue, particularly for technologically advanced process equipment, whose performance mainly depends on the quality of supply. Problems with PQ such as voltage swells/sags, interruptions, and harmonics are defined by any voltage, current, or frequency abnormalities causing damage or failure of the end-user equipment. Outages and interruptions lead to malfunctioning of end-user equipment or sensitive loads, such as diagnostic equipment in healthcare facilities, clinics, educational institutions, and detention centers, while further increasing significant economic losses. Custom power devices (CPDs) are recommended for enhancing power quality, and the best and most economical solution is considered to be the dynamic voltage restorer (DVR). Several methods are suggested to improve the PQ by using the dynamic voltage restorer; among them, most encouraging ways are to use a multilevel inverter (MLI) in the dynamic voltage restorer. This article combines the latest work of the literature, as well as a detailed discussion on PQ issues of the grid-integrated renewable energy sources (RESs), DVR principle with its operating procedures, system components, energy storage-based DVR topologies, DVR control unit, and DVR power converter-based topologies. In addition, synthesis of energy storage, control strategies, and multilevel inverters for DVR. This review benefits those interested in investigating DVR as a relevant and comprehensive reference.

1. Introduction

In the smart era, microprocessor-controlled devices or digital, electronic, and nonlinear devices are extensively used in all sectors of the industry. Nearly all these devices are sensitive, have electrical supply disruptions at any minute, and cannot be operated properly. In addition, several supplies have also been increased, which degrades power quality (PQ). Problems that happen because of inadequate power quality are data errors, automatic resets, memory losses, UPS alarms, equipment failures, software corruptions, circuit board failures, power supply problems, and overheating of electrical distribution systems. Considering these realities, PQ has become progressively critical. Not only PQ issues but also the issues related to voltage are also most important from sensitive nonlinear loads and end-users [1, 2].

The use of sensitive loads such as diagnostic equipment in health centers, educational institutions, and detention centers over several years has been fourfold, which leads to a concern with the quality of power of sensitive loads [3]. If power quality is insufficient, serious economic losses, losses in manufacturing, outage of sensitive and critical loads, and lack of information could have serious consequences [4]. Consequently, high power quality is essential for utilities, customers, and producers of electrical appliances too. The essential power quality issues include voltage swells, sags, harmonics, transients, flickers, fluctuations, and interruptions [5]. These are discussed in the next section. The sensitive and critical loads must prevent these issues in terms of power quality and voltage disturbances. In this regard, a wide range of solutions has been introduced including the best and most efficient solution for the compensation and mitigation of voltage disturbance known as custom power devices (CPDs) [6]. They act as compensating devices, each with its own control and application. CPDs such as a parallel-connected distribution static synchronous compensator (DSTATCOM), are used for correcting the power factor; for voltage compensation, the dynamic voltage restorer (DVR) is used and is connected in series; a parallel-series connected unified power quality conditioner (UPQC) can simultaneously inject voltage in series and current in parallel; however, UPQC and DSTATCOM are larger and more expensive, rather than DVR [7]. In modern power systems, the most serious and usual power quality issues are voltage sags, and DVR is used as the least expensive voltage sag solution [8].

When a voltage disturbance occurs on the supply side, the DVR supplies the required voltage to the load side. The DVR also protects from supply-side disturbances to sensitive and critical loads [9, 10]. This means that the DVR is important to compensate for voltage sags and to protect the sensitive load. The DVR is the best CPD since it has low costs, has small sizes, and can respond quickly to voltage disturbances. As an example, the DVR installation cost for the 2–10 MVA power supply is USD 300/kVA, while uninterruptible power supplies (UPSs) installation costs are USD 500/kVA. The servicing and operating costs of DVR are approximately 5% of its capital investment; however, it is much higher (about 15%) [1]. UPQC is a DSTATCOM-DVR combination with two power converters; hence, the structure of the DVR is, therefore, less than UPQC. DVR and DSTATCOM are closely related; however, DVR is used to protect the sensitive loads from supply interruptions, whereas DSTATCOM is used to protect critical loads from load-side disturbances. Furthermore, the DVR quickly (less than 1/4 cycle) responds to voltage disturbances, unlike other CPDs, such as the static VAR compensator (SVC) (2-3 cycle) [11].

Many topologies of DVR from different points of view of energy storages, power converters, and control systems have been investigated to improve power quality, cut costs, and improve the performance of DVR [12]. Furthermore, it has become widely attractive to modify DVR topology and integrate renewable energy resources with the DVR. Some general reviews on DVRs were carried out that a detailed study is lacking on modified DVR configurations and integration with renewable energy [13, 14]. Significant research is being conducted on DVR innovation and is now advanced but not many of the survey papers in the published literature are accessible. Remya et al. reviewed the DVR and reported on the challenges of the DVR systems [15]. Farhadi-Kangarlu et al. reported the combined overall DVR topologies, compensation techniques, and control strategies [16]. Significant research development in DVR technology for fifteen years after the first installation of DVR was published by El-Gammal et al. [17]. This paper intends to give a comprehensive evaluation of different components of DVR structure, as well as the integration of distributed generations into multi-inverter-based DVR. This article provides a significant contribution in the following ways:

(i) Discussion of the power quality difficulties associated with RES integration into the grid
(ii) To understand the working principles of DVR, the basic components, alternative DVR topologies from an energy storage approach, DVR control units, and DVR compensation techniques are provided
(iii) Discussion and extensive study of different grid-connected multilevel inverters, as well as multilevel inverter-based DVR integration with distributed generation, for optimizing voltage profile

Engineers and researchers working on the issues of power quality and the mitigation of voltage disturbances will be able to use them on an extensive basis.

The remainder of the article is organized accordingly. Section 2 describes the power quality problems of RES connected to the grid, grid-integrated RES requirements, PQ standards, classifications, causes, and effects. The most important custom power device and applications have also been clarified. In Section 3, the principle of DVR and its various operating modes, DVR circuit components, and DVR topologies are presented from the point of view of energy storage. Following this, Section 4 reviews DVR control units and compensating techniques. The analysis of various grid-tied multilevel inverters with their advantages and disadvantages along with their performance indices and, finally, an elaborated review on multilevel inverter-based DVRs are provided in Section 5; the conclusions and scope of future work are given in Section 6.

2. Power Quality Issues in Grid-Connected Renewable Energy Sources

There is considerable global attention to the utilization of renewable energy sources (RESs) for electricity generation. This is because of the negative environmental effects of fossil fuels being burned to convert energy, which emits an enormous amount of CO_2 and other greenhouse gases into the air. Figure 1 depicts a few of the renewable energy sources.

Renewable energy use rose by 3 percent as the demand for all other fuels declined, according to the IEA, Paris World Energy Review 2021 [18]. The main driver was a 7 percent increase in renewable energy generation. Renewable energy accounts for a 29% share of global electricity production in 2020, up from 27% in 2019. In 2021, the production of renewable energy will be more than 8% expanding to 8,300 TWh, the fastest growth year-on-year since the 1970s. Two-thirds of the renewable energy growth will be supported by solar PV and wind. The growth of renewable energy alone in China in 2021 was almost half expected, followed by the USA, the EU, and India shown in Figure 2. The wind is set to grow by 275 TWh (almost 17 percent), the greatest increase in renewable energy production, which is significantly higher than in 2020. China will remain the biggest market for PV, and there is expansion

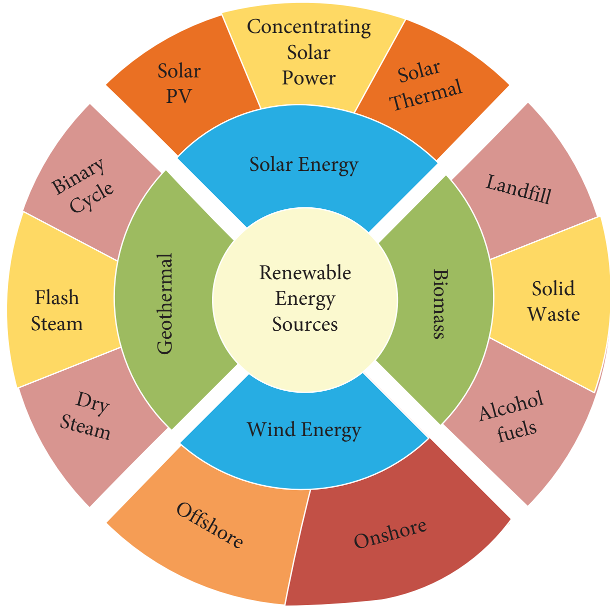

Figure 1: Major renewable energy sources.

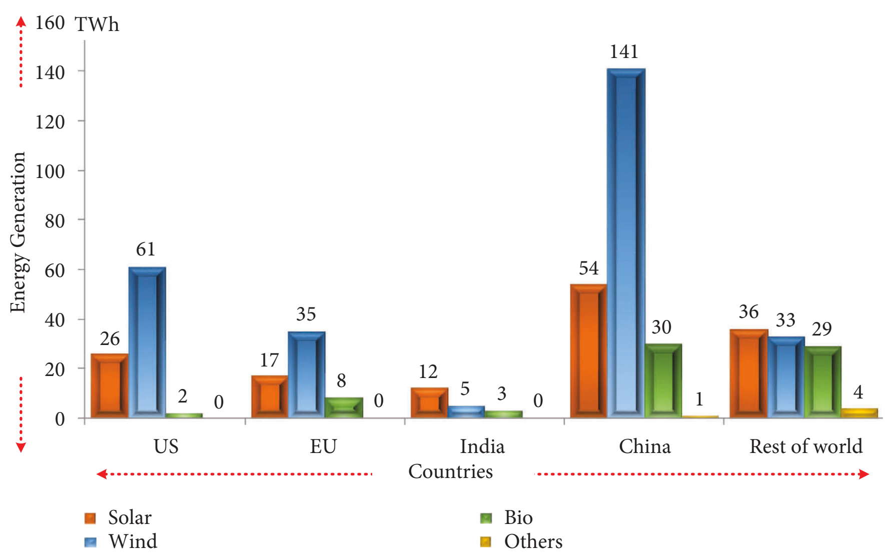

Figure 2: Worldwide increased technology and renewable power generation in 2020-2021.

in the United States with ongoing federal and state policy support. The new solar PV capacity additions will recover rapidly from COVID-19-related delays in India in 2021, with strong policy support in Brazil and Vietnam driven by large political support for distributed solar PV applications. The new solar PV capacities increased in Brazil and Vietnam. The total electricity generated by solar photovoltaic systems in 2021 is projected to grow to 145 TWh or almost 18 percent. Renewable sources in the electricity generation mix are expected to increase their proportion by 30 percent in 2021, all the time from all renewable sources. In combination with nuclear, carbon-free sources, the world coal plants' output in 2021 is much higher than that.

According to the IEA's 2021 Renewable Energy Market Update [19], renewable energy is the only power source for which consumption has risen despite the pandemic by 2020, while other fuel consumption has decreased. In light of current commercial and political changes, the renewable energy market investigates new global renewable power add-ons for 2021 and 2022. It also establishes a modern biofuel production prediction for these years, as the industry experienced significant losses due to a fall in transportation demand during the pandemic. It is expected to maintain the exceptional level of renewable energy add-ons and that 270 GW will become operational in 2021 and 280 GW in 2022. This expansion is more than 50% higher than the annual capacity rise record set in 2017–2019, implying that renewables will account for 90% of global capacity growth in both 2021 and 2022, as indicated in Figure 3.

2.1. Requirements for Grid-Integrated RES. Although some renewable energy sources are linked to the transmission system, most of them are linked to the distribution system. The operators of both distribution (DSOs) and transmission systems (TSOs) have been facing significantly higher levels of penetration of renewable sources, especially PV and wind systems, and many other strategies to replace conventional power plants with RES have been launched [20]. These changes have forced electrical system operators to take into account the impact of that penetration on grid stability. TSOs and DSOs have introduced new regulations at PCC, a common point of connection between the power grid and RES [21, 22]. RESs have the potential to handle various disturbances, increase the stability of voltage and frequencies and reliability, and improve power quality and security of power grids; they are required to act as traditional power plants [23]. The new requirements include standards of PCC power quality [24], voltage regulation [25], frequency regulation [26, 27], voltage stability support through reactive power injection [28], frequency stability support through active power control [26, 27], and voltage ride through (VRT) [29–34]. VRT is further subcategorized into (i) LVRT (low-voltage ride through) [30], (ii) ZVRT (zero-voltage ride through) [33], and (iii) HVRT (high-voltage ride through) [34]. In [30], the energy storage system was controlled by LVRT, and reactive power supports the grid; the limitations are overshooting, high fluctuations, superimposition, additional investment costs, periodic inspection, and maintenance, as specified in the grid code, whereas in [32], STATCOM and SVC control the LVRT; it injects reactive currents and improves the VRT capacity; however, there are no data about the change of DC-link voltage during grid faults; also, the complexity and costs increase. Voltage ride-through standards in different countries are tabulated in Table 1.

2.2. Power Quality. Power quality for electricity suppliers and their customers has become an important concern. From the point of view of customers, the consequences of disturbances in terms of financial loss can be between hundreds to millions of dollars. Power quality issues lead to losses of consumer satisfaction and also losses of load or income from the point of view of utilities. Quick incidents such as voltage transients, swells/sags, voltage impulses, high-frequency noise, and faults are power quality issues; generally, these are identified as any deviation from the standard voltage source. Hence, issues of power quality affect electrical equipment directly [35–37]. The percentage sharing of major power quality issues is shown in Figure 4.

Disturbances that could lead to problems with power quality may be an operation of unbalanced and nonlinear loads, start or switch off huge loads such as motors, energization of transformers and capacitor banks, or failure of devices such as transformers and wires, lightning, and natural events. The two main standards for power quality issues are the IEC and the IEEE. Table 2 contains the latest revisions to these standards [38–48], and the time required for RES to clear the abnormalities when exposed to abnormal voltage and frequency [49] is listed in Table 3.

Table 4 lists the most important issues of power quality and their definitions, and Table 5 provides reasons and effects of problems of power quality together with their duration and magnitude. IEC 61000-3-2 (1995-03), IEEE-519, and IEC/TS 61000-3-4 (1998-10) establish guidelines for limiting harmonic problems. IEEE P1564 and P1547a address the voltage sag issues. The first deals with the impacts of voltage sag, while the second deals with ways to stabilize a system through voltage sag mitigation. The flicker problem characterizes IEC 61000-4-15. IEEE 1159–1995 characterizes general problems with power quality. IEEE 1250–1995 and IEEE P1409 discuss the impacts and corresponding solutions on power quality issues. IEEE Standard P1547 discusses microgrid characteristics and their interconnections with the power system.

2.2.1. Power Quality Improvement (PQI) Techniques. Various PQI research aimed at minimizing problems with PQs are reported, and the ideal grid integration of renewable energy sources is promoted; however, every mitigation technique creates certain difficulties; hence, it will continue to be an active research sector in the future too. Current quality improvement (CQI) and voltage quality improvement (VQI) strategies are two types of PQI techniques that emphasize renewable energy integration, as shown in Figure 5. The VQI technology addresses voltage variations and frequency mitigation in DGs. Further subclassifications of VQI techniques may include energy storage (ES) [50], custom power devices (CPDs) [51], optimization of energy conversion [52, 53], spinning reserve [54], and a few additional unique technologies based on the variable frequency transformer (VFT) [55] and the virtual sync machine [56]. Further CQI technologies can be divided into passive filters (PFs) [57], active power filters (shunt and series) [58], smart impedance [59], hybrid filters [60], and multifunctional DGs [61].

2.2.2. Custom Power Devices (CPDs). Critical equipment protection against voltage sags and interruption is supplied with storage units. Examples of storage systems include flywheel energy storage system (FESS), superconducting magnetic energy storage (SMES), uninterruptible power supply (UPS), ultracapacitors (UCAPs), and batteries. They are used to mitigate the required energy due to faults and voltage drops. The most efficient method of mitigating voltage slags is by using custom power devices (CPDs); they ensure that the quality and reliability of supply are guaranteed to customers [62, 63]. Table 6 contains the most important CPDs to mitigate the issues related to power quality.

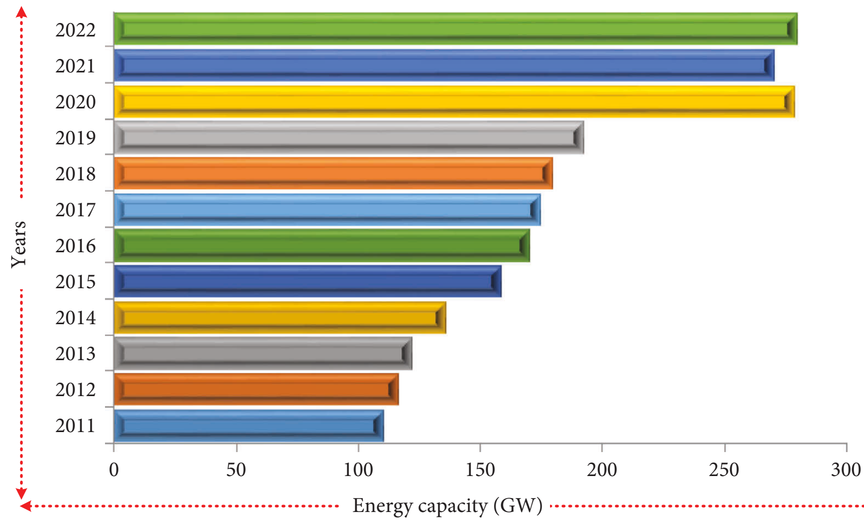

Figure 3: Net renewable capacity additions, by renewable energy market update 2021, IEA.

Table 1: Voltage ride-through standards in different countries.

Parameters	Country	Regulation			
		During fault		After fault	
		$t_{max.}$ (s)	$V_{min.}$ (%)	$t_{max.}$ (s)	$V_{max.}$ (%)
LVRT	UK	0.14	15	1.2	80
	Denmark	0.5	20	1.5	90
	US (NERC)	0.625	15	3.0	90
	China	0.625	20	2.0	90
	Japan	1.0	20	1.2	80
	US (PREPA)	0.60	15	3.0	85
	Romania	0.625	15	3.0	90
ZVRT	Canada	0.15	0	1.0	85
	Germany	0.15	0	1.5	90
	Australia	0.45	0	0.45	80
	US (WECC)	0.15	0	1.75	90
	Spain	0.15	0	1.0	85
	Malaysia	0.15	0	1.5	90
	Italy	0.2	0	1.5	85
	South Africa	0.15	0	2.0	85
		During fault (caused voltage increase)			
		$t_{max.}$ (s)		$V_{min.}$ (%)	
HVRT	Denmark	0.1		120	
	Germany	0.1		120	
	Spain	0.25		130	
	US (NERC)	1.0		120	
	US (WECC)	1.0		120	
	US (PREPA)	1.0		140	
	South Africa	0.15		120	
	Malaysia	Continuous		120	
	Australia	0.06		130	
	Italy	0.1		125	
	Romania, China, Canada, and the UK	Not defined		Not defined	

3. Dynamic Voltage Restorer

DVR is a compensating device having a series impedance that is serially connected between the PCC (point of common coupling) and the load as shown in Figure 6. It supplies the required voltage during sag to synchronize the load voltage and permits the switching of real and reactive power between DVR and distribution systems [64]. Westinghouse manufacturing company (part of Siemens) introduced the first DVR in August 1996, with the support of the Electric Power Research Institute (EPRI), with an installed capacity of 2 MVA at Duke Power Company located in North

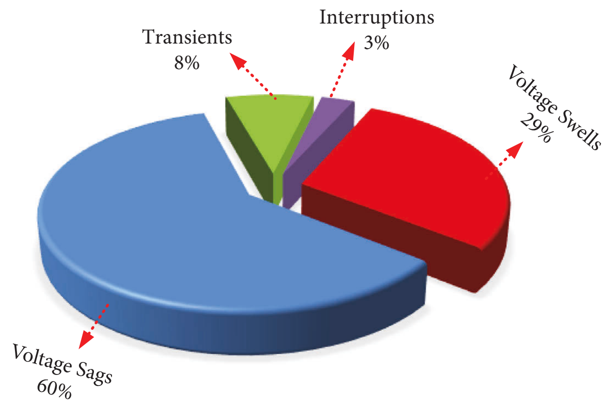

Figure 4: Percentage quantity of major PQ problems.

Table 2: Power quality standard and their recommendations.

References	PQ standard	Recommendations
[38]	IEEE 519	Harmonic limitation of current and voltage.
[39]	IEC 61000-3-2	Limitation of harmonic current (device input current ≤ 16 A).
[40]	IEC/TS 61000-3-4	Limitation of harmonic current (device input current > 16 A).
[41]	IEEE P1564	Sag performance indication and characterization.
[42]	IEEE P1547a	Allow the equipment to improve stability through voltage mitigation.
[43]	IEC 61000-4-15	An obvious sign of fluctuations/flicker characterization.
[44]	IEEE 1159	Definition and regulating of power quality in alternating power systems (AC) and their influence on customer devices
[45]	IEEE 1250	AC system voltage disturbances, their impact on sensitive equipment, and harmonic limitation.
[46]	IEEE P1409	Progress in standard custom power devices.
[47]	IEEE 141	Voltage regulation, property maintenance, preservation, reliability, simplicity, and flexibility.
[48]	IEEE P1547	Distributed generations (DGs) integration with power systems.

Carolina (USA) on 12.47 kV distribution systems having three voltage source inverters and three injection transformers with the in-phase compensation technique [10, 15].

The equivalent circuit of DVR is obtained by connecting a voltage source V_{Comp} in between the source (V_S) and load (V_L) with their respective impedances Z_S and Z_L as shown in Figure 7. At PCC source, the current I_S is divided into I_L and IoT, where I_L is the sensitive load current and I_{OT} is another load current. The voltage at PCC is represented by V_G, and the voltage compensated by DVR is V_{DVR}. Resistance R and inductance L are obtained from the impedance Z of the filter and injection transformer, and the values of R_{DVR} and X_{DVR} are related to V_{DVR}. The impedance of the source, load, and DVR are Z_S, Z_L, and Z_{DVR}, respectively.

P_S is the real power, and Q_S is the reactive power of supply.

P_L is the real power, and Q_L is the reactive power of the load.

P_{DVR} is the real power, and Q_{DVR} is the reactive power supplied by the DVR.

The voltage across sensitive load V_L is given by

$$\begin{aligned} V_L(t) &= V_G(t) + V_{\text{DVR}}(t) + Ri_L(t) + L\frac{di_L}{dt}, \\ X_{\text{DVR}} &= \frac{V_{\text{DVR}}^2}{S_{\text{DVR}}} X p.u., \\ R_{\text{DVR}} &= \frac{V_{\text{DVR}}^2}{S_{\text{DVR}}} R p.u., \\ Z_{\text{DVR}} &= \frac{V_{\text{DVR}}^2}{S_{\text{DVR}}} Z p.u. \end{aligned} \tag{1}$$

The percentage of voltage handling capacity u_{DVR} and current handling capacity i_{DVR} of DVR is given by [65]

$$\begin{aligned} u_{\text{DVR}}\% &= \frac{V_{\text{DVR}}}{V_{s,\text{rated}}} 100\%, \\ i_{\text{DVR}}\% &= \frac{I_{\text{DVR}}}{I_{L,\text{rated}}} 100\%. \end{aligned} \tag{2}$$

I_{DVR} is the current rating of DVR, $V_{S,\text{ rated}}$ is the rated supply voltage, and $I_{L,\text{rated}}$ is the rated load current of DVR [66].

Table 3: Response to abnormal grid voltage and frequency.

Standard	Voltage (V)	Clearing time (sec)
Abnormal response of grid voltage		
IEEE 1547 Rule 21	$V < 45\%$	0.16
	$45\% < V < 60\%$	1
	$60\% < V < 88\%$	2
	$110\% < V < 120\%$	1
	$120\% < V$	0.16
IEC 61727	$V < 50\%$	0.1
	$50\% < V < 85\%$	2
	$110\% < V < 135\%$	2
	$135\% < V$	0.05
IEEE 929	$V < 50\%$	6*
	$50\% < V < 88\%$	120*
	$110\% < V < 120\%$	120*
	$120\% < V$	6*
VDE-AR-N-4105	$V < 80\%$	0.1
	$V > 110\%$	0.1
AS 4777	$V < 200\ V$	2
	$V > 270$ V	2
Abnormal response of grid frequency		
IEEE 1547A Rule 21	$f < 57$	0.16
	$57 < f < 59.5$	2
	$60.5 < f < 62$	2
	$62 < f$	0.16
IEC 61727	±1	0.2
IEEE 929	$f < 59.5$	6*
	$f > 60.5$	6*
VDE-AR-N-4105	$f < 51.5$	0.1
	$f < 47.5$	0.1
AS 4777	$f < 45$	2
	$f > 55$	2
Rule 21	$f > 60.5$	0.16
	$f < 59.3$	0.16

*Cycles

DVR mainly consists of a bypass switch, injection transformer, filter, inverter, and DC-link capacitor or energy storage as shown in Figure 8. DVR can be categorized into $1-\phi$ DVR shown in Figure 8 and $3-\phi$ DVR shown in Figure 9. A bypass switch is used to connect the DVR to the line during the injection mode and disconnect the DVR under standby operation. The injection transformer will adjust the DVR output voltage and isolate DC to AC systems. High-frequency harmonics present in DVR output voltage to attenuate this LC filter are used. The voltage is maintained as constant during transient by using a DC-link capacitor; hence, a steady-state operating range of DVR will improve. For deep voltage sags, the external energy storage supplies the desired real power to the load. The most essential part of DVR is the inverter; it produces the required controllable voltage for compensation.

The dynamic voltage restorer works in three operating modes. They are (i) voltage compensating or active or injecting mode, (ii) standby mode, and (iii) fault current limiting or protecting mode. When the voltage disturbance occurs within the operating range of the DVR. at that instant. the bypass switch is open and DVR switches to active mode and feeds the grid with the required voltage. Once the voltage is in its normal range, the bypass switch will close and end the compensation mode. It is not necessary to inject voltage into the grid under normal conditions; hence, the DVR is left out through a bypass switch to reduce the power loss in the DVR by restricting the inverse effect on line voltage; this mode is known as the standby mode. Sometimes, high current flows through DVR due to SC fault on the load side which will cause damage to the injection transformer and DVR components; hence, the identification of downstream fault is necessary to protect the DVR [67]. The protection scheme of DVR is presented in Figure 10. It provides an alternative path to the fault current through breakers, thyristors, and varistors and ensures that the current path should be present. If the current path is not present, a severe overvoltage appears at the terminals of the injection transformer [66, 68].

By lowering the fault current, the DVR disables both main and backup protection. As a result, the duration of the defect may be extended. As a result, using a DVR to reduce the fault current to zero, interrupt it, and send a trip signal to the upstream relay or circuit breaker is preferred (CB). The ability to inject 100% of the voltage is required for the FCI function. As a result, the series transformer and VSC power ratings would be almost three times higher than those of a standard DVR with 30%–40% voltage injection capabilities. As a result, the DVR will cost extra. The economic feasibility of such a DVR is determined by the cost of the DVR, and the importance of the sensitive load is protected by the DVR.

3.1. DVR Topologies. The DVR can be categorized into various groups, related to the configuration of energy storage, location of the filter, presence of the injection transformer, and structure of the converter. Figure 11 shows various categories of system topologies.

3.1.1. Location of the Filter. Usually, the high-frequency or carrier frequency switching technique is used in DVRs. Hence, the output voltage is embodied with higher-order harmonics; thus, it is required to attenuate the harmonics, and for that, generally a low-pass LC filter is used [69–73]. As indicated in Figure 12, the filter is connected to the inverter side [72] or the supply side [73]. The converter side filter has the advantage that it does not allow the higher harmonic currents into the series transformer; hence, the rating of a transformer will decrease; also, the dv/dt stresses on the transformer are reduced. However, the presence of a passive element will produce an extra drop over the transformer. A capacitor is connected to the series transformer in the case of a grid-side filter scheme. It will solve the issues related to the presence of the inductor in the inverter side filter. However, this topology has poor efficiency as compared to the previous one for harmonic reduction.

3.1.2. Presence of an Injection Transformer. In DVR, the inverter generates the required compensation voltage and is injected through the injection transformer. Based on

Table 4: Description of power quality issues.

PQ issues	Characteristics	Expression	Constraints
Normal		$x(t) = \sin(\omega t)$	$\omega = 2\pi f$ rad/s
Voltage dip/sag	A decrease in RMS voltage	$x(t) = [1 - \alpha(u(t - t_1) - u(t - t_2))]\ \sin\ (\omega t)$	$0.1 \le \alpha \le 0.9$, $T \le t_2 - t_1 \le 9T$
		With harmonic $x(t) = [1 - \alpha(u(t - t_1) - u(t - t_2)^*$ $[\alpha_1 \sin(\omega t) + \alpha_3 \sin(3\omega t) + \alpha_5 \sin(5\omega t)]$	$0.1 \le \alpha \le 0.9$, $T \le t_2 - t_1 \le 9T$, $0.05 \le \alpha_3,\ \alpha_5 \le 0.15$ $\Sigma(\alpha_i)^2 = 1$
Voltage swell/ rise	An increase in RMS voltage	$x(t) = [1 + \alpha(u(t - t_1) - u(t - t_2))]\ \sin\ (\omega t)$	$1.1 \le \alpha \le 0.8$, $T \le t_2 - t_1 \le 9T$
		With harmonic $x(t) = [1 + \alpha(u(t - t_1) - u(t - t_2))]^*$ $[\alpha_1 \sin(\omega t) + \alpha_3 \sin(3\omega t) + \alpha_5 \sin(5\omega t)]$	$0.1 \le \alpha \le 0.8$, $T \le t_2 - t_1 \le 9T$, $0.05 \le \alpha_3,\ \alpha_5 \le 0.15$, $\Sigma(\alpha_i)^2 = 1$
Transient	A sudden voltage change, current change, or both	$x(t) =$ $\sin(\omega t) + \alpha e^{-(t - t_1/\tau)}(u(t - t_1) - u(t - t_2))\sin(2\pi f n t)$	$0.1 \le \alpha \le 0.8$, $0.5\,T \le t_2 - t_1 \le 3T$, $300\text{ Hz} \le fn \le 900\text{ Hz}$, $8\text{ ms} \le \tau \le 40\text{ ms}$
Harmonic	The distorted voltage or current waveform is due to the existence of integral multiples in fundamental frequency	$x(t) = \alpha_1 \sin(\omega t) + \alpha_3 \sin(3\omega t) + \alpha_5 \sin(5\omega t) + \alpha_7\ \sin(7\omega t)$	$0.05 \le \alpha 3, \alpha 5,\ \alpha 7 \le 0.15$ $\Sigma(\alpha_i)^2 = 1$
Voltage flicker/ fluctuation	Fluctuations or a random change in the amplitude of the voltage	$x(t) = [1 - \alpha\ \sin(2\pi\beta t)]\sin\ (\omega t)$	$1.1 \le \alpha \le 0.2$, $5\text{ Hz} \le \beta \le 20\text{ Hz}$
Voltage interruption	Reduced supply voltage or charge current to below 0.1 pu	$x(t) = [1 - \alpha(u(t - t_1) - u(t - t_2))]\ \sin\ (\omega t)$	$0.9 < \alpha \le 1$, $T \le t_2 - t_1 \le 9T$

injection transformers, there are two topologies: injection transformer-based DVR topologies and transformerless DVR topologies.

(1) Transformerless DVR Topologies. In some DVR topologies, the injection transformer is removed to overcome the issues associated with core saturation and inrush currents present in the transformer; such topologies are named transformerless topologies [74] shown in Figure 13. The benefits of transformerless DVR topologies are less weight and a significant reduction in volume and price [75, 76]. However, the converter must allow the full voltage; hence, for better efficiency of higher voltage applications, multilevel inverters are used. A transformerless DVR presented in [77] consists of a buck-boost converter with five bidirectional switches. It has the advantages of compact structure and lightweight. However, due to bidirectional switches, this converter experiences a commutation problem and high cost. To overcome the tough commutation problem, Zhou et al. [78] proposed a DVR with an indirect AC/AC converter heaving six unidirectional switches.

(2) Transformer-Based DVR Topologies. For isolation, an injection transformer is required; in the case of DC-link in DVR, it is activated from the supply or load side via a rectifier; however, if energy is received from battery storage in DVR, the injection transformer is not required because the battery works as a floating DC source [79]. The major issues associated with injection transformers are saturation and protection of the transformer. The solutions to the saturation problems in the injection transformer have been addressed in [80–83]. Figure 14 represents transformer-based DVR.

3.1.3. Energy Storage. In DVR, energy storage means external energy devices (not for DC-link capacitors) are used to inject real power into the grid. Depending on energy storage, there are two DVR topologies: (i) without energy storage topologies and (ii) with energy storage topologies.

(1) Without Energy Storage. By connecting a series converter, a shunt converter (mostly rectifier), or an AC-AC converter to the grid, the required compensating energy is directly received in this method. The converter is added to either the grid side or load side which are presented in Figures 15 and 16 , respectively. Preliminary research was carried out on DVR without DC-link before 1996 [84]. A few developments in this topology were reported in [85–87] after the development of bidirectional switch escalating the progress of AC-AC converter-based DVR [88]. According to the nature of voltage sags, a control scheme is proposed to compensate for the sag with phase jump in [89]. In these topologies, a considerable amount of supply voltage is present at the time of sag, and this residual voltage is utilized to boost and protest the full load at rated voltage. However, during fault conditions, it draws more current from the line; hence, upstream loads have higher voltage drops.

(2) With Energy Storage. The required compensation energy is drawn from a variable DC-link (capacitor supported or self-charging) shown in Figure 17 or from a constant DC-

Table 5: Characteristics, causes, and effects of power quality issues.

PQ issues	Causes	Category	Magnitude (pu) and duration	Effects	
Voltage dip/ sag	Start of huge loads, loading of grid, variations in supply voltage, inrush current, faults, and irregular connection	Instantaneous	0.1–0.9	Motor overload or decay, lock-up, and data inaccurate	0.5–30 cycles
		Momentary	0.1–0.9		30 cycles–3 sec
		Temporary	0.1–0.9 3 sec–1 min		
Voltage swell/ rise	Stop/start of large loads, variations in supply voltage, inrush current, and irregular connection	Instantaneous	1.1–1.8 0.5–30 cycles	Loss of data, damage to equipment, lock-up, and data inaccurate	
		Momentary	1.1–1.4		30 cycles–3 sec
		Temporary	1.1–1.2		3 sec–1 min
Transient	Stop/start of large loads, lightning, snubber circuits, and incorrect connection to the transformer	Impulsive: Nanosecond	— <50 nsec	Electrical equipment interference, loss of data, flickering of lights, and harm to sensitive appliances	
		Impulsive: Microsecond	— 50 nSec–1 msec		
		Impulsive: Millisecond	— >1 msec		
		Oscillatory: Low frequency	0–4 0.3–50 msec		
		Oscillatory: Medium frequency	0–8 20 μsec		
		Oscillatory: High frequency	0–4 5 μsec		
Voltage interruption	Insulation failure and disturbance in control	Instantaneous	<0.1	Disturbance of data processing devices	0.5–30 cycles
		Momentary	<0.1		30 cycles–3 sec
		Temporary	<0.1		3 sec–1 min
Harmonic	Nonlinear loads	—	Steady-state	Data unfaithful, lock-up, motors and transformers overheating, and losses in electrical equipment	0–20%
Voltage fluctuation/ flicker	Load switching and supply voltage fluctuations	—	Intermittent	Flickering of light, over and under voltages, and damage to the load-side device	0.1–7%

link (external energy storage supported) shown in Figure 18. In capacitor-supported topology, the discharging energy from the DC-link capacitor is injected into the grid during the active mode. In the standby mode, the DC-link capacitor is charged and stores the required energy. It is more economical since there is no need for external storage. However, the stored energy in the DC-link capacitor is limited; hence, it is inadequate to compensate the deep sags for high pf loads in a lengthy period. Constant DC-link topology requires direct energy storage devices, such as SMES, supercapacitors, and batteries, and also an extra high-rated energy converter is connected to transfer the large stored energy to a low-rated DC-link storage to maintain a constant voltage during sag, but the size and capital cost of the DVR get increased.

The energy storage of intermittent renewable sources is an extensive area of research since energy storage is utilized in several applications in the grid, including energy shifting, electricity supply capability, supporting frequencies and voltages, and the management of electricity bills [90–92]. Energy storage technologies are pumped hydroelectric (PHS) [93], compressed air energy storage (CAES) [94], flywheel energy storage (FES) [95], battery energy storage (BES) [96], thermal storage [97], and hydrogen [98]. Table 7 provides a technical and economic summary of key energy storage technologies. According to the International

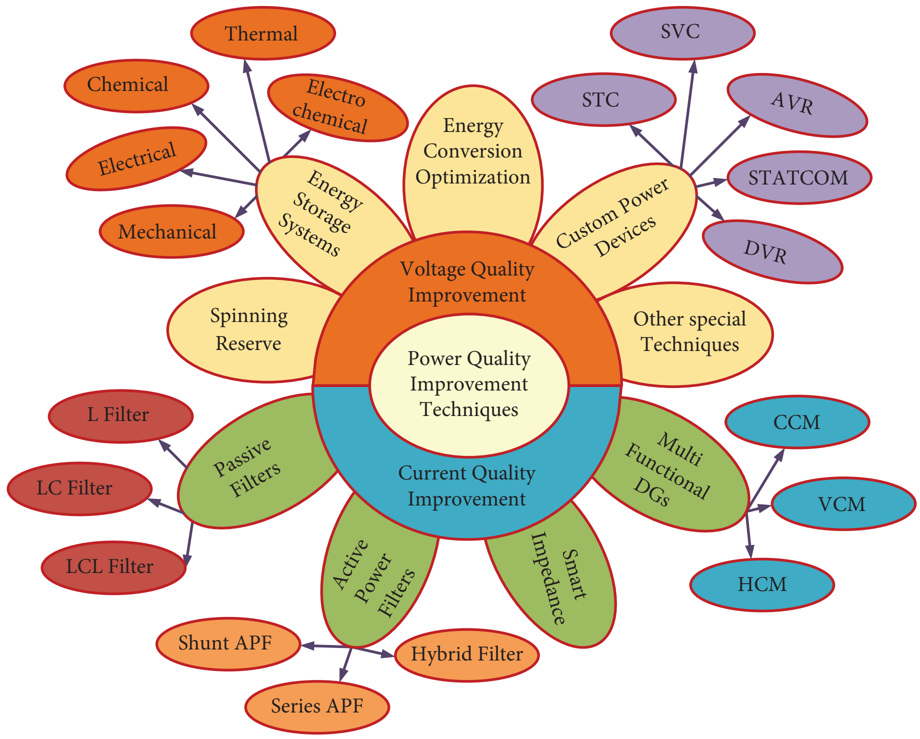

Figure 5: Power quality improving techniques for integration of renewable energy.

Table 6: Applications of the CPDs.

Custom power devices (CPDs)	Applications/functions
Distribution static synchronous compensator	Current harmonics, power factor, load voltage/current balancing, and flicker.
Active power filter	Harmonic distortion and transient.
Interline power flow controller	Transient, damping oscillation, voltage control, and reactive power flow control.
Dynamic voltage restorer	Voltage balancing, voltage sags/swells, flicker, and voltage regulation.
Static current limiter solid-state circuit breaker	Disconnects the faulted circuit and fault current limitation.
Solid-state transfer switch	Voltage sag/swell and transmitting power from another feeder.
Static synchronous series compensator	Fault current limitation, control of current, and active/reactive power.
Static VAR compensator	Flicker and unsymmetrical loads.
Static synchronous compensator	Transient, damping oscillation, and voltage fluctuation/flicker.
Surge arrester	Overvoltage and transient.
Unified power flow controller	Voltage and active/reactive power control, fault current limitation, and transient.
Uninterruptible power supply	Emergency power shortage.
Unified power quality conditioner	Voltage/current balancing, voltage sags/swells, harmonics, power factor, fluctuations, and harmonic load current.
Transient voltage surge suppressors	Voltage transient.

Hydroelectricity Association (IHA), PHS is the most advanced and well-established storage technology in the world, with a total installed capacity of 153 GW in 2018 and is expected to increase by almost 50 percent to about 240 GW by 2030 [112].

A PHS system can support seasonal management, time-shifting, peak lopping, back-up, filling of the valley, and energy management. It is, however, geographically constrained, capital-intensive, and frequently delayed owing to environmental permission. Technology in CAES can provide services of flexible power quality, but it also suffers from the same problem as PHS such as geographically limited. During the industrial revolution, flywheel technology was quickly developed as the mechanism for smoothing steam engines [95]. Energy storage batteries are an electrochemical storage system that delivers quality services in power and were recently used to supply variable renewable storage systems such as solar PV and wind, in part driven by reductions in battery costs. Several technologies for batteries are covered in [113] from advanced lead acids widely used in automotive

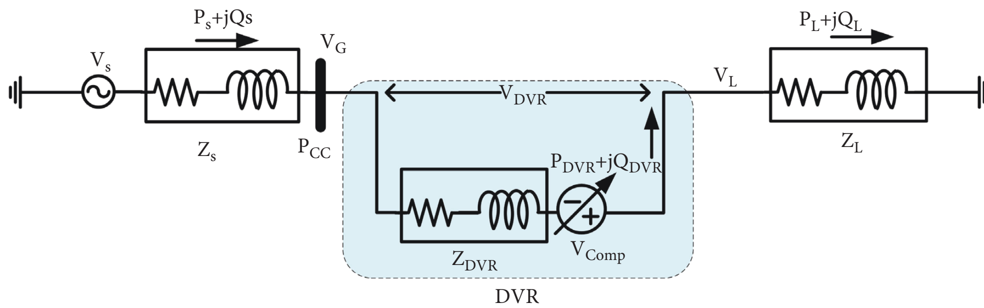

Figure 6: Basic structure of the dynamic voltage restorer.

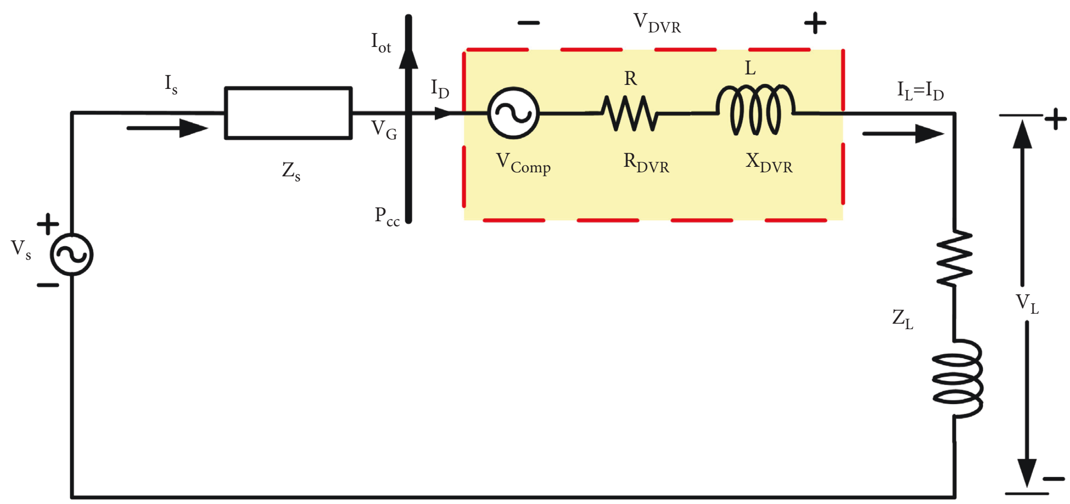

Figure 7: Equivalent model of the dynamic voltage restorer.

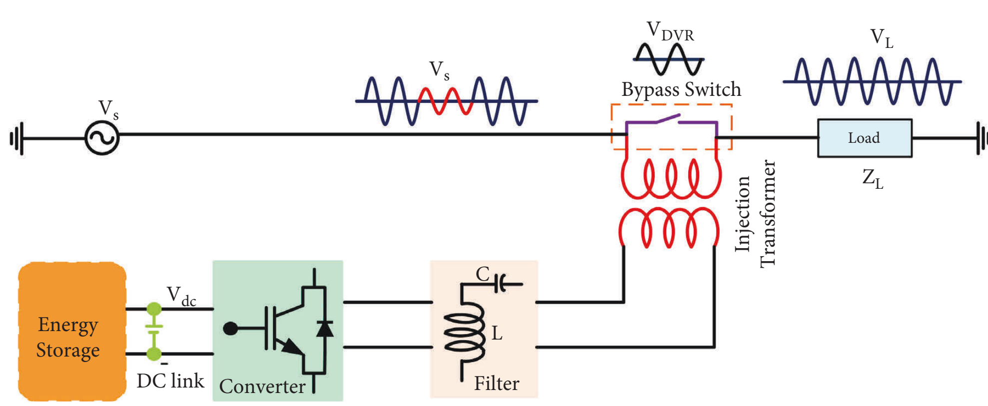

Figure 8: Schematic representation of $1-\phi$ DVR.

and heavy goods vehicles to the development of flow battery technologies that could be used in the power storage market. However, the most popular technology for portable and power storage systems has emerged from lithium-ion battery systems. Lithium-ion batteries have a low self-discharge rate, have a high energy density, are flexible and lightweight, and require little maintenance when compared to other battery technologies, making them the most popular. However, depending on the ambient conditions, lithium-ion systems necessitate temperature monitoring, and certain installations have cooling systems. The worldwide demand for batteries is increasing, with the use of batteries for portable and energy storage devices.

The benefits of various energy storage (ES) technologies such as energy density, cycle lifetime, and specific power can be combined with those of hybrid energy storage systems (HESS). Furthermore, combined technologies can differ in their electricity characteristics significantly; for example,

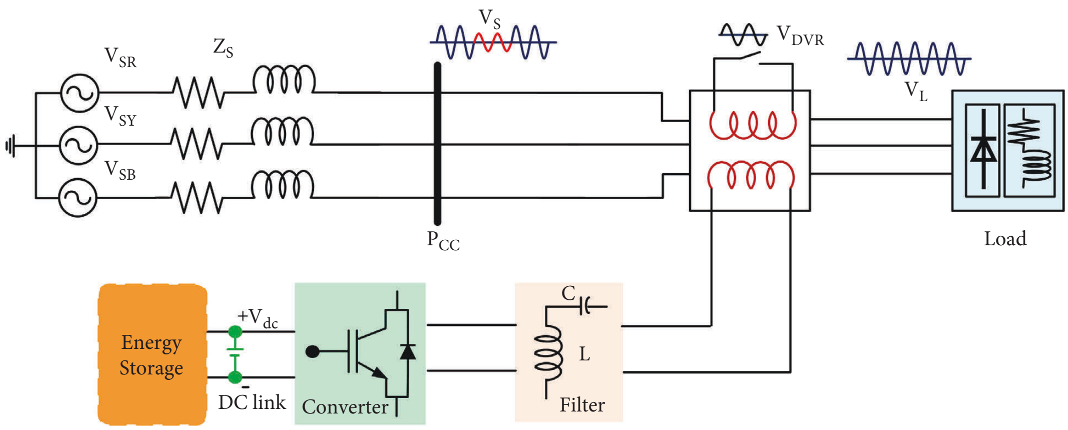

Figure 9: Schematic representation of $3-\phi$ DVR.

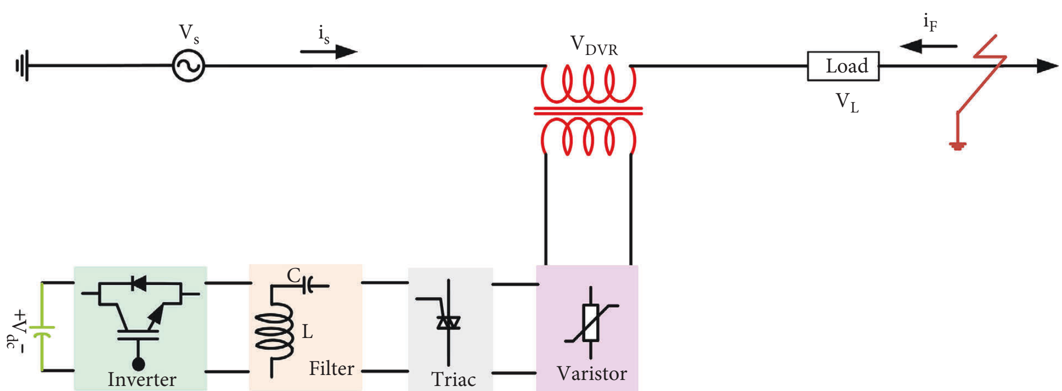

Figure 10: Protection scheme of the dynamic voltage restorer.

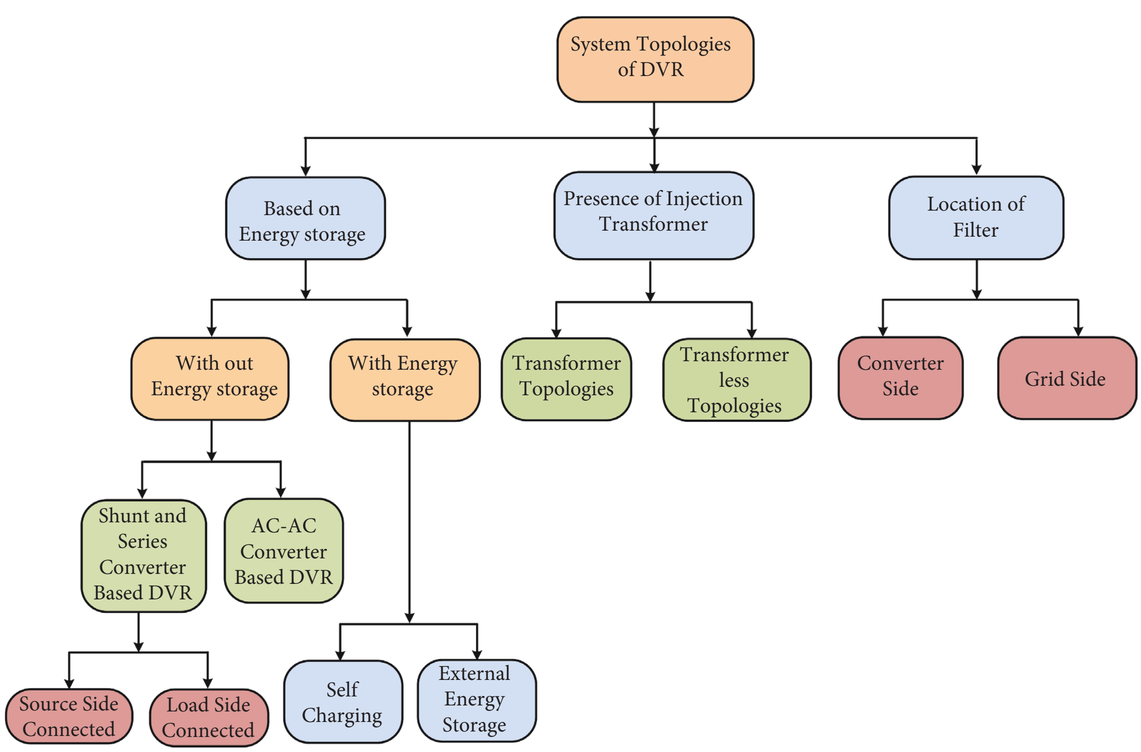

Figure 11: Classification of DVR system topologies.

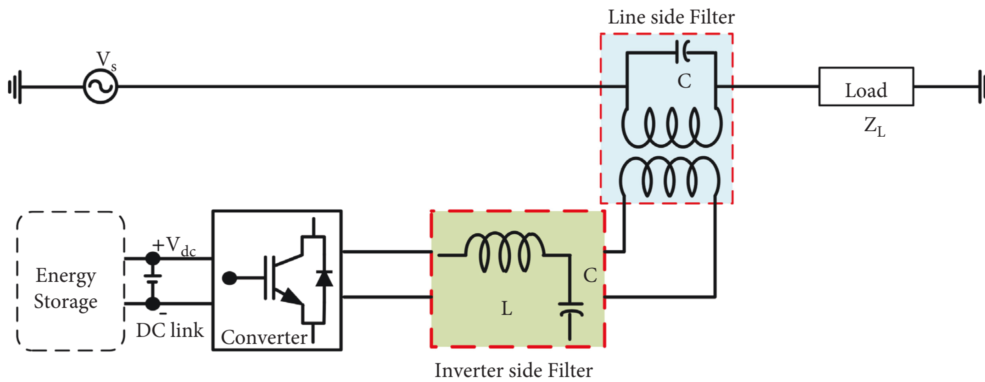

Figure 12: Different locations of the filter in DVR.

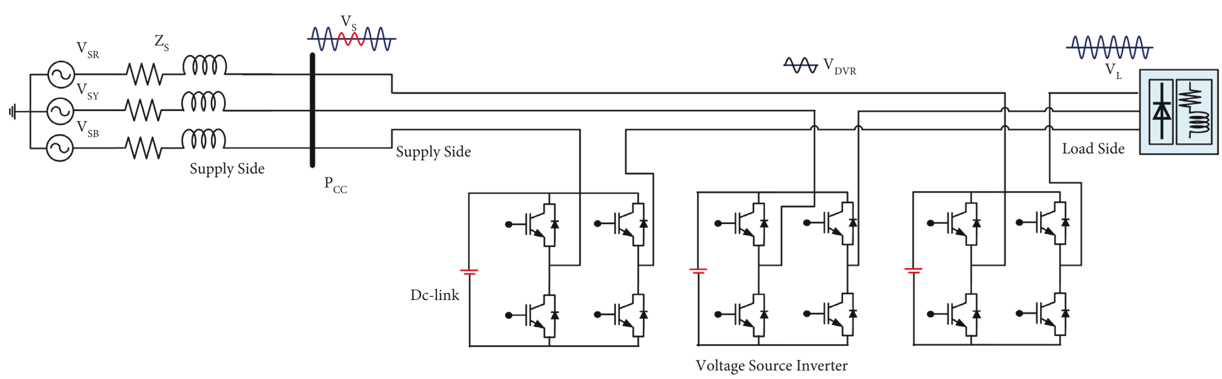

Figure 13: Transformerless DVR [15].

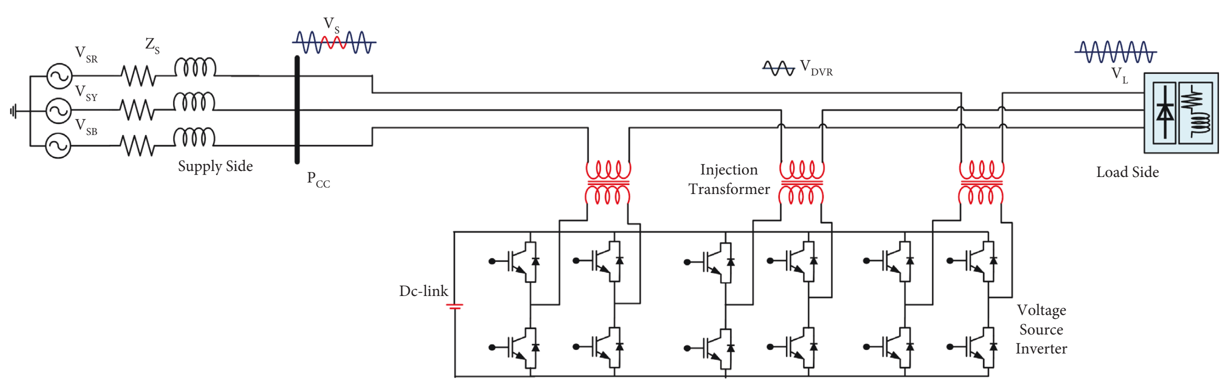

Figure 14: The transformer connected to DVR [15].

cut-off voltage prevents overload. A PE interface is thus important in controlling the both terminal voltage and power flow of individual devices in the HESS between various ES devices. Several configurations have been proposed and discussed that connect each HESS to ES device to the common DC-link [114–119].

HESS integration can be implemented by utilizing cascaded modular converters and existing PE devices. For example, the typical HESS composed of batteries and supercapacitor can be integrated into the MMC by connecting the DC-link to the battery, and connecting the submodules to the supercapacitors or connecting the batteries and supercapacitors to various submodules. Advanced control algorithms can control the active power supplied by DC-links/batteries and submodules/supercapacitors in the AC power [120]. Table 8 lists major electronic power suppliers to the commissioned BESS utilities and their solutions.

A capacitor-supported DVR was proposed by Nielsen and Blaabjerg [122]; it gives comparatively less performance for deep sags. Narrow sags, that persist not more than one minute, are compensated by using an ultra-capacitor-based DVR [123]. Wang and Venkataramanan [88] reported that flywheel is an effective technology for short-term energy

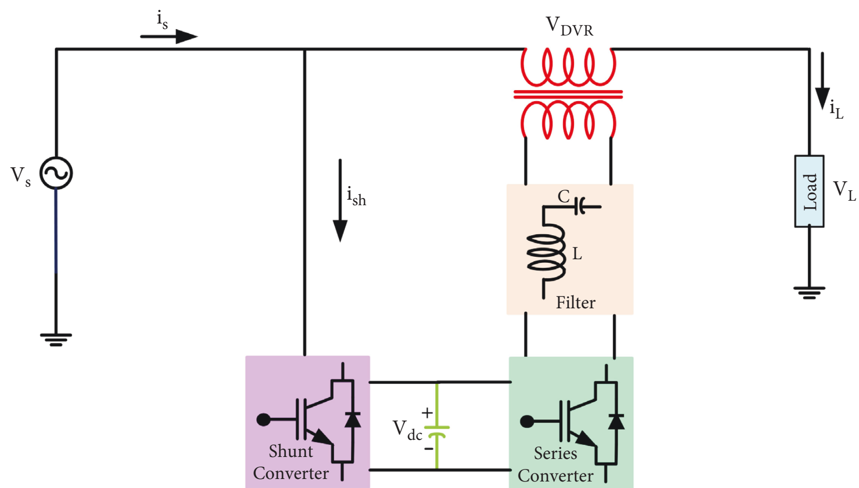

FIGURE 15: DVR connected at the grid side.

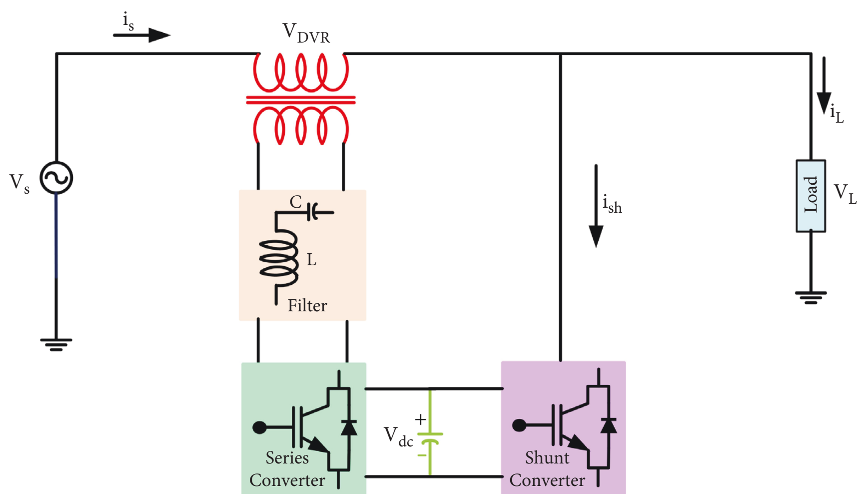

FIGURE 16: DVR connected at the load side.

storage. Kim et al. [124] proved that SMES is capable to mitigate the narrow voltage sags for MJ/750 kVA DVR. Shi et al. [125] presented that SMES is effectively mitigating the sags persistence of 100 ms. Superconducting magnetic energy storage (SMES)-based DVRs are analyzed for voltage sag compensation and technically validated in [126–128]. However, as compared to DVR supported with regular battery energy storage (BES), the SMES-based DVR systems are uneconomical because of the high capital cost of SMES coils [129]. To overcome this, hybrid energy storage (HES) was introduced by Shim et al. [130]; in that, they reported SMES/HES is suitable for getting smooth output from renewable energy sources. Gee et al. [131] presented that SMES or battery energy storage systems based on DVR are well suited for three-phase loads. MW-class SMES integrated with SFCL-based DVR for voltage sag compensation is proposed and demonstrated in [132].The potentials and constraints of various DVR topologies are listed in Table 9.

4. Control Systems in DVR

The control system plays a vital role in the DVR, and it goes through several stages; these include (a) detecting voltage disturbance, (b) generating the reference voltage, and (c) controlling the converter. The systematic procedure of the control system and different types of techniques used in the detecting voltage disturbance unit, reference generation unit, voltage and current controllers, and PWM pulse generator are presented in Figure 19.

The efficiency of the control algorithm is completely dependent on the accuracy and quality of the techniques used in voltage detection. Input data received by the detecting unit is the measured voltage on the supply or load or both sides. The operating mode of DVR is decided by this stage whether DVR operates as standby mode or active mode or protection mode, by using traditional or advanced detection techniques. In traditional voltage peak detection

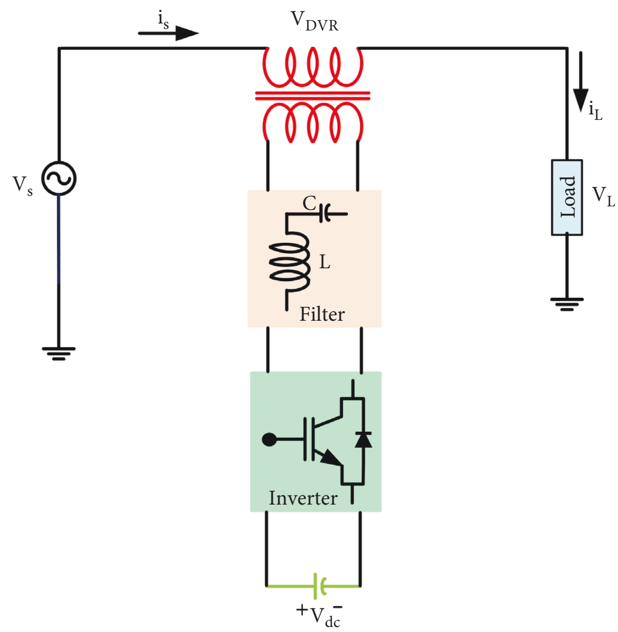

FIGURE 17: DVR with variable DC-link.

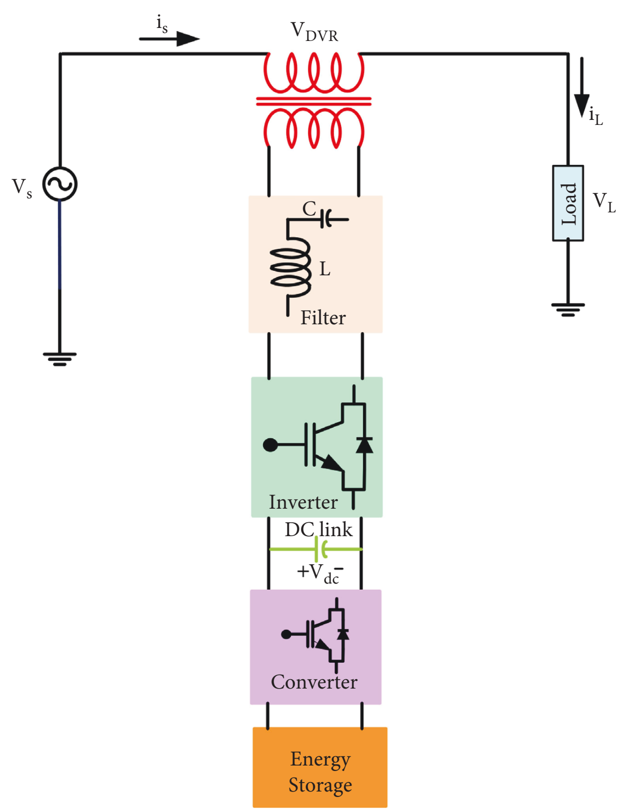

FIGURE 18: DVR with constant DC-link.

[133], RMS detection [134] are used, whereas in advanced detection, wavelet [135], Kalman filtering [136], discrete Fourier transform(DFT) [74], fast Fourier transform (FFT) [136], numerical matrix [137], missing voltage [135], rotating DQ reference frame [90], and synchronously rotating frame (SRF) [89] are used. If there is no voltage disturbance, then the bypass switch is turned ON and DVR acts as the standby mode. If any load side fault is detected,

Table 7: Technical parameters of different energy storage technologies.

Parameters	Mechanical			Electrochemical						Electrical		Hydrogen	Thermal
	PHS	FES	CAES	Pb-A	Ni-Cd	Na-S	NaNiCl2	Li-ion	VRFB	SCES	SMES		
Power range (MW)	10–5000 [99–102] 1000–3000 [103]	0.1–20 [99] < 0.25 [104] 0–0.25 [100, 102] 0.01–0.25 [105] 0–1.65 [106] 0–10 [103]	5–1000 [99] 5–300 [100–102] 100–3000 [103] 50–350 [91]	0–40 [99] 0–20 [100, 101] 0.05–10 [91]	0–40 [99, 101]	0.05–34 [99] 0.05–8 [101]	0–3 [102] 0.05–2 [101]	0–100 [99] 0–1 [100] 0–0.1 [101] 0.015–50 [91]	0.3–3 [100]	0–0.3 [100, 101]	0.1–10 [100, 101]	0–50 [101] 0.1–15 [91]	50–250 [91]
Energy density (Wh/l)	0.5–1.5 [100, 102, 105]	20–80 [102, 104]	3–6 [100–102]	50–80 [100, 101] 50–100 [107]	60–150 [99, 101]	150–250 [100, 102]	150–180 [102]	200–500 [101, 102] 200–350 [107]	16–33 [100] 20–70 [108]	2.5–15 [102] 2–10 [107]	0.2–2.5 [102]	—	—
Power density (W/l)	0.5–1.5 [104, 109]	1000–2000 [102, 104]	0.5–2 [100, 101]	10–400 [100, 101]	150–300 [99]	150–230 [100, 102]	220–300 [102]	500–2000 [102]	0.5–2 [108]	500–5000 [102]	1000–4000 [102]	—	—
Round trip efficiency (%)	75–85 [99], 65–87 [100, 102] 70–85 [105]	93–95 [99] 90–95 [105] 90–93 [109]	70–89 [99] 50–89 [100, 101] 70–79 [109]	70–90 [99] 75–80 [100]	60–65 [99] 85–90 [100]	85–90 [99] 80–90 [100, 102]	85–90 [102]	85–90 [100, 102] ~90–97 [104]	85–90 [100] 75–82 [109]	90–95 [100, 102] 95–98 [109]	95–98 [100, 102] 95 [109]	35–40 [91]	14–18 [91]
Discharge time (ms-hr)	1–24 hr+ [99, 100, 102, 105]	Ms–15 min [99, 102, 105]	1–24 hr+ [99, 100, 102]	Sec-hr [99–101]	Sec-hrs [100]	Sec-hr [99, 100, 102]	Sec–h [102]	Min–hr [99, 100, 102]	Sec-10 hrs [100]	Ms–hr [99]	Ms–8 sec [99]	12+ [91]	1–24+ [101]
Response time (ms-h)	sec-min [99] min [104, 105] 1-2 min [100]	<4 ms-sec [99], sec [105]	1–15 min [99], 1-2 min [100]	5–10 ms [99], sec [100]	20 ms-sec [99], sec [100]	1 ms [99]Sec [100]	<sec [108]	20 ms-s [99]	Sec [100]	8 ms [99]	<100 ms [99]	—	—
Lifetime (yr)	40–60 [99, 101, 102, 104]	15 + [99], 15 [100–102]	20–40 [99]	3–15 [99], 5–15 [100, 101]	10–20 [99, 100]	10–15 [99, 100, 102]	10–14 [102]	5–15 [99, 100]	5–10 [100]	20+ [99, 100]	20+ [99, 100]	—	—
Daily self discharge (%)	Very small [100, 104] 0.00 [110]	100 [101] 24–100 [110]	Small [101, 104] 0.00 [110]	0.1–0.3 [100, 101] 0.033–1.10 [110]	0.2–0.6 [100, 101] 0.07–0.71 [110]	20 [100, 102, 110]	11.89–26.25 [110]	0.1–0.3 [100, 101] 0.03–0.33 [110]	Small [100]	20–40 [99, 100] 0.46–40 [110]	10–15 [99, 100] 1–15 [110]	0 [91]	0.05–1 [101]
Power cost $ (kW)	2000–4300 [99] 600–2000 [100, 102] 500–2000 [105]	250–350 [99, 100, 102] 271–380 [111]	400–1000 [99] 400–800 [102] 1411–1628 [111]	300–600 [99, 101] 200–300 [100] 326–651 [111]	500–1500 [99]	1000–3000 [99, 101, 102], 380–3256 [111]	150–300 [102]	900–4000 [99] 10200–4000 [100, 101] 1303–4342 [111]	600–1500 [100] 651–1628 [111]	100–450 [99] 271–480 [111]	200–489 [99] 200–300 [101] 217–326 [111]	540–4809 [91]	—
Energy cost $ (kWh)	5–100 [99–101, 109] 1–291.20 [110] 217–271 [111]	1000–14,000 [99] 500–1000 [100] 1000–5000 [101, 102]200–150,000 [110] 1085–5427 [111]	2–120 [99] 2–50 [101] 1–140 [110] 217–271 [111]	200–400 [99, 101, 110] 120–150 [100] 50–1100 [110] 54–337 [111]	400–2400 [99] 800–1500 [104] 330–3500 [110]	300–500 [99, 101] 150–900 [110] 326–543 [111]	100–200 [102] 100–345 [110]	600–3800 [99] 300–1300 [100] 2000–4000 [110] 651–2714 [111]	150–1000 [100] 100–2000 [110] 190–1085 [111]	300–2000 [99] 100–94,000 [110]	1000–10,000 [101] 5000–1,080,000 [110] 1085–10854 [111]	2–15 [91]	—
Environmental impact	High/medium [99–101, 110]	Very low [99–101, 110]	Medium/low [99–101, 110]	High [100, 101, 110]	High [100, 110]	High [100, 110]	Medium/low [110]	Medium/low [100, 110]	Medium/low [100, 110]	Very low [100, 110]	Low [100, 110]	—	—
Specific power (W/kg)	—	—	—	75–300 [91] 180 [106]		150–230 [91] 150–240 [106]	150–200 [91] 174 [106]	150–315 [91] 500–2000 [106]	80–150 [106]	~100,000 [91]	—	—	—
Specific energy (Wh/kg)	0.5–1.5 [101]	10–30 [101] 5–80 [91]	30–60 [101]	35–50 [91] 30–50 [101]	50–75 [101] 45–80 [91]	175 [91] 150–240 [101]	70–90 [91]	75–200 [101] 120–200 [91]	25–35 [91] 10–30 [101]	0.05–5 [91]	—	400–1000 [91]	80–200 [101]
Technology maturity	Very mature/fully commercialized [99, 104, 105, 110]	Mature/commercializing [100, 102, 104, 105, 110]	Proven/ commercializing [100, 110]	Very mature/fully commercialized [104, 105, 110]	Very mature/ fully commercialized [99, 100, 110]	Proven/ commercializing [99, 100, 110]	Proven/ commercializing [102, 110]	Proven/ commercializing [99, 100]	Proven/ commercializing [100, 110]	Proven/ commercializing [99, 110]	Proven/ commercializing [99, 110]	Proven [106]	Proven [106]

Table 8: Major power electronic unit providers for commissioned utility BESS [121].

PE provider	Battery technology	DC-DC stage	Power/energy (MW/MWh)	AC/DC voltage (V)		Topology	Module power level
				V_{AC}	V_{DC}		
ABB	Li-ion	No	20/6.67	415–690	975–1200	2L/3L	72 kW–1 MW
Parker SSD	Li-ion	No	12/4	400–480	720–1200	2L/3L	1.2–2.2 MW
Dyna power	Li-ion	—	11/4.4	—	750–1150	2L/3L	1 MVA
Mitsubishi	Li-ion	—	20/6.33	300	—	2L/3L	0.5 MW
Enercon	Li-ion	Yes	10/10	—	—	2L/3L	300 kW
Nidec	NaS	Yes	12/96	—	—	2L	1.2–2.5 MW
General electric	Lead acid	—	21/14	480	431–850	2L/3L	1.25 MW
S and C electric	Lead acid	Yes	10/0.14	480	460–800	2L/3L	1 MW/1.25 MVA
Extreme power	Advanced lead acid	—	10/7.5	480	750–1200	2L	1.5 MVA
Younicos	Advanced lead acid	—	36/24	415–690	975–1200	2L/3L	250 kVA

Table 9: Potentials and constraints of various DVR topologies.

Location of filter	Inverter side	Higher-order current harmonics are eliminated before entering the injected transformer. The fundamental component consists of voltage drop and phase shift. Influence the control system in the DVR.
	Line side	The control system in the DVR is not affected. Less efficient than inverter side connected filter.
Injection transformer (IT)	Without IT	Minimizing the size, weight, and cost. Saturation and inrush current issues are not present. Not recommended for high voltage applications.
	With IT	The voltage rating of the inverter is proportional to the turn ratio of the transformer. Preferable for high voltage applications. Downstream fault current protection of the transformer is difficult. Saturation and inrush current issues are present in the transformer. Requires high-frequency transformer. Efficiency is relatively poor.
Energy storage (ES)	Without ES	Cost-effective. Small and modular design. Suited for strong electrical grids. The burden on the grid is more and hard to control.
	With ES	Better performance. Less burden on the grid. Easy to control. High cost. When the energy stored is lost, the capability of compensation reduced.

then DVR comes into protected mode. Once it detects voltage disturbance, then the DVR comes into active mode and generates the magnitude and phase angle of the reference voltage in the reference generation unit by using a suitable compensation technique (explained in a further subsection) and is injected through the converter. This information is computed by using different phase-locked loops (PLLs).

Figure 20 depicts a rotating DQ reference frame controller. The error signal and change in error signal drive the PI controller, which analyses the input and generates controller output. The PWM receives the controller output as a reference voltage. The inverter is controlled by the pulses generated by the PWM pulse generator. The magnitude and phase angle of the reference voltage are generated using a correction approach and are fed into the multilayer inverter. This data are derived using phase-locked loops (PLLs).

Many papers [138] have recently introduced a variety of PLL schemes such as the synchronous reference frame PLL (SRF-PLL) [139, 140], the dual second-order generalized integrator PLL (DSOGI-PLL) [141], the double synchronous reference frame PLL (DSRF-PLL) [142], and the enhanced PLL (EPLL) [143]. Table 10 illustrates the comparison between the strong and weak sides of the selected PLL algorithms.

For reference generation, the coordinate transformation (Park and Clark) method [144], the symmetric component estimation method [145], and the instantaneous power theory (PQR) method [146] are used. The converter is controlled either by an open-loop (feed-forward) controller or a closed-loop (feedback) controller [147]. In open-loop control, the generated voltage reference is straightly given as a reference to the PWM. However, in the closed loop, the generated reference voltage is fed to the controllers such as passive-based controller [148], two degrees of freedom

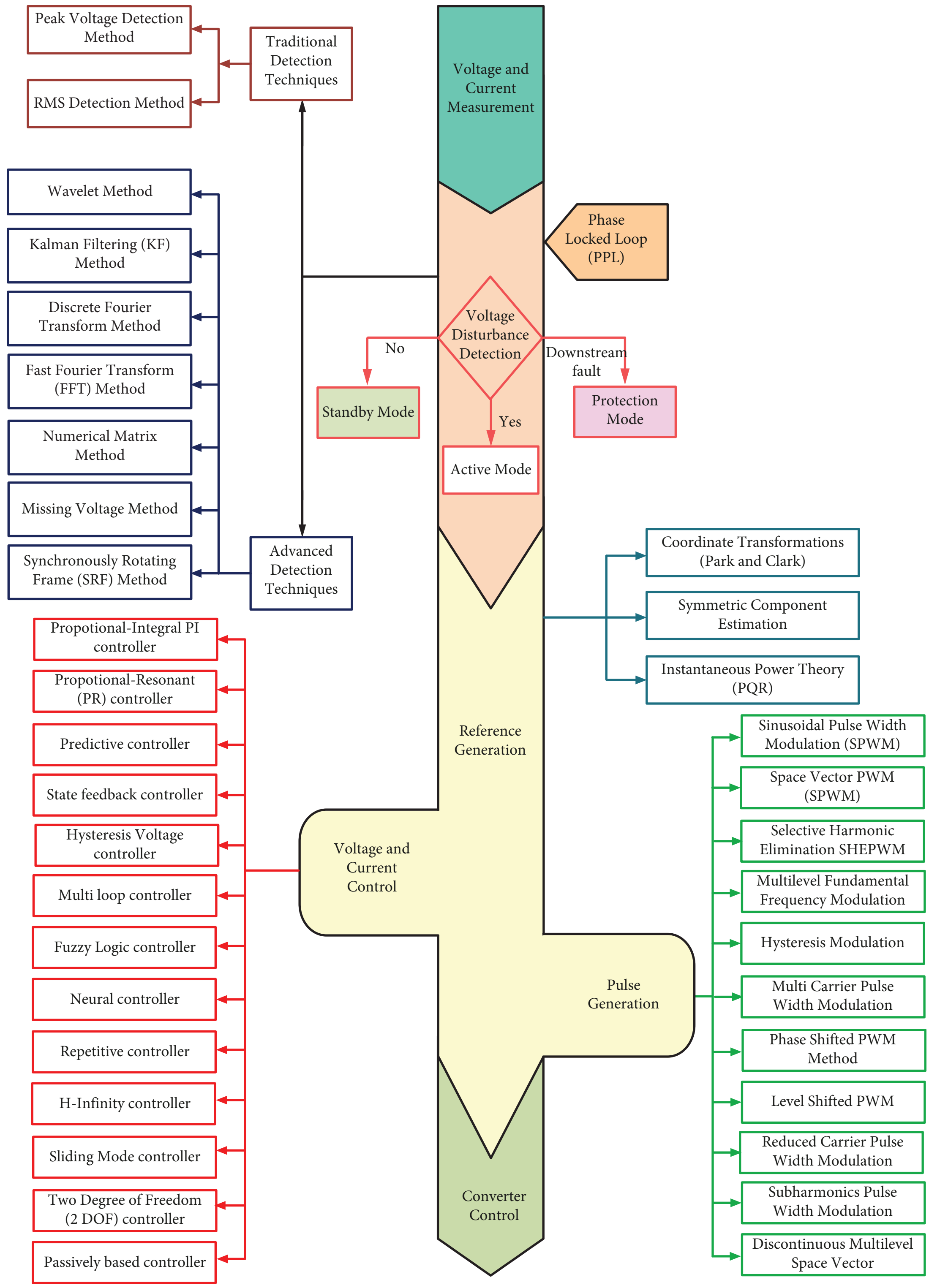

FIGURE 19: Different techniques at various stages in the control strategy of DVR.

(2DOF) [149], sliding mode [150], H-infinity [151], repetitive [152], neural [153], fuzzy logic [154], multiloop [88], hysteresis voltage [155], state feedback [156], predictive [157], and proportional-resonant (PR) [133]. The controller output is given as a reference voltage to the PWM. The operation of the controller is controlled by the pulses generated by the PWM pulse generator. Sinusoidal PWM [158], space vector PWM (SVPWM) [159], multilevel fundamental frequency [160], selective harmonic elimination (SHEPWM) [161], hysteresis modulation [162], multicarrier

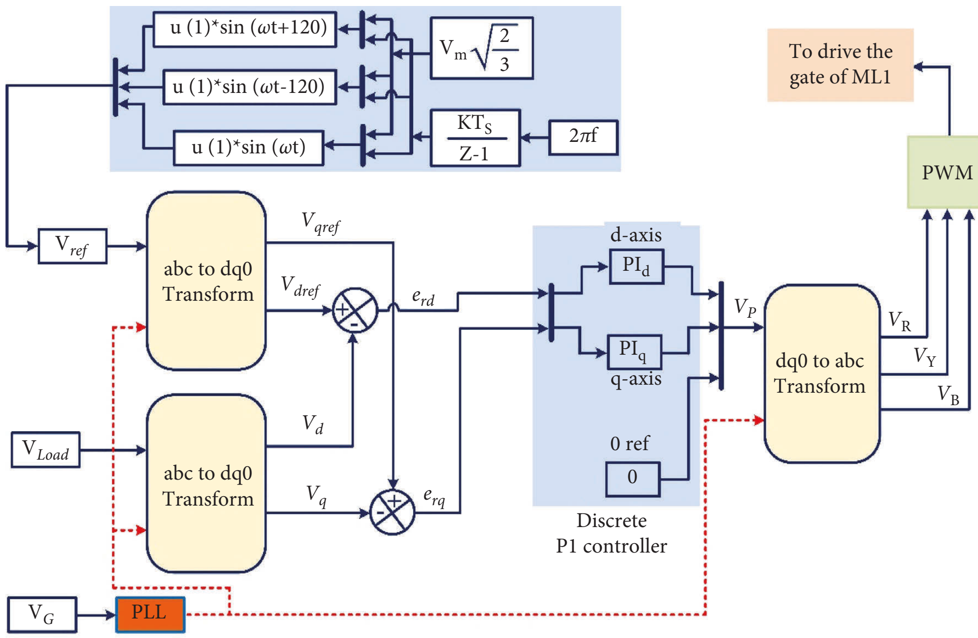

FIGURE 20: Rotating DQ reference frame controller.

TABLE 10: PLL synchronization schemes and performance comparisons.

PLL methods	SRF-PLL	DSOGI-PLL	DSRF-PLL	EPLL
Advantages	(i) Easy implementation (ii) Computational burden is less (iii) DC offset (iv) Fast dynamic response (v) Stability	(i) Fast dynamic response (ii) Unbalanced voltage (iii) Phase jumping (iv) Variations and rise in frequency (v) Stability (vi) DC offset	(i) Harmonics (ii) Unbalanced voltage (iii) Stability (iv) DC offset (v) Computational burden is less (vi) Load rising (vii) Phase jumping	(i) Harmonics (ii) Stability (iii) Phase jumping (iv) DC offset
Limitations	(i) Voltage unbalances (ii) Phase jump (iii) Frequency rising and overshoot (iv) Load rising (v) Harmonics	(i) Load rising (ii) Average implementation (iii) Harmonic (iv) Computational burden is high (v) Simplicity	(i) Frequency rising and overshoot (ii) Simplicity (iii) Average implementation	(i) The dynamic response is slow (ii) Frequency rising and variations (iii) Load rising (iv) Average implementation (v) Simplicity (vi) Voltage unbalances

PWM [163], phase-shifted PWM [164], level-shifted PWM [165], reduced carrier PWM [166], subharmonics PWM [167], and discontinuous multilevel space vector modulation [168] are the various modulation techniques used to generate the pulses. Table 11 represents the comparison of different linear controllers, and Table 12 represents the comparison of different control strategies used in grid-connected three-phase four-leg inverters.

4.1. Compensation Techniques Used in DVR. The required DVR output voltage is achieved by using a suitable compensating technique. The selection of compensation strategy depends on the reference produced by the reference generation unit because it influences the phase-locked loop (PLL), which leads to a key task in synchronization of grid voltage. Hence, by using the proper compensation technique, the PLL output is controlled. Different compensation strategies are presented in Figure 21.

4.1.1. Presag Compensation (PSC). In this strategy load voltage is maintained with the presag voltage; therefore, no voltage disturbance is sensed by the load because the load voltage is having the same magnitude and phase angle [66]; hence, it is also known as the voltage quality optimized technique. The vector representation of PSC is shown in Figure 22. During sag, the DVR is controlled by adding more

Table 11: Comparison of various linear controllers.

Parameter	Feedback	Feedforward
Stability	Can be unstable	Good
Response time	Medium and controllable	Fast and depends on the system
Measures	Load side voltage	Grid side voltage
Transient overshoot	Controllable	Not easy to control
Steady-state error	Can be eliminated	High
Switching harmonics	Penetrate the control	Do not penetrate the control
Compensation of asymmetrical fault	Good	Possible but slow
Compensation of DVR generated voltage	Can be reduced	Difficult to control

**Composite controller measures the load side voltage for feedback and grid voltage for feedforward, and the response time of it has a strength of both feedforward and feedback.

Table 12: Comparison of different control strategies.

Reference	Reference frame	Control technique		Modulation
		Voltage control	Current control	
[169]	*abc* frame	PR	*P*	SPWM
[170]		Repetitive	—	3D SVPWM
[171]		Hysteresis	—	Hysteresis
[172, 173]		*P* + resonant	—	—
[174–176]		Predictive	—	—
[177]		Sliding mode	—	3D SVPWM
[178]	Stationary frame	PR and PI	*P*	SPWM
[179]		PR	—	
[180, 181]		PR	PR	
[182]		PR	*P*	
[183]	dqo frame and stationary frame	Integral	—	3D SVPWM
[184]	dqo frame	PI	*P*	SPWM
[185, 186]		PI	PI	
[187]		PID and PD	—	
[188, 189]		PI	PI	3D SVPWM
[190]		PI	PI	
[191]		PI and resonant	—	
[192]		State feedback	—	
[193]		Pole-placement	—	—

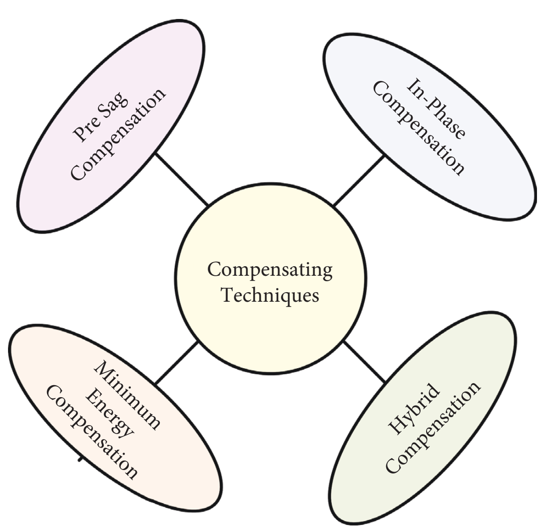

Figure 21: Classification of DVR compensation techniques.

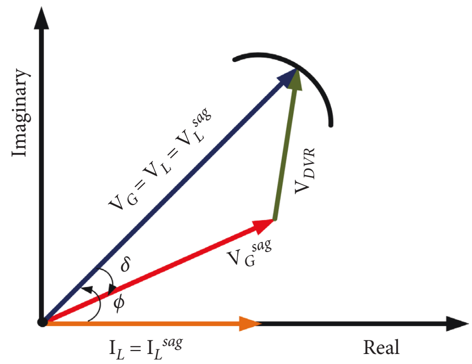

Figure 22: Presag compensation technique.

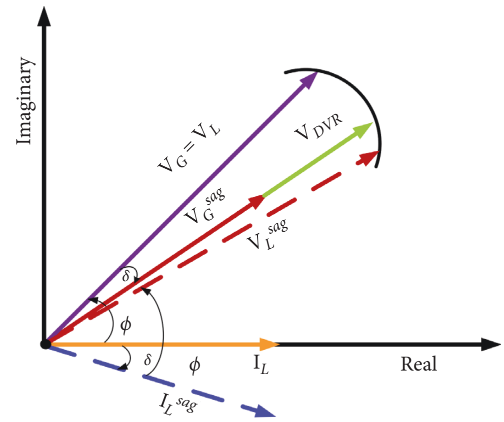

Figure 23: In-phase compensation technique.

real power which affects the rating of direct energy storage or energy received from the grid; hence, the requirement of energy source to supply active power will increase apart from reactive power injected by the inverter. It is acceptable for both balanced and unbalanced sensitive loads heaving phase jump or not. (3) gives the magnitude of $V_{\mathrm{DVR},}$ and the phase angle of V_{DVR} is obtained from equation (4).

$$V_{\mathrm{DVR},p} = \sqrt{2}\sqrt{\left(V_L\right)^2 + \left(V_G^{Sag}\right)^2 - \left(2V_L V_{G,p}^{Sag}\cos\left(\delta_p\right)\right)}, \quad (3)$$

$$\llcorner V_{\mathrm{DVR},p} = \tan^{-1}\left(\frac{V_L \sin\phi - V_{G,p}^{Sag}\sin\left(\phi - \delta_p\right)}{V_L\cos\phi - V_{G,p}^{Sag}\cos\left(\phi - \delta_p\right)}\right), \quad (4)$$

where V_{DVR} is the DVR injected voltage, ϕ is the phase angle between V_L and I_L, V_G^{Sag} is the grid voltage at sag, δ is the corresponding angle of phase jump to V_G^{Sag}, and p is the corresponding phase of the supply voltage (a, b, or c).

4.1.2. In-Phase Compensation (IPC). If any disturbance in the supply voltage concerning the magnitude, then DVR restores the same voltage in phase with the supply voltage [194]; hence, it is known as voltage amplitude optimized control. The vector representation of IPC is shown in Figure 23. This technique reduces the requirements of supplying real power but is unable to compensate for the phase angle of load voltage which may cause harm to some sensitive loads. The injected voltage V_{DVR} is given by

$$V_{\mathrm{DVR},p} = \sqrt{2}\left|V_L - V_{G,p}^{Sag}\right|. \quad (5)$$

4.1.3. Minimum Energy Compensation (MEC). DVR voltage is controlled by adding voltage at 90° to the load current [195]. The vector representation of MEC is shown in Figure 24. This technique minimizes the capacity of energy storage by drawing more real power from the grid, and this minimization is inversely proportional to the sag depth. Equations (6) and (7) represent the magnitude and phase angle of $V_{\mathrm{DVR},}$ respectively.

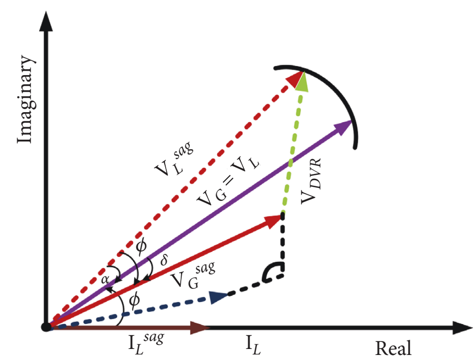

Figure 24: Minimum energy compensation technique.

$$V_{\mathrm{DVR},p} = \sqrt{2}\sqrt{\left(V_L\right)^2 + \left(V_G^{Sag}\right)^2 - \left(2V_L V_{G,p}^{Sag}\cos\left(\delta_p + \alpha\right)\right)}, \quad (6)$$

$$\llcorner V_{\mathrm{DVR},p} = \tan^{-1}\left(\frac{V_L \sin(\phi + \alpha) - V_{G,p}^{Sag}\sin\left(\phi - \delta_p\right)}{V_L\cos(\phi + \alpha) - V_{G,p}^{Sag}\cos\left(\phi - \delta_p\right)}\right), \quad (7)$$

where α is a shifted phase angle between V_{DVR} and $I_{L.}$

4.1.4. Hybrid Compensation. The benefits of previous compensation techniques are mixed to develop a hybrid compensation technique. This technique avoids a large DC-link capacitor [146]. In the proposed compensation strategy in [196], first, the load voltage restores via the PSC strategy and catches a transition to the MEC strategy. Figure 25 shows the transformation between presag to in-phase compensation. In the beginning, the presag technique is applied to compensate for the voltage sag as shown in Figure 25(a). Once the DC-link voltage reaches a specific point, then it starts to change the compensation strategy, and the systematic synchronization of grid voltage was carried out by phase look loop (PLL) as shown in Figures 25(b) and 25(c). In this way, the phase angle is gradually changed, till it is in phase with the grid voltage as shown in Figure 25(d). The mapping of different compensation techniques used for

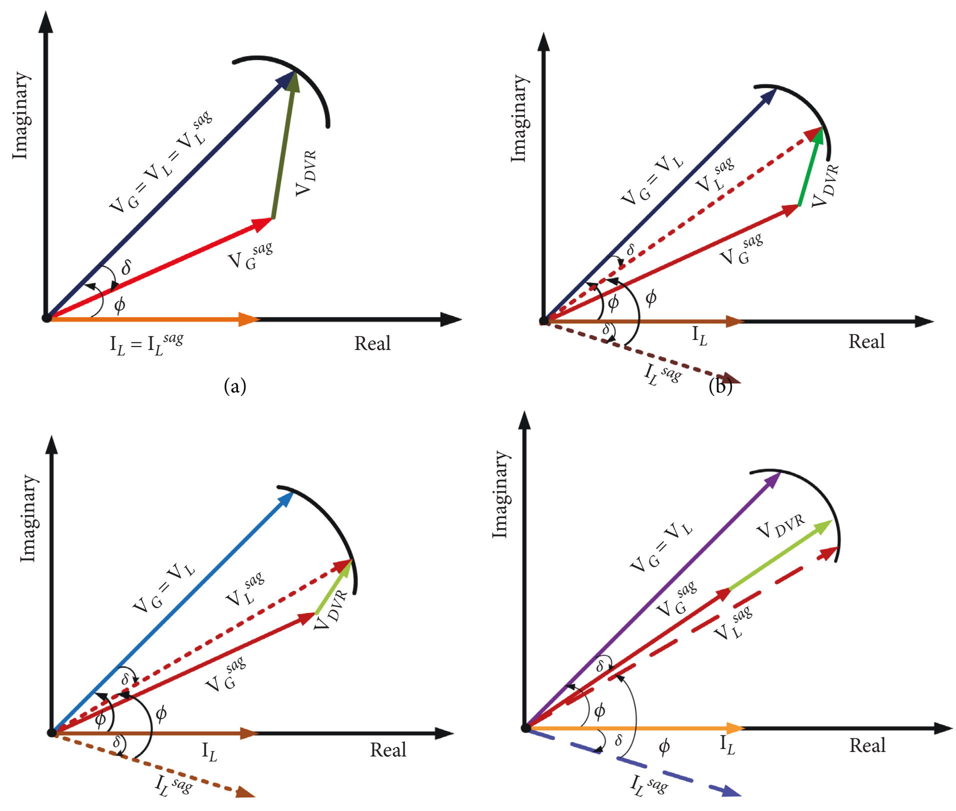

FIGURE 25: Hybrid compensation technique: (a) presag compensation, (b, c) change from presag to in-phase, and (d) in-phase compensation.

various applications is shown in Figure 26, and Table 13 compares the performance of several compensating strategies.

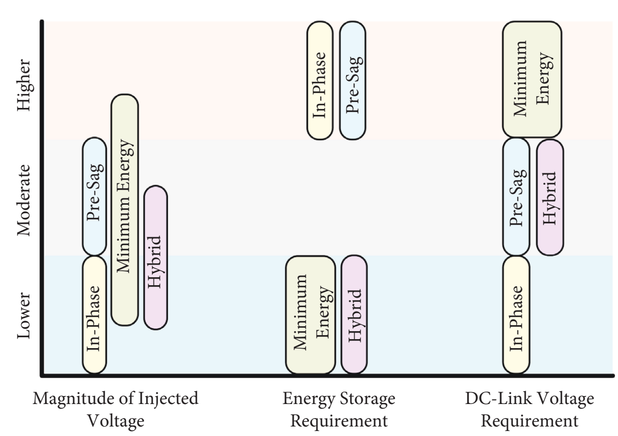

FIGURE 26: Mapping of compensation strategies.

5. Inverter Topologies

In many industrial applications, MLIs have found their extensive influence such as UPFC, drives with high power and medium voltage, DSTATCOM, electric vehicles (EV), active power filters, DVR, microgrid, grid integrated or standalone photovoltaic (PV) systems, and numerous other fields [197]. Because of the power and voltage rating limits on power-semiconductor devices, two-level voltage sources (VSIs) were mostly limited to low voltage and medium power applications. Furthermore, these pulse width (PWM) inverters have been affected by excessive switching losses caused by high-frequency switching. These constraints motivated the introduction of a multilevel inverter (MLI), which generates many voltage levels on the inverter output using a variety of voltage sources, capacitors, and power semiconductor devices [198]. To keep MLIs economical for grid-connected renewable energy applications, current advancements in MLIs have focused on reducing switch counts, gate driver circuits, and DC supply, as well as improving the quality of power and fault-tolerant capability [199].

Depending on supply DVR is classified into single phase and three phase. Based on the inverter, each one is again divided into different topologies, and they are shown in Figure 27. Half-bridge inverters [200] and H-bridge (full-bridge) inverters [201] are familiar inverter topologies in single-phase DVR. Besides that, numerous multilevel inverters, matrix converters, and impedance-fed inverters [202] are used for both single and three-

Table 13: Comparison of various compensation techniques.

Parameters	IPC	PSC	MEC
Load recommended	Linear	Nonlinear	Linear
Regains	Only magnitude of voltage and not phase angle jump	Both magnitude and phase angle jump of voltage	Only magnitude of voltage and not phase angle jump
Device ratings	Storage devices and injection transformers require minimum ratings	Storage devices and injection transformers require higher ratings	Required high-rated inverter
PLL performance at load condition	PLL must be synced with source voltage, and hence, it will not be locked during compensating	PLL must be synced with source voltage, PLL will be locked, and the phase angle will be restored as quickly as feasible if the failure occurs	PLL must be synced with source voltage, hence it will not be locked during compensating
Power requirement	Real and reactive power	Real and reactive power	Only reactive power
Distortion	Distortion is not minimized by phase jump	The method causes the lowest distortion	—
The magnitude of the injected voltage	Minimum	Maximum	Very high in comparison with other methods
Reliability	Causes transient and circulating current	Reliable for the protection of sensitive loads without transient or circulating current	Undesirable phase shifts are present during voltage sag compensation
Outcomes	Voltage disturbance is not fully eliminated	The voltage disturbance is eliminated although the phase angle jumps are different in every phase	Voltage disturbance is not fully eliminated
Compensation strength	Balanced and unbalanced voltage sag	Balanced and unbalanced voltage sag	—

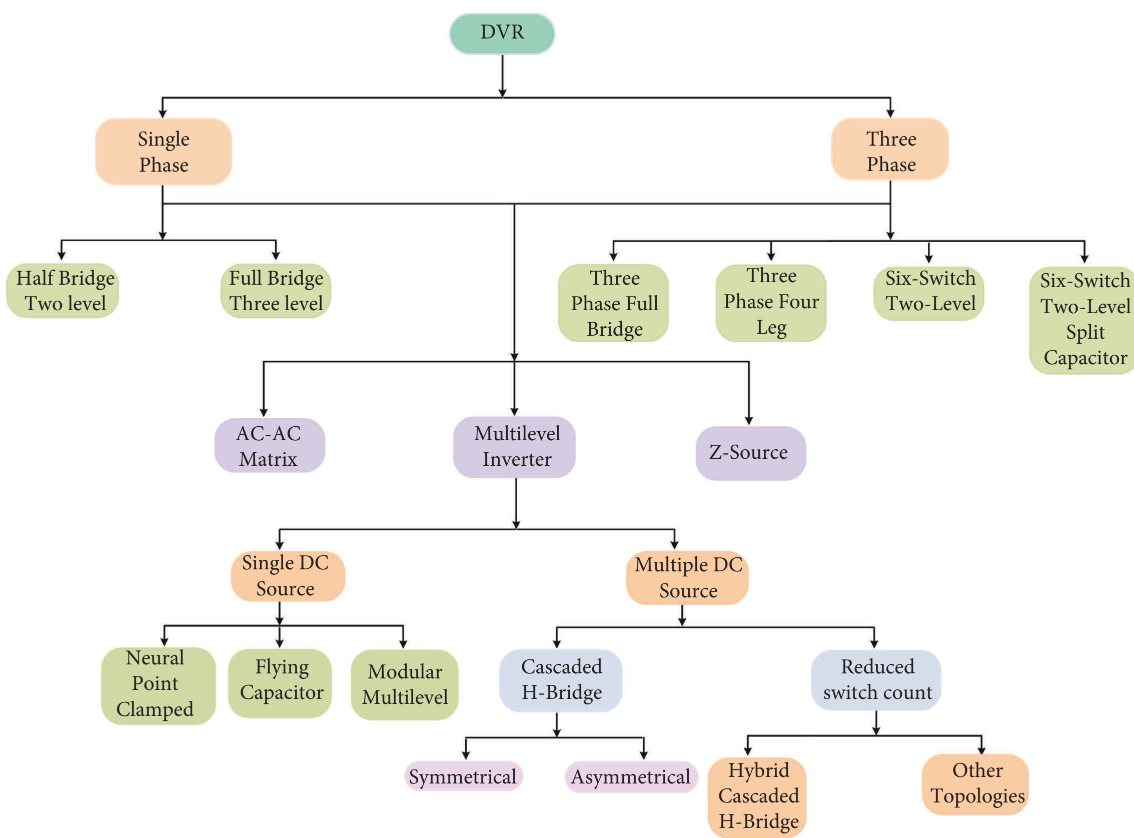

Figure 27: Different inverter topologies in DVR.

phase DVRs. AC-AC converter-based DVRs [78, 203] are used to mitigate the PQ problems without a DC-link capacitor as shown in Figure 28. However, during voltage sag, AC-AC converters draw huge current from the grid. Thus, these are not suitable for long-duration voltage sag mitigation in weak grids. For deep voltage sag, Z-source

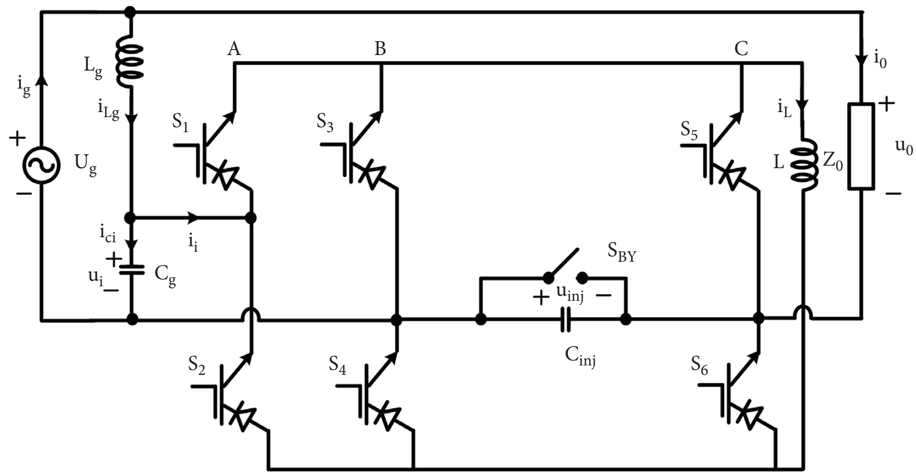

Figure 28: AC-AC converter-based DVR [78].

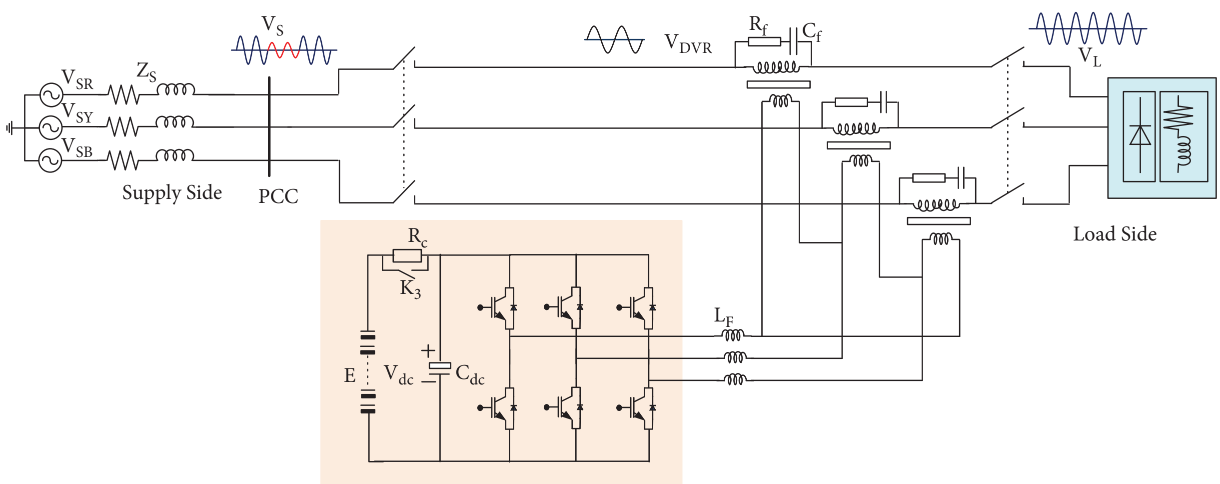

Figure 29: $3-\phi$ full-bridge inverter-based DVR [205].

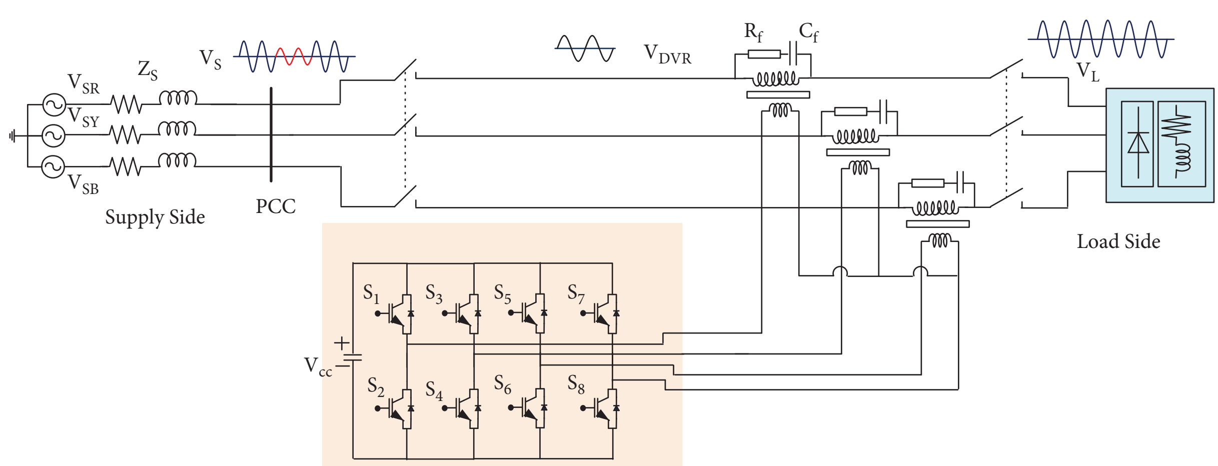

Figure 30: $3-\phi$ four leg inverter [206].

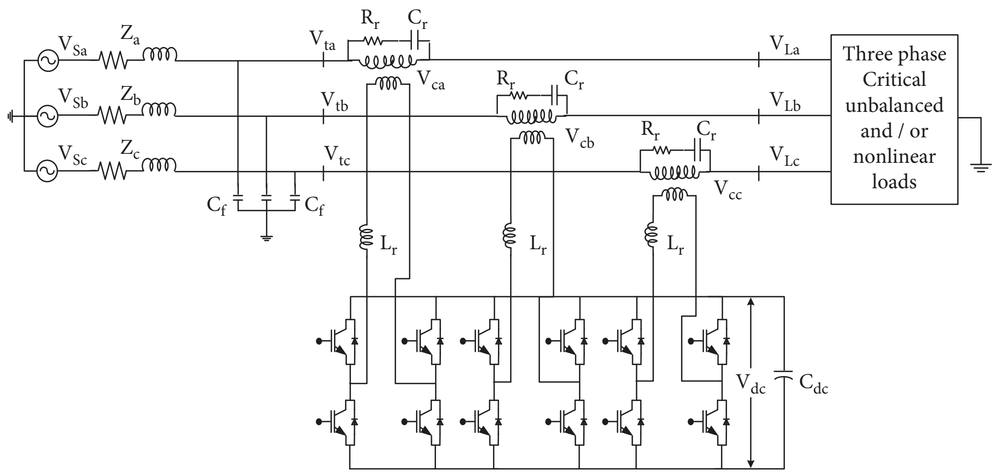

Figure 31: $3-\phi$ six-switch two-level inverter-based DVR [207].

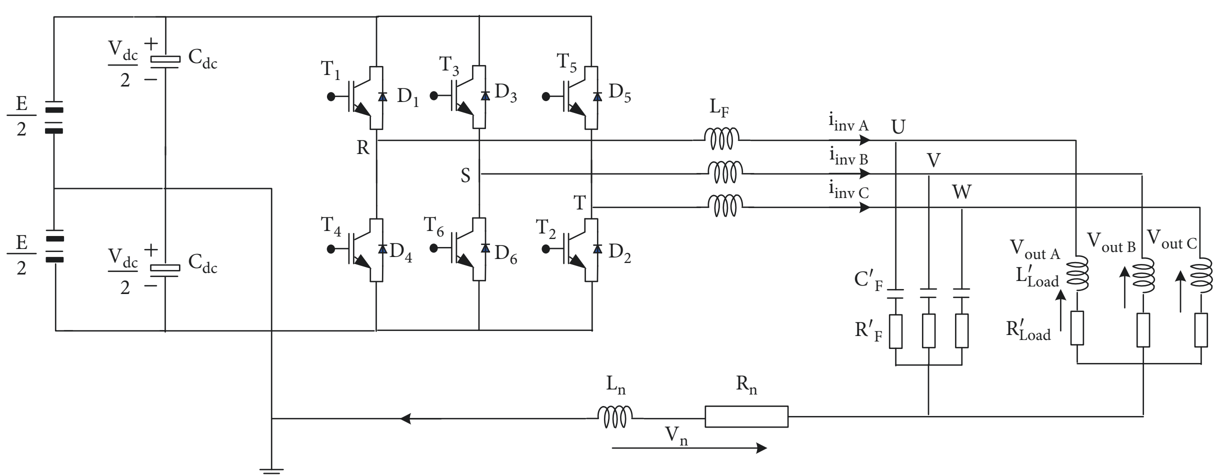

Figure 32: $3-\phi$ six-switch split capacitor inverter-based DVR [208].

Table 14: Merits and demerits of various inverter topologies in DVR.

Ref. no.	Inverter topology	Strengths	Weaknesses
[200]	$1-\phi$ half-bridge inverter	The switch count is reduced and it is quite inexpensive	The harmonic content of the output voltage is high
[201]	$1-\phi$ full bridge inverter	Preferably for high voltage systems	Quite high harmonic content
[205]	$3-\phi$ full bridge inverter	Smooth control and cheap	dv/dt stress is higher, resulting in electromagnetic interference
[206]	$3-\phi$ four-leg inverter	The DC-link capacitor balancing problem does not exist	Additionally, two more switches are required
[207]	$3-\phi$ six switch inverter	The requirement for power semiconductor devices is less, with simple topology	Compensation for unbalanced voltages is difficult
[208]	$3-\phi$ split capacitor six switches four-wire inverter	Able to compensate for unbalanced voltages	DC-link capacitor balancing will face input/output voltage ratio issues
[203]	AC-AC converter	Variable and constant energy sources are not required	Lower efficiency for heavy sag in the substandard grid
[204]	Z-source inverter	Capable to supply the voltage for lower DC-link during deep voltage sag	A number of LC elements are required and shoot through the problem

Table 15: Comparison of various two-level inverter topologies in DVR.

Ref. no.	Inverter topology	Energy storage	Injection transformer	Compensation technique	Capabilities	No. of levels	Modulation technique
[10]	VSI inverter	Capacitor	Present	—	Only sag	2	PWM
[80]	VSI inverter	Constant source	Present	—	Only sag	2	Space vector PWM
[134]	VSI inverter	Electrolytic capacitors	Present	PSC	Only sag	2	PWM
[200]	$1-\phi$ half-bridge inverter	Capacitor	Not present	—	Only sag	2	PWM
[201]	$1-\phi$ full bridge inverter	Constant source	Present	—	Both	2	PWM
[205]	$3-\phi$ three wire inverter	Lead-acid batteries	Present	PSC to IPC	Only sag	2	Voltage space vector PWM
[206]	$3-\phi$ four-leg inverter	Constant source	Not present	—	Only sag	2	—
[207]	$3-\phi$ six-switch inverter	Capacitor	Present	—	Only sag	2	—
[208]	$3-\phi$ split capacitor six switch four wire inverter	Lead-acid batteries	Present	PSC to IPC	Only sag	2	Voltage space vector projection method
[209]	VSI inverter	Capacitor	Present	—	Only sag	2	PWM
[210]	VSI inverter	Constant source	Present	MEC	Only sag	2	PWM
[211]	$3-\phi$ three-wire	Lead-acid batteries	Present	PSC to IPC	Only sag	2	Space vector PWM
[212]	$3-\phi$ half-bridge inverter	Constant source	Present	PSC	Only sag	2	PWM
[213]	VSI inverter	Constant source	Present	PSC and IPC	Both	2	Space vector PWM

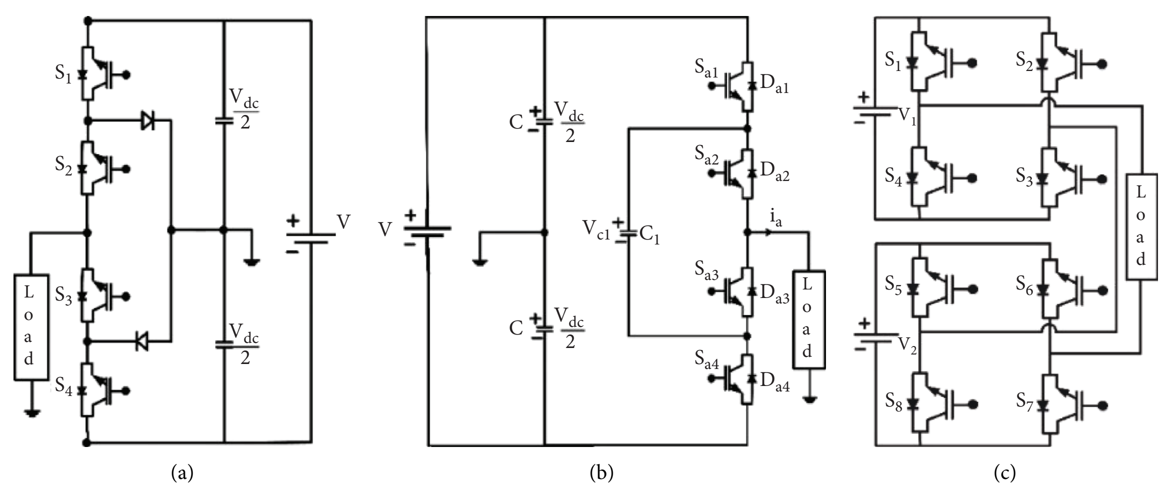

Figure 33: Classical multilevel inverter topologies [198]. (a) NPC. (b) FC. (c) CHB.

converter-based DVR with less DC-link voltage was presented in [204], although it requires more storage elements and also suffers from shoot-through.

Full-bridge, four-leg, six-switch, and six-switch split capacitor topologies are the most common traditional inverter topologies used in three-phase DVR. In [205], the authors implemented a DVR by using a three-phase full-bridge PWM voltage-source inverter supplied by lead-acid batteries for real power support as shown in Figure 29; the DVR can compensate the voltage swells/sags using the voltage-space-vector PWM (VSVPWM) approach and the software phase-locked loop (SPLL), thus keeping the load voltages at 1.0 p.u. A 4-leg VSC-based DVR shown in Figure 30; the DVR provides closed-loop control for producing unbalanced 3-phase voltages with a zero-sequence component, and the DVR's response during voltage sags is instant, with less than 8 ms delay. The extraction of sequence components accounts for the majority of the time delay [206].

Six-switch two-level voltage-source inverter-based DVR with a common DC capacitor (C_{dc}) shown in Figure 31 was proposed in [207]. In this topology, to safeguard unbalanced

Table 16: Quantitative and qualitative comparison of classical MLI topologies.

Indices		NPC MLI	FC MLI	CHB MLI	
				Symmetric	Asymmetric
Quantitative	N_{sw}	$2(N_{lel}-1)$	$2(N_{lel}-1)$	$2(N_{lel}-1)$	$4(\log_2(N_{lel}+1)-1)$
	N_{so}	1	1	$(N_{lel}-1)/2$	$\log_2(N_{lel}+1)-1$
	N_{dc}	$(N_{lel}-1)$	$(N_{lel}-1)$	0	0
	N_{cd}	$(N_{lel}-1) * (N_{lel}-2)$	0	0	0
	N_{cc}	0	$(N_{lel}-1) * (N_{lel}-2)/2$	0	0
	V_{block}	$2(N_{lel}-1)V$	$2(N_{lel}-1)V$	$2(N_{lel}-1)V$	$4(2^{N_{so}-1})V$
Qualitative	Complexity	Low	High	Medium	High
	Redundancy	Line	Phase and line	Phase	None
	Modularity	Yes	Yes	Yes	None
	Structure	Bulky	Bulky	Light	Light
	Source/switch utilization	Poor	Good	Good	Poor
	Fault tolerance	Medium	High	High	Low
	Cost	Low	High	Medium	Medium
Features		Switches are exposed to less voltage stress than, a single DC source	Fault-tolerant, modularity, single dc source, and natural charge balancing	Fewer components needed, fault-tolerant, modular, reliable, symmetric, and asymmetric structure	
Limitations		Uneven blocking voltage across diodes	More switching losses, high clamping capacitors needed, and unbalanced voltage between clamping capacitors	Required more isolated dc supplies, lack of modularity due to asymmetry, and increases the components requirement	
Applications		FACTS, DSTATCOM, UPFC, active filter, and low switching frequency applications	High switching frequency and high-velocity MV drive applications	HEVs, EVs, stand-alone PV systems, active filter, grid integrated PV, and WECS	

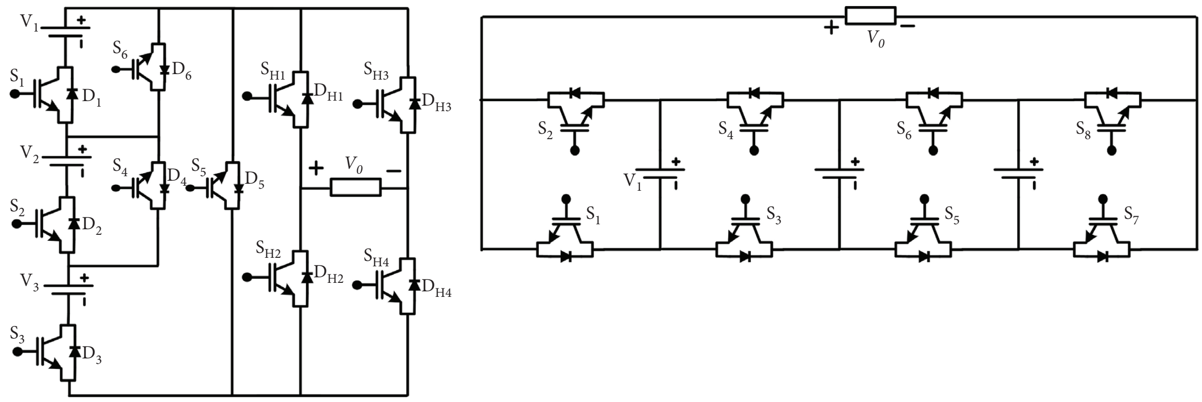

(a) (b)

Figure 34: Reduced components topologies (a) with H-bridge [219]and (b) without H-bridge [197].

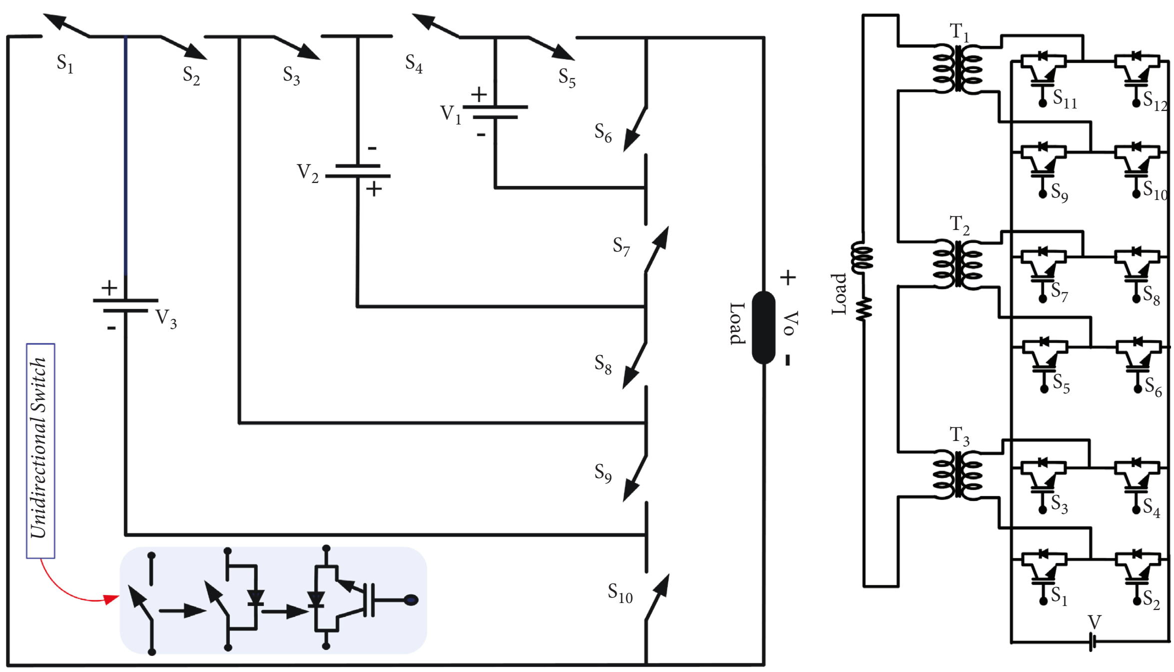

(a) (b)

Figure 35: Miscellaneous hybrid topologies: (a) MV/HV and high-power applications [256] and (b) LV supply from standalone PV arrays [258].

and nonlinear loads, a simple generalized technique for generating instantaneous reference compensating voltages for managing self-supported DVR based on basic SRFT was devised. A fundamental positive-sequence extractor has been suggested, which extracts three fundamental positive-sequence phase voltages from just two unbalanced and/or distorted line voltages. A six-switch split capacitor shown in Figure 32 was implemented in [208]; here, a 3-D voltage space vector PWM algorithm has been implemented for the control of the three-phase four-wire inverter, and the positive, negative, and zero sequence components of the terminal voltages were controlled instantaneously. A DVR with a three-phase split capacitor inverter was studied, which can inject three distinct voltages in series with the main circuit to maintain the voltage waveform at the sensitive load. Usually, two-level voltage source inverter-based DVR [201–207] is suitable for low voltage. Merits and demerits of various inverter designs of DVR are reported in Table 14, and a comparison of various conventional two-level inverter topologies of DVR is tabulated in Table 15.

However, for higher power, two-level voltage source inverters are not suitable because the switches will block large voltage, and more dv/dt creates electromagnetic interference; to get better from these issues, multilevel inverter (MLI) is the best option. The benefits of MLIs are lower output voltage step, high power quality, fewer switching

Table 17: Comparison of various hybrid MLI topologies.

Topology			N_{SW}	N_{Lel}	N_{So}	N_d	N_C	TSV	PIV	Findings
With H-bridge	Symmetric	[221]	$(N_{lel}+1)$	$6(n+3)$	$(N_{lel}-1)/2$	—	—	$23(N_{lel}-45)/6$	$(N_{lel}-1)/2$	Features: reduced components, modularity, both symmetric and asymmetric, low cost, space and losses, and multilevel DC-link. Demerits: bidirectional and variety switches required, not suitable for MV applications, complex switching, and no fundamental switching operation. Applications: PV stand-alone, fuel cells, EVs, grid-tied PV systems, and LV applications.
		[222]	$2(N_{lel}-1)$	$2n+1$	$(N_{lel}-1)/2$	—	—	$2(N_{lel}-1)$	$(N_{lel}-1)/2$	
		[223]	$2(N_{lel}-1)$	$2n+1$	$(N_{lel}-1)/2$	—	—	$2(N_{lel}-1)$	$(N_{lel}-1)/2$	
		[224]	$2(N_{lel}-1)$	$2n+1$	$(N_{lel}-1)/2$	—	—	$2(N_{lel}-1)$	$(N_{lel}-1)/2$	
		[225]	$(N_{lel}+3)$	$2n+1$	$(N_{lel}-1)/2$	—	—	$3(N_{lel}-1)$	$(N_{lel}-1)/2$	
		[226]	$(N_{lel}+3)$	$4n+1$	$(N_{lel}-1)/4$	—	—	$2(N_{lel}-1)$	$(N_{lel}-1)/2$	
		[227]	$3(N_{lel}+5)/2$	$4n+1$	$(N_{lel}-1)/2$	—	—	$3.5(N_{lel}-1)$	$(N_{lel}-1)/2$	
		[228]	$3(N_{lel}-1)/2$	$4n+1$	$(N_{lel}-1)/2$	—	—	$2(N_{lel}-1)$	$(N_{lel}-1)/2$	
		[229]	$2(N_{lel}+3)/3$	$6n+3$	$(N_{lel}-1)/2$	—	—	$3(N_{lel})-4$	$(N_{lel}-1)/2$	
		[230]	$(N_{lel}+9)/2$	$2n+1$	$(N_{lel}-1)/2$	$(N_{lel}-1)/2$	—	$3(N_{lel})-4$	$(N_{lel}-1)/2$	
		[231]	$2(N_{lel}+11)/3$	$6n+1$	1	—	$2(N_{lel}+3)/3$	$8(N_{lel}+4)/3$	$(N_{lel}-1)/2$	
		[232]	$(N_{lel}+5)/2$	$2n+3$	$(N_{lel}-1)/2$	$(N_{lel}-3)/2$	—	$(5N_{lel}-7)/2$	$(N_{lel}-1)/2$	
	Asymmetric	[233]	$4m$	3^m	m	—	—	$2(3^m-1)$	$(3^m-1)/2$	
		[226]	$4(m+1)$	$2(3^m)-1$	m	—	$2m$	$3(3^m-1)$	$(3^m-1)/2$	
		[227]	$3m+4$	$2(3^{m/2})-1$	m	—	—	$2(3^{(m+2)/2}-2)$	$(3^{m/2}-1)$	
		[234]	$2m+4$	3^m	m	—	—	$3(3^m-1)$	$(3^m-1)/2$	
		[235]	$m+4$	3^m	m	m	—	$2.5(3^m-1)$	$(3^m-1)/2$	
		[236]	$2m+4$	3^m	m	—	—	$3(3^m-1)$	$(3^m-1)/2$	
		[237]	$(5m+13)/3$	$3^{(m}+^{2)/3}$	m	-	-	$19(3^{(m-1)/3})-15$	$1.5(3^{(m-1)/3})-1$	
		[238]	$6m$	$2(3^m)-1$	m	m	m	$5(3^m-1)$	(3^m-1)	
Without H-bridge	Symmetric	[239]	$(N_{lel}+1)$	$2n+1$	$(N_{lel}-1)/2$	—	—	$2(N_{lel}-1)$	$(N_{lel}-1)/2$	Features: reduced switch count, symmetric and asymmetric, low losses, less size and cost, and self-balancing of dc bus. Demerits: asymmetric mode requires a large number of switches, dc sources, diodes, less fault-tolerant, has uneven power loss, and poor semiconductor utilization. Applications: MV/HV, UPS, FACTS, stand-alone PV, and RES.
		[240]	$3(N_{lel}-1)/2$	$4n+1$	$(N_{lel}-1)/2$	$2(N_{lel}-1)$	—	$5(N_{lel}-1)/2$	$(N_{lel}-1)$	
		[241]	$7(N_{lel}-1)/8$	$8n+1$	$3(N_{lel}-1)/8$	$(N_{lel}-1)/2$	—	$13(N_{lel}-1)/16$	$11(N_{lel}-1)/8$	
	Asymmetric	[242]	$3(N_{lel}-1)/2$	$2n+1$	$(N_{lel}-1)/2$	—	—	$3(N_{lel}-1)$	$2(N_{lel}-1)$	
		[243]	$5(N_{lel}-1)/6$	$12n+1$	$(N_{lel}-1)/3$	—	—	$5(N_{lel}-1)/3$	$5(N_{lel}-1)/12$	
		[244]	$3(N_{lel}-1)/4$	$16n+1$	$(N_{lel}-1)/4$	—	—	$5(N_{lel}-1)/2$	$(N_{lel}-1)/2$	
		[245]	$(N_{lel}+11)/2$	$2n+1$	$(N_{lel}-1)/2$	$(N_{lel}-1)/2$	—	$9(N_{lel}-1)/4$	$(N_{lel}-3)/2$	
		[246]	$(N_{lel}+1)$	$2n+5$	$(N_{lel}-1)/2$	—	—	$3N_{lel}-7$	$(N_{lel}-1)$	
		[247]	$(N_{lel}+5)$	$4n+1$	1	—	$(N_{lel}+3)/2$	$(N_{lel}+9)/4$	1	
Miscellaneous hybrid		[249]	$3(N_{lel}-1)/4$	$16n+1$	$(N_{lel}-1)/8$	—	$(N_{lel}-1)/4$	$(N_{lel}-1)/30$	$(N_{lel}-1)/2$	Features: high efficiency and reliability, reduced switches, asymmetric, and fundamental frequency modulation. Demerits: complex due to capacitors and transformers. Applications: MV/HV and stand-alone PV.
		[250]	$3(N_{lel}-1)/4$	$16n+1$	$(N_{lel}-1)/16$	$(N_{lel}-1)/8$	$(N_{lel}-2)/5$	$5(N_{lel}-2)/3$	$(N_{lel}-1)/4$	
		[251]	$5(N_{lel}-1)/4$	$8n+1$	$(N_{lel}-1)/4$	-	$(N_{lel}-1)/4$	$(N_{lel}-1)$	—	
		[256]	$(N_{lel}-1)/2$	$10n+1$	$(N_{lel})/7$	—	—	$(N_{lel}-1)/5$	—	

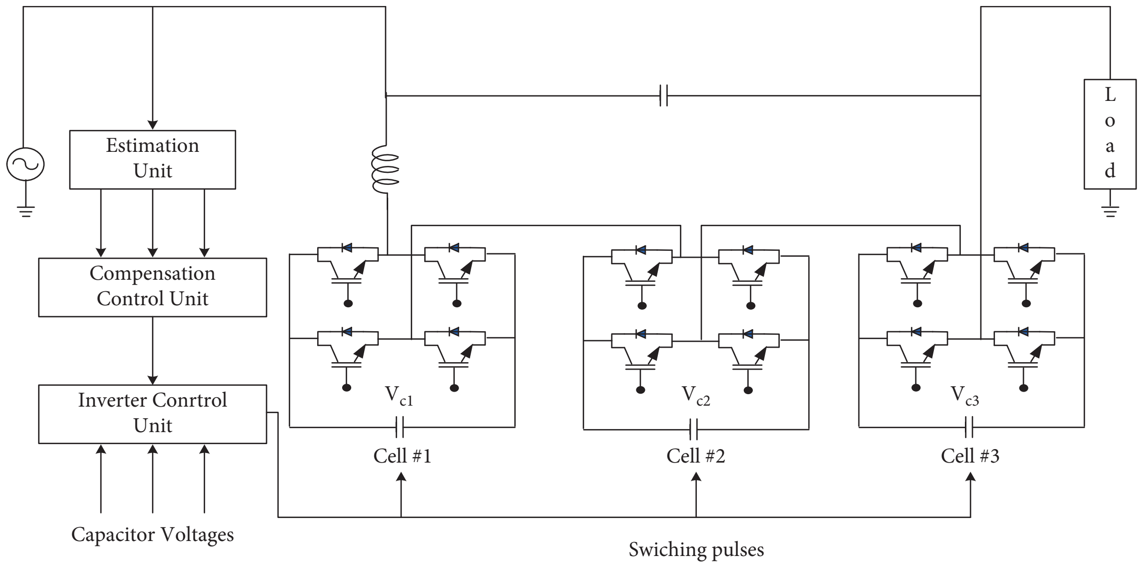

FIGURE 36: DVR with a cascaded H-bridge multilevel converter [144].

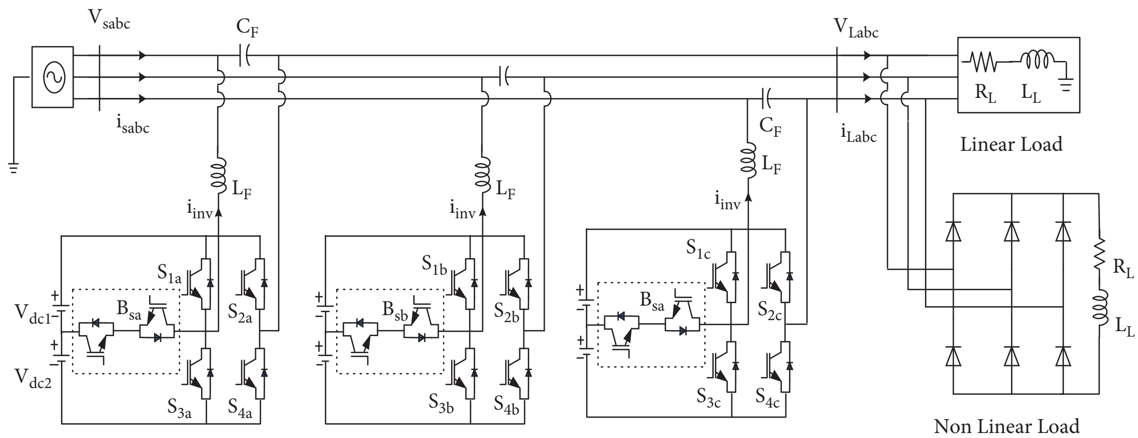

FIGURE 37: Reduced switch count (T-type) MLI-based DVR [263].

losses, minimum harmonics, and better electromagnetic compatibility.

MLIs are useful for high-voltage applications due to their capacity to synthesize output-voltage waveforms with an expanded harmonic spectrum and achieve a higher voltage with a limited maximum device rating. A multilevel output can be produced by properly arranging power-switching semiconductive devices and voltage sources. MLIs are classified into two types: classical MLIs and recent hybrid MLIs.

5.1. Classical Multilevel Inverter Topologies. Conventional MLI topologies are commonly employed in a wide range of manufacturing and grid-connected renewable energy systems. Classical topologies are popular because they have a modular structure, are easy to manage, have low harmonic distortion, are fault-tolerant, and have low switching losses. The familiar classical multilevel inverter topologies are diode-clamped (or) neutral-point clamped (NPC), flying capacitor (FC), and cascaded H-bridge (CHB) inverters shown in Figure 33. Certain performance metrics and terms used often in MLIs are as follows: N_{sw} is the switch count, N_{so} is DC sources, N_{lel} is the number of voltage levels, N_{cc} is clamping capacitors count, N_d is the diode count, N_{cd} is the count of clamping diodes, N_{dc} is the number of DC-link capacitors, V_{blk} is the total blocking voltage, PIV is the peak inverse voltage, and TSV is the total standing voltage of MLI. Table 16 presents quantitative and qualitative comparisons between classical MLI topologies. All these topologies have their positives and difficulties. Capacitor voltage balancing is difficult when the voltage level increases in the case of diode-clamped MLI; hence, these are restricted to three levels. However, most of the industries use three-level NPC inverter. Flying capacitor MLI requires more DC capacitors for higher voltage levels. However, there is flexibility to set the switching combinations feasible for

Table 18: Comparison of various multilevel inverter topologies in DVR.

Ref. no.	Inverter topology	Energy storage	Injection transformer	Compensation technique	Compensation capabilities	Switches/ phase	No. of levels	Modulation technique	THD
[77]	Buck-boost AC/AC converter	Without DC-link	Not present	IPC	Both	5	5	Pulse width modulation	—
[78]	Three leg AC/AC converter	Without DC-link	Not present	IPC	Both	6	—	High frequency PWM	2.02
[203]	Direct AC–AC converter	Without DC-link	Present	PSC	Only sag	4	—		—
[163]	Diode clamped	Constant source	Present	—	Only sag	24	5	Multicarrier PWM	—
[164]	Flying-capacitor	Constant source	Present	—	Only sag	24	5	Phase shifted PWM	—
[144]	CHB MLI	DC-link	Present	Zero energy	Only sag	24	13	Pulse width modulation	—
[261]	CHB MLI	DC-link	Not present	MEC	Only sag	8	7	Phase shift PWM	—
[160]	CHB MLI	Constant source	Present	—	Only sag	16	9	Fundamental frequency modulation	2.8
[165]	$3-\phi$ phase inverters	Constant source	Present	—	Only sag	—	5	Level shifted PWM	—
[263]	T-type MLI	Without DC-link	Not present	IPC	Both	8	5	Reduced carrier PWM	2.77
[264]	CHB MLI	Constant source	Present	MEC	Only sag	12	7	Phase shifted carrier based PWM	—
[159]	$3-\phi$ phase six switch inverter	Constant source	Present	IPC	Both	-	3	Space vector PWM	—
[265]	CHB MLI	DC-link	Present	Hybrid	Only sag	12	7	Phase shift PWM	—
[157]	CHB MLI	DC-link	Present	Positive and negative sequence	Only sag	40	-	Carrier phase shifting sine Wave PWM	1.94
[266]	CHB MLI	DC-link	Not present	Hybrid	Both	16	9	Multicarrier PWM	—
[259]	TCHB MLI	DC-link	Present	IPC, PSC	Only sag	5	5	Pulse width modulation	4.78
[168]	CHB MLI	DC-link	Not present	Postsag	Only sag	—	17	Discontinuous multilevel space vector modulation	—
[260]	Simplified four level inverter	DC-link	Not present	—	Only sag	8	7	—	1.23
[267]	CHB MLI	Constant source	Present	MEC	Only sag	12	7	Phase shifted carrier PWM	1.73
[158]	HB MLI	DC-link	Present	Hybrid	Only sag	—	—	SPWM	
[268]	CHB MLI	Constant source	Not present	—	Only sag	20	11	—	—
[269]	RC MLI	Constant source	Present	PSC	Only sag	12	23	Nearest level voltage control	1.28

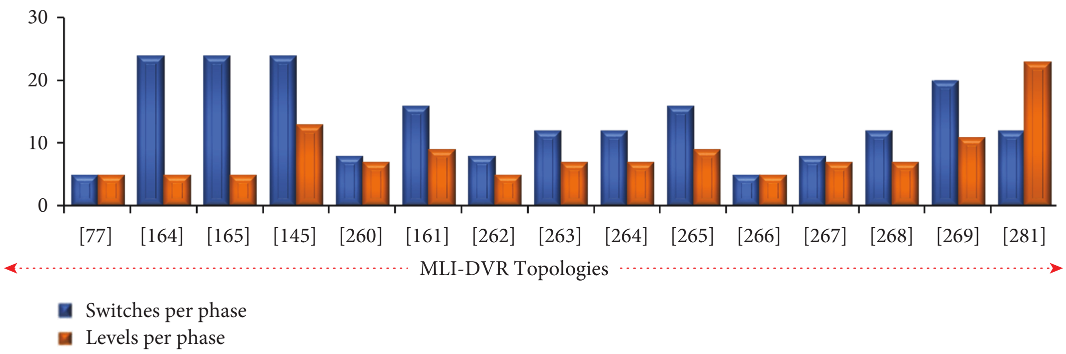

Figure 38: Comparisons of various MLI-based DVR topologies.

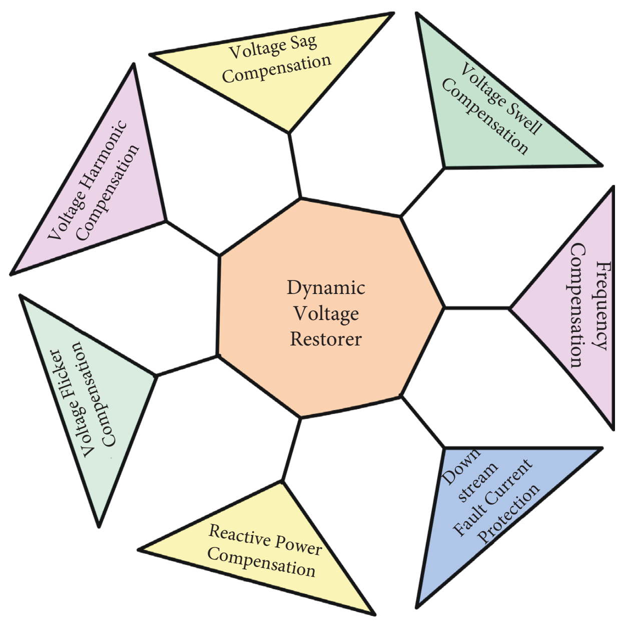

Figure 39: Functions of DVR.

DC capacitor voltage balance [164]. Due to its modularity characteristic, CHB MLI topology becomes more reliable and popular. However, each bridge needs an isolated DC source, and for higher levels, the requirement for switches also increases [144].

5.2. Hybrid MLI Topologies. Recently, many hybrid topologies have been proposed by researchers mainly emerging from conventional topologies to attain power quality issues and high grid code standards economically [214–220]. Recent hybrid MLI topologies are mainly classified into reduced components with H-bridge topologies [221–238]; they have separate blocks for polarity and level generation and are best suited for LV applications, as shown in Figure 34(a). Reduced components without H-bridge topologies [239–247], capable of generating bipolar waveform, consisting of several unit cells connecting in serial, are mainly used in medium voltage (MV) applications, as shown in Figure 34(b). Miscellaneous hybrid topologies are primarily designed for high power and MV/HV applications [248–257], as shown in Figure 35(a), whereas, some other topologies [258] use variable turn ratio transformers to generate more voltage levels while improving the LV supply from fuel cells, and standalone PV arrays are as shown in Figure 35(b). In MV grid-connected power systems, traditional topologies are still commonly employed. However, the worsening penetration and compliance with power quality and the high grid code standards measures of renewable power systems have led scientists to invent new RC topologies for MVs and high-power applications in modern times. In these topologies, there is no separate H-bridge to create polarity; other benefits include modularity, fault tolerance, high reliability, and reduced space requirements. The comparison of various hybrid MLI topologies is presented in Table 17.

In [77], a new DVR topology based on a buck-boost AC/AC converter was proposed. It contains five bidirectional switches, an inductor, and a capacitor, and the topology's most notable feature is the lack of an injection transformer,

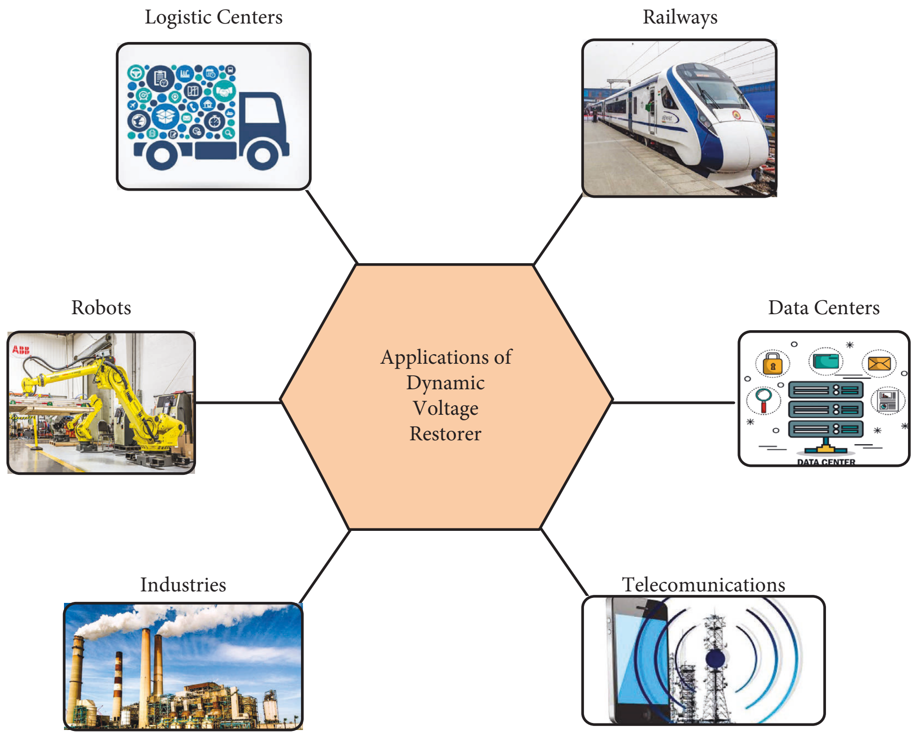

Figure 40: Applications of DVR.

allowing for a direct connection to the grid without the need for storage elements. As a result, as compared to conventional topologies, this topology has less physical volume, mass, and cost. A DVR with a cascaded H-bridge multilevel converter was proposed in [144] that could connect directly to the MV network without the use of an injection transformer as shown in Figure 36. The voltage restoration is achieved by the capacitors as energy storage using the zero active power compensation technique.

DVR with five levels reduced the number of power circuit components. TCHB inverter [259] was used to mitigate the voltage sag using two voltage compensation schemes, in-phase and presag compensation. In [260], the authors proposed an S4L inverter-based DVR with a single DC power source and reduced switch count; thus, it is more cost-effective. Furthermore, it generates seven levels, which greatly aids in the reduction of the system's harmonic problem. Interline DVR with a CHB multilevel inverter was proposed by Shahabadini et al. [261] to mitigate the voltage sag with better THD. An adjustable DC-link connected MLI-based DVR is suggested in [160] , which is suitable for compensation of both long- and short-period sag. DVR with an open-end winding transformer having reduced inverter loss and lower harmonics is proposed in [165]. A cascaded OEW transformer-based DVR is reported in [262] with better voltage levels and reduced THD even though it does not require extraclamping diodes. The number of switches required for n-level voltage in conventional MLI is $N_{sw} = 2(n - 1)$. For a definite voltage level, these topologies require a high number of switches; thus, the required gate drivers, size, and cost are increased. To overcome these, a T-type MLI-based DVR is proposed for medium- and high-power applications in [263] which is shown in Figure 37, and a comparison of various multilevel inverter topologies in DVR is tabulated in Table 18. A comparison of various multilevel inverter topologies in DVR is shown in Figure 38.

In addition to mitigating the sag and swelling, the DVR can execute other functions such as compensation of selective voltage harmonics [86, 270, 271], mitigation of voltage flickers [272–274], reactive power compensation [275], and frequency compensation [276]. Protection of the DVR [277] is very important during the fault at the load side of the DVR; otherwise, the same downstream fault current is present in the DVR, and it may damage the DVR. This protection is achieved by making an alternative path for the fault current through breakers, thyristors, and varistors. However, other proposals [85, 270, 278–280] also actively limit the downstream fault current. Various functions and applications of DVR are presented in Figures 39 and 40, respectively.

6. Conclusions and Future Scope

A systematic review of different types of DVR systems and the future scope of the relevant literature are discussed in this article. Studies reviewing the DVR include many areas, but specifically, power quality issues, energy-storage topology, absence of energy, and controlled strategies are covered in this paper. DVR configurations based on power converters and control units at different stages are described in detail based on the latest literature. In the orientation towards the integration of renewable energy sources, certain updated and upgraded DVR configurations are also presented. This review supports the selection of the best, most cost-effective, and high-performance DVR configuration based on the requirements of researchers and scientists working on this prospective research [281].

Future research could be conducted in several areas of the literature. The following are some essential considerations; however, they are not exhaustive:

(i) The efficiency of the DVR circuit is limited by VSI, filter, and transformer losses. The buck nature of the VSI output voltage necessitates the use of a boost converter between the energy storage and the inverter, which adds more switches, controls, and complexity. By using a multilevel inverter in place of VSI partly or entirely, the need for filters can be eliminated, resulting in fewer switching losses. This allows us to increase DVR's efficiency, LVRT capacity, cost performance, deep sag/swell compensation, reliability, and harmonic compensation.

(ii) The depth of the sag and duration of the sag determines the storage capacity. If there is a long-term sag, the energy storage capacity declines and the DVR's compensating property gets reduced. The strategy used during the detection stage unit may be modified, particularly when it comes to deep/long voltage sags/swells to the extent that the detection process is highly reliable.

(iii) DG and DVR integration has gained popularity due to its reliable features. Future research should take into account the integration of DVR with microgrids and smart grids which will improve power quality for the end-users.

Data Availability

No data were used to support this study.

Conflicts of Interest

The authors declare that they have no conflicts of interest.

References

[1] S. Santoso, M. F. McGranaghan, R. C. Dugan, and H. Wayne Beaty, *Electrical Power Systems Quality*, McGraw-Hill Education, New York, USA, 2012.

[2] A. Baggini, *Handbook of Power Quality*, John Wiley & Sons, Hoboken, New Jersey, USA, 2008.

[3] M. H. J. Bollen, "Understanding power quality problems," in *Voltage Sags and Interruptions*IEEE press, New York, USA, 2000.

[4] A. Kusko, *Power Quality in Electrical Systems*, McGraw-Hill Education, New York, USA, 2007.

[5] W. E. Brumsickle, R. S. Schneider, G. A. Luckjiff, D. M. Divan, and M McGranaghan, "Dynamic sag correctors: cost-effective industrial power line conditioning," *IEEE Transactions on Industry Applications*, vol. 37, no. 1, pp. 212–217, 2001.

[6] A. Moreno-Muñoz, *Power Quality: Mitigation Technologies in a Distributed Environment*, Springer Science & Business Media, Berlin, Germany, 2007.

[7] H. Liao and J. V. Milanović, "On capability of different FACTS devices to mitigate a range of power quality phenomena," *IET Generation, Transmission & Distribution*, vol. 11, no. 5, pp. 1202–1211, 2017.

[8] M. F. McGranaghan, D. R. Mueller, and M. J. Samotyj, "Voltage sags in industrial systems," *IEEE Transactions on Industry Applications*, vol. 29, no. 2, pp. 397–403, 1993.

[9] A. Ghosh and G. Ledwich, "Compensation of distribution system voltage using DVR," *IEEE Transactions on Power Delivery*, vol. 17, no. 4, pp. 1030–1036, 2002.

[10] N. H. Woodley, L. Morgan, and A. Sundaram, "Experience with an inverter-based dynamic voltage restorer," *IEEE Transactions on Power Delivery*, vol. 14, no. 3, pp. 1181–1186, 1999.

[11] K. R. Padiyar, *FACTS Controllers in Power Transmission and Distribution*, New Age International (P) Limited, Publishers, Chennai, Tamil Nadu, 2007.

[12] A. Moghassemi and S. Padmanaban, "Dynamic voltage restorer (DVR): a comprehensive review of topologies, power converters, control methods, and modified configurations," *Energies*, vol. 13, no. 16, p. 4152, 2020.

[13] B. P. Babu and V. Indragandhi, "A review on dynamic voltage restorer in power systems concerned to the issues of power quality IOP conference series: materials science and engineering," *IOP Publishing*, vol. 623, no. 1, Article ID 012015, 2019.

[14] J. Praveen, B. P. Muni, S. Venkateshwarlu, and H. V. Makthal, "Review of dynamic voltage restorer for power quality improvement,"vol. 1, pp. 749–754, in *Proceedings of the 30th Annual Conference of IEEE Industrial Electronics Society, 2004. IECON 2004*, vol. 1, pp. 749–754, IEEE, Busan, Korea (South), November 2004.

[15] V. K. Remya, P. Parthiban, and V. Ansal, "Dynamic Voltage Restorer (DVR)–areview," *Journal of Green Engineering*, vol. 8, 2018.

[16] M. Farhadi-Kangarlu, E. Babaei, and F. Blaabjerg, "A comprehensive review of dynamic voltage restorers," *International Journal of Electrical Power & Energy Systems*, vol. 92, pp. 136–155, 2017.

[17] M. A. El-Gammal, A. Y. Abou-Ghazala, and T. I. El-Shennawy, "Fifteen years of the dynamic voltage restorer: a literature review," *Australian Journal of Electrical and Electronics Engineering*, vol. 8, no. 3, pp. 279–287, 2011.

[18] Iea, *Global Energy Review 2021*, IEA, Paris, 2021.

[19] Iea, *Renewable Energy Market Update 2021*, IEA, Paris, 2021.

[20] H. X. Li, D. J. Edwards, M. R. Hosseini, and G. P. Costin, "A review on renewable energy transition in Australia: an updated depiction," *Journal of Cleaner Production*, vol. 242, Article ID 118475, 2020.

[21] A. Battaglini, J. Lilliestam, A. Haas, and A. Patt, "Development of SuperSmart Grids for a more efficient utilisation of electricity from renewable sources," *Journal of Cleaner Production*, vol. 17, no. 10, pp. 911–918, 2009.

[22] A. Q. Al-Shetwi, M. Hannan, K. P. Jern, M. Mansur, T. Mahlia, and T. M. I. Mahlia, "Grid-connected renewable energy sources: review of the recent integration requirements and control methods," *Journal of Cleaner Production*, vol. 253, Article ID 119831, 2020.

[23] T. R. Ayodele, A. Jimoh, J. L. Munda, and J. T. Agee, "Challenges of grid integration of wind power on power system grid integrity: a review," *World*, vol. 3, no. 6, pp. 618–626, 2020.

[24] E. Hossain, M. R. Tur, S. Padmanaban, S. Ay, and I. Khan, "Analysis and mitigation of power quality issues in

distributed generation systems using custom power devices," *IEEE Access*, vol. 6, pp. 16816–16833, 2018.

[25] A. Shetwi, Q. Ali, S. M. Zahim, and R. N. Lina, "A review of the fault ride through requirements in different grid codes concerning penetration of PV system to the electric power network," *ARPN: Journal of Engineering and Applied Sciences*, vol. 10, no. 21, pp. 9906–9912, 2015.

[26] H. Bevrani, H. Golpîra, A. R. Messina, N. Hatziargyriou, F. Milano, and T. Ise, "Power system frequency control: an updated review of current solutions and new challenges," *Electric Power Systems Research*, vol. 194, Article ID 107114, 2021.

[27] M. Sedighizadeh, M. Esmaili, and S. M. Mousavi-Taghiabadi, "Optimal energy and reserve scheduling for power systems considering frequency dynamics, energy storage systems and wind turbines," *Journal of Cleaner Production*, vol. 228, pp. 341–358, 2019.

[28] K. H. Oon, C. K. Tan, A. H. A. Bakar, H. S. Che, H. Mokhlis, and H. A. Illias, "Establishment of fault current characteristics for solar photovoltaic generator considering low voltage ride through and reactive current injection requirement," *Renewable and Sustainable Energy Reviews*, vol. 92, pp. 478–488, 2018.

[29] A. Q. Al-Shetwi, M. Z. Sujod, and F. Blaabjerg, "Low voltage ride-through capability control for single-stage inverter-based grid-connected photovoltaic power plant," *Solar Energy*, vol. 159, pp. 665–681, 2018.

[30] J. I. Y. Ota, T. Sato, H. Akagi, and H. Akagi, "Enhancement of performance, availability, and flexibility of a battery energy storage system based on a modular multilevel cascaded converter (MMCC-SSBC)," *IEEE Transactions on Power Electronics*, vol. 31, no. 4, pp. 2791–2799, 2016.

[31] M. Castilla, J. Miret, A. Camacho, J. Matas, and L. García de Vicuña, "Voltage support control strategies for static synchronous compensators under unbalanced voltage sags," *IEEE Transactions on Industrial Electronics*, vol. 61, no. 2, pp. 808–820, 2014.

[32] L. N. Popavath and P. Kaliannan, "Photovoltaic-STATCOM with low voltage ride through strategy and power quality enhancement in a grid integrated wind-PV system," *Electronics*, vol. 7, no. 4, p. 51, 2018.

[33] A. Q. Al-Shetwi and M. Z. Sujod, "Grid-connected photovoltaic power plants: a review of the recent integration requirements in modern grid codes," *International Journal of Energy Research*, vol. 42, no. 5, pp. 1849–1865, 2018.

[34] V. Gevorgian and S. Booth, "Review of prepa technical requirements for interconnecting wind and solar generation," National Renewable Energy Lab.(NREL), Golden, CO (United States), No. NREL/TP-5D00-57089, 2013.

[35] A. Moghassemi, M. Hosseini, and J. Olamaei, "Power quality improvement of grid-connected photovoltaic systems using Trans-z-source inverter under partial shading condition," *Iranian Journal of Science and Technology, Transactions of Electrical Engineering*, vol. 44, no. 4, pp. 1429–1447, 2020.

[36] R. Madhusudan and G. Ramamohan Rao, "Modeling and simulation of a distribution STATCOM (D-STATCOM) for power quality problems-voltage sag and swell based on Sinusoidal Pulse Width Modulation (SPWM)," in *Proceedings of the IEEE-International Conference On Advances In Engineering, Science And Management (ICAESM-2012)*, pp. 436–441, IEEE, Nagapattinam, India, March 2012.

[37] A. Ghosh and G. Ledwich, *Power Quality Enhancement Using Custom Power Devices*, Springer science & business media, Berlin, Germany, 2012.

[38] Ieee 519, *Recommended Practice and Requirements for Harmonic Control in Electric Power Systems*, IEEE, Piscataway, NJ, USA, 2014.

[39] Iec 61000-3-2, *Electromagnetic Compatibility (EMC)—Part 3-2: Limits—Limits for Harmonic Current Emissions (Equipment Input Current _16 A Per Phase)*, IEC, Geneva, Switzerland, 2018.

[40] Iec Ts 61000-3-4, *Electromagnetic Compatibility (EMC)—Part 3-4: Limits—Limitation of Emission of Harmonic Currents in Low-Voltage Power Supply Systems (Equipment with Rated Current Greater than 16 A)*, IEC, Geneva, Switzerland, 1998.

[41] Ieee P1564, *Guide for Voltage Sag Indices*, IEEE, Piscataway, NJ, USA, 2014.

[42] *IEEE Standard for Interconnecting Distributed Resources with Electric Power Systems_Amendment 1*, pp. 1–16, 2014, IEEE Standard 1547a-2014 (Amendment to IEEE Standard 1547-2003).

[43] Iec 61000-4-15, *Electromagnetic Compatibility (EMC)—Part 4-15: Testing and Measurement Techniques—Flickermeter—Functional and Design Specifications*, IEC, Geneva, Switzerland, 2017.

[44] Ieee 1159, *Recommended Practice for Monitoring Electric Power Quality*, IEEE, Piscataway, NJ, USA, 2019.

[45] Ieee 1250, *Guide for Identifying and Improving Voltage Quality in Power Systems*, IEEE, Piscataway, NJ, USA, 2018.

[46] Ieee P1409, *Draft Guide for the Application of Power Electronics for Power Quality Improvement on Distribution Systems Rated 1 kV through 38 kV*, IEEE, Piscataway, NJ, USA, 2012.

[47] eee 141, "I," *Recommended Practice for Electric Power Distribution for Industrial Plants*, IEEE, Piscataway, NJ, USA, 1986.

[48] Ieee P1547, *Approved Draft Standard Conformance Test Procedures for Equipment Interconnecting Distributed Energy Resources with Electric Power Systems and Associated Interfaces*, IEEE, Piscataway, NJ, USA, 2020.

[49] R. Panigrahi, S. K. Mishra, S. C. Srivastava, A. K. Srivastava, and N. N. Schulz, "Grid integration of small-scale photovoltaic systems in secondary distribution network-a review," *IEEE Transactions on Industry Applications*, vol. 56, no. 3, pp. 3178–3195, 2020.

[50] H. Ibrahim, A. Ilinca, and J. Perron, "Energy storage systems-characteristics and comparisons," *Renewable and Sustainable Energy Reviews*, vol. 12, no. 5, pp. 1221–1250, 2008.

[51] M. Bajaj and A. K. Singh, "Grid integrated renewable DG systems: a review of power quality challenges and state-of-the-art mitigation techniques," *International Journal of Energy Research*, vol. 44, no. 1, pp. 26–69, 2020.

[52] C. Evangelista, P. Puleston, F. Valenciaga, and L. M. Fridman, "Lyapunov-designed super-twisting sliding mode control for wind energy conversion optimization," *IEEE Transactions on Industrial Electronics*, vol. 60, no. 2, pp. 538–545, 2013.

[53] I. Munteanu, S. Bacha, A. Bratcu, J. Guiraud, and D. Roye, "Energy-reliability optimization of wind energy conversion systems by sliding mode control," *IEEE Transactions on Energy Conversion*, vol. 23, no. 3, pp. 975–985, 2008.

[54] J. Zhu, G. Jordan, and S. Ihara, "The market for spinning reserve and its impacts on energy prices,"vol. 2, pp. 1202–1207, in *Proceedings of the 2000 IEEE Power Engineering Society Winter Meeting. Conference Proceedings (Cat. No.*

00CH37077), vol. 2, pp. 1202–1207, IEEE, Singapore, January 2000.
[55] A. Merkhouf, P. Doyon, and S. Upadhyay, "Variable frequency transformer—concept and electromagnetic design evaluation," *IEEE Transactions on Energy Conversion*, vol. 23, no. 4, pp. 989–996, 2008.
[56] R. Hesse, D. Turschner, and H.-P. Beck, "Micro grid stabilization using the virtual synchronous machine (VISMA)," in *Proceedings of the International Conference on Renewable Energies and Power Quality (ICREPQ'09)*, pp. 15–17, Valencia, Spain, April 2009.
[57] J. C. Das, "Passive filters-potentialities and limitations," *IEEE Transactions on Industry Applications*, vol. 40, no. 1, pp. 232–241, 2004.
[58] D. Li, T. Wang, W. Pan, X. Ding, and J. Gong, "A comprehensive review of improving power quality using active power filters," *Electric Power Systems Research*, vol. 199, Article ID 107389, 2021.
[59] R. B. Gonzatti, S. C. Ferreira, C. H. da Silva, R. R. Pereira, L. E. Borges da Silva, and G Lambert-Torres, "Smart impedance: a new wikay to look at hybrid filters," *IEEE Transactions on Smart Grid*, vol. 7, no. 2, pp. 837–846, 2016.
[60] B. Singh, V. Verma, A. Chandra, and K. Al-Haddad, "Hybrid filters for power quality improvement," *IEE Proceedings - Generation, Transmission and Distribution*, vol. 152, no. 3, pp. 365–378, 2005.
[61] H. Khalid and A. Shobole, "Existing developments in adaptive smart grid protection: a review," *Electric Power Systems Research*, vol. 191, Article ID 106901, 2021.
[62] A. Chandra, G. K. Singh, and V. Pant, "Protection of AC microgrid integrated with renewable energy sources–A research review and future trends," *Electric Power Systems Research*, vol. 193, Article ID 107036, 2021.
[63] M. Z. Degefa, I. B. Sperstad, H. Sæle, and S. Hanne, "Comprehensive classifications and characterizations of power system flexibility resources," *Electric Power Systems Research*, vol. 194, Article ID 107022, 2021.
[64] V. Cárdenas, M. A. González-García, and R. Álvarez-Salas, "A dynamic voltage restorer with the functions of voltage restoration, regulation using reactive power, and active filtering," *Electric Power Components and Systems*, vol. 43, no. 14, pp. 1596–1609, 2015.
[65] J. G. Nielsen, *Design and Control of a Dynamic Voltage Restorer*, Institut for Energiteknik, Aalborg Universitet, Aalborg, Denmark, 2002.
[66] J. G. Nielsen, F. Blaabjerg, and N. Mohan, "Control strategies for dynamic voltage restorer compensating voltage sags with phase jump,"vol. 2, pp. 1267–1273, in *Proceedings of the APEC 2001. Sixteenth Annual IEEE Applied Power Electronics Conference And Exposition (Cat. No. 01CH37181)*, vol. 2, pp. 1267–1273, IEEE, Anaheim, CA, USA, March 2001.
[67] L. A. Moran, I. Pastorini, J. Dixon, and R. Wallace, "A fault protection scheme for series active power filters," *IEEE Transactions on Power Electronics*, vol. 14, no. 5, pp. 928–938, 1999.
[68] M. J. Newman and D. G. Holmes, "An integrated approach for the protection of series injection inverters," *IEEE Transactions on Industry Applications*, vol. 38, no. 3, pp. 679–687, 2002.
[69] S. Sasitharan and M. K. Mishra, "Design of passive filter components for switching band controlled DVR," in *Proceedings of the TENCON 2008-2008 IEEE Region 10 Conference*, pp. 1–6, IEEE, Hyderabad, India, November 2008.
[70] H. Kim, J.-H. Kim, and S.-K. Sul, "A design consideration of output filters for dynamic voltage restorers,"vol. 6, pp. 4268–4272, in *Proceedings of the 2004 IEEE 35th Annual Power Electronics Specialists Conference (IEEE Cat. No. 04CH37551)*, vol. 6, pp. 4268–4272, IEEE, Aachen, Germany, June 2004.
[71] G. Chen, M. Zhu, X. Cai, J. Song, Y. Zhou, and C. Ma, "Optimization of the LC filter based on double impact factors for cascaded H-bridge DVR," in *Proceedings of the 2013 IEEE 8th Conference on Industrial Electronics and Applications (ICIEA)*, pp. 1184–1190, IEEE, Melbourne, VIC, Australia, June 2013.
[72] S. S. Choi, B. H. Li, and D. M. Vilathgamuwa, "Design and analysis of the inverter-side filter used in the dynamic voltage restorer," *IEEE Transactions on Power Delivery*, vol. 17, no. 3, pp. 857–864, 2002.
[73] B. H. Li, S. S. Choi, and D. M. Vilathgamuwa, "Design considerations on the line-side filter used in the dynamic voltage restorer," *IEE Proceedings - Generation, Transmission and Distribution*, vol. 148, no. 1, pp. 1–7, 2001.
[74] B. H. Li, S. S. Choi, and D. M. Vilathgamuwa, "Transformerless dynamic voltage restorer," *IEE Proceedings - Generation, Transmission and Distribution*, vol. 149, no. 3, pp. 263–273, 2002.
[75] B.-H. Kwon, G.-Y. Jeong, S.-H. Han, and D.-H. Lee, "Novel line conditioner with voltage up/down capability," *IEEE Transactions on Industrial Electronics*, vol. 49, no. 5, pp. 1110–1119, 2002.
[76] T. B. Soeiro, C. A. Petry, L. A. C. Lopes, and A. J. Perin, "High-efficiency line conditioners with enhanced performance for operation with non-linear loads," *IEEE Transactions on Industrial Electronics*, vol. 59, no. 1, pp. 412–421, 2012.
[77] D. Nazarpour, M. Farzinnia, and H. Nouhi, "Transformerless dynamic voltage restorer based on buck-boost converter," *IET Power Electronics*, vol. 10, no. 13, pp. 1767–1777, 2017.
[78] M. Zhou, Y. Sun, M. Su et al., "Transformer-less dynamic voltage restorer based on a three-leg ac/ac converter," *IET Power Electronics*, vol. 11, no. 13, pp. 2045–2052, 2018.
[79] B. H. Li, S. S. Choi, and D. M. Vilathgamuwa, "On the injection transformer used in the dynamic voltage restorer,"vol. 2, pp. 941–946, in *Proceedings of the PowerCon 2000. 2000 International Conference on Power System Technology. Proceedings (Cat. No. 00EX409)*, vol. 2, pp. 941–946, IEEE, Perth, WA, Australia, December 2000.
[80] C. Fitzer, A. Arulampalam, M. Barnes, and R. Zurowski, "Mitigation of saturation in dynamic voltage restorer connection transformers," *IEEE Transactions on Power Electronics*, vol. 17, no. 6, pp. 1058–1066, 2002.
[81] T. Jimichi, H. Fujita, and H. Akagi, "An approach to eliminating DC magnetic flux from the series transformer of a dynamic voltage restorer," *IEEE Transactions on Industry Applications*, vol. 44, no. 3, pp. 809–816, 2008.
[82] D. A. Fernandes, F. F. Costa, and M. A. Vitorino, "A method for averting saturation from series transformers of dynamic voltage restorers," *IEEE Transactions on Power Delivery*, vol. 29, no. 5, pp. 2239–2247, 2014.
[83] T. Jimichi, H. Fujita, and H. Akagi, "A dynamic voltage restorer equipped with a high-frequency isolated DC–DC converter," *IEEE Transactions on Industry Applications*, vol. 47, no. 1, pp. 169–175, 2011.
[84] G. Venkataramanan, B. K. Johnson, and A. Sundaram, "An AC-AC power converter for custom power applications,"

IEEE Transactions on Power Delivery, vol. 11, no. 3, pp. 1666–1671, 1996.

[85] A. Farooqi, M. M. Othman, M. A. M. Radzi, I. Musirin, S. Z. M. Noor, and I. Z. Abidin, "Dynamic voltage restorer (DVR) enhancement in power quality mitigation with an adverse impact of unsymmetrical faults," *Energy Reports*, vol. 8, pp. 871–882, 2022.

[86] V. Babu, K. S. Ahmed, Y. M. Shuaib, and M. Manikandan, "Power quality enhancement using dynamic voltage restorer (DVR)-Based predictive space vector transformation (PSVT) with proportional resonant (PR)-Controller," *IEEE Access*, vol. 9, pp. 155380–155392, 2021.

[87] M. Ramasamy and S. Thangavel, "Experimental verification of PV based dynamic voltage restorer (PV-DVR) with significant energy conservation," *International Journal of Electrical Power & Energy Systems*, vol. 49, pp. 296–307, 2013.

[88] B. Wang and G. Venkataramanan, "Dynamic voltage restorer utilizing a matrix converter and flywheel energy storage," *IEEE Transactions on Industry Applications*, vol. 45, no. 1, pp. 222–231, 2009.

[89] S. Jothibasu and M. K. Mishra, "A control scheme for storageless DVR based on characterization of voltage sags," *IEEE Transactions on Power Delivery*, vol. 29, no. 5, pp. 2261–2269, 2014.

[90] D. Prasad and C. Dhanamjayulu, "Solar PV integrated dynamic voltage restorer for enhancing the power quality under distorted grid conditions," *Electric Power Systems Research*, vol. 213, Article ID 108746, 2022.

[91] M. M. Rahman, A. O. Oni, E. Gemechu, A. Kumar, and K. Amit, "Assessment of energy storage technologies: a review," *Energy Conversion and Management*, vol. 223, Article ID 113295, 2020.

[92] N. McIlwaine, A. M. Foley, D. J. Morrow et al., "A state-of-the-art techno-economic review of distributed and embedded energy storage for energy systems," *Energy*, vol. 229, Article ID 120461, 2021.

[93] J. P. Deane, B. P. Ó. Gallachóir, and E. McKeogh, "Techno-economic review of existing and new pumped hydro energy storage plant," *Renewable and Sustainable Energy Reviews*, vol. 14, no. 4, pp. 1293–1302, 2010.

[94] A. Foley and I. Díaz Lobera, "Impacts of compressed air energy storage plant on an electricity market with a large renewable energy portfolio," *Energy*, vol. 57, pp. 85–94, 2013.

[95] E. Dragoni, "Mechanical design of flywheels for energy storage: a review with state-of-the-art developments," *Proceedings of the Institution of Mechanical Engineers - Part L: Journal of Materials: Design and Applications*, vol. 233, no. 5, pp. 995–1004, 2019.

[96] C. Quann and T. H. Bradley, "Renewables firming using grid scale battery storage in a real-time pricing market," in *Proceedings of the 2017 IEEE Power & Energy Society Innovative Smart Grid Technologies Conference (ISGT)*, pp. 1–5, IEEE, Washington, DC, USA, April 2017.

[97] P. Kohlhepp, H. Harb, H. Wolisz, S. Waczowicz, D. Müller, and V. Hagenmeyer, "Large-scale grid integration of residential thermal energy storages as demand-side flexibility resource: a review of international field studies," *Renewable and Sustainable Energy Reviews*, vol. 101, pp. 527–547, 2019.

[98] A. Chapman, K. Itaoka, K. Hirose et al., "A review of four case studies assessing the potential for hydrogen penetration of the future energy system," *International Journal of Hydrogen Energy*, vol. 44, no. 13, pp. 6371–6382, 2019.

[99] C. K. Das, O. Bass, G. Kothapalli, T. S. Mahmoud, and D. Habibi, "Overview of energy storage systems in distribution networks: placement, sizing, operation, and power quality," *Renewable and Sustainable Energy Reviews*, vol. 91, pp. 1205–1230, 2018.

[100] A. K. Rohit, S. Rangnekar, and S. Rangnekar, "An overview of energy storage and its importance in Indian renewable energy sector: Part II–energy storage applications, benefits and market potential," *Journal of Energy Storage*, vol. 13, pp. 447–456, 2017.

[101] H. Chen, T. N. Cong, W. Yang, C. Tan, Y. Li, and Y. Ding, "Progress in electrical energy storage system: a critical review," *Progress in Natural Science*, vol. 19, no. 3, pp. 291–312, 2009.

[102] M. Aneke and M. Wang, "Energy storage technologies and real life applications–A state of the art review," *Applied Energy*, vol. 179, pp. 350–377, 2016.

[103] S. . Faias, P. Santos, J. Sousa, and R. Castro, "An overview on short and long-term response energy storage devices for power systems applications," *System*, vol. 5, p. 6, 2008.

[104] X. Luo, J. Wang, M. Dooner, and J. Clarke, "Overview of current development in electrical energy storage technologies and the application potential in power system operation," *Applied Energy*, vol. 137, pp. 511–536, 2015.

[105] F. Nadeem, S. M. S. Hussain, P. K. Tiwari, A. K. Goswami, and T. S. Ustun, "Comparative review of energy storage systems, their roles, and impacts on future power systems," *IEEE Access*, vol. 7, pp. 4555–4585, 2019.

[106] S. R. Sinsel, R. L. Riemke, and V. H. Hoffmann, "Challenges and solution technologies for the integration of variable renewable energy sources-a review," *Renewable Energy*, vol. 145, pp. 2271–2285, 2020.

[107] M. Ourahou, W. Ayrir, B. El Hassouni, and A. Haddi, "Review on smart grid control and reliability in presence of renewable energies: challenges and prospects," *Mathematics and Computers in Simulation*, vol. 167, pp. 19–31, 2020.

[108] H. A. Behabtu, M. Messagie, T. Coosemans et al., "A review of energy storage technologies' application potentials in renewable energy sources grid integration," *Sustainability*, vol. 12, no. 24, Article ID 10511, 2020.

[109] S. Ben Elghali, R. Outbib, and M. Benbouzid, "Selecting and optimal sizing of hybridized energy storage systems for tidal energy integration into power grid," *Journal of Modern Power Systems and Clean Energy*, vol. 7, no. 1, pp. 113–122, 2019.

[110] S. Sabihuddin, A. E. Kiprakis, and M. Mueller, "A numerical and graphical review of energy storage technologies," *Energies*, vol. 8, no. 1, pp. 172–216, 2014.

[111] A. K. S. Maisanam, A. Biswas, and K. K. Sharma, "An innovative framework for electrical energy storage system selection for remote area electrification with renewable energy system: case of a remote village in India," *Journal of Renewable and Sustainable Energy*, vol. 12, no. 2, Article ID 024101, 2020.

[112] International Hydropower Association, *2018 Hydropower Status Report*, https://www.hydropower.org/status-report, 2018.

[113] B. Kale and S. Chatterjee, "Electrochemical energy storage systems: India perspective," *Bulletin of Materials Science*, vol. 43, no. 1, pp. 96–15, 2020.

[114] X. Tan, Q. Li, and H. Wang, "Advances and trends of energy storage technology in microgrid," *International Journal of Electrical Power & Energy Systems*, vol. 44, no. 1, pp. 179–191, 2013.

[115] A. Etxeberria, I. Vechiu, H. Camblong, and J.-M. Vinassa, "Comparison of three topologies and controls of a hybrid energy storage system for microgrids," *Energy Conversion and Management*, vol. 54, no. 1, pp. 113–121, 2012.

[116] S. Lemofouet and A. Rufer, "Hybrid energy storage system based on compressed air and super-capacitors with maximum efficiency point tracking (MEPT)," *IEEE Transactions on Industry Applications*, vol. 126, no. 7, pp. 911–920, 2006.

[117] R. A. Dougal, S. Liu, and R. E. White, "Power and life extension of battery-ultracapacitor hybrids," *IEEE Transactions on Components and Packaging Technologies*, vol. 25, no. 1, pp. 120–131, 2002.

[118] L. Gao, R. A. Dougal, and S. Liu, "Power enhancement of an actively controlled battery/ultracapacitor hybrid," *IEEE Transactions on Power Electronics*, vol. 20, no. 1, pp. 236–243, 2005.

[119] W. Li and G. Joos, "A power electronic interface for a battery supercapacitor hybrid energy storage system for wind applications," in *Proceedings of the 2008 IEEE Power Electronics Specialists Conference*, pp. 1762–1768, IEEE, Rhodes, Greece, June 2008.

[120] F. Guo and R. Sharma, "A modular multilevel converter with half-bridge submodules for hybrid energy storage systems integrating battery and ultracapacitor," in *Proceedings of the 2015 IEEE Applied Power Electronics Conference and Exposition (APEC)*, pp. 3025–3030, IEEE, Charlotte, NC, USA, March 2015.

[121] G. Wang, G. Konstantinou, C. D. Townsend et al., "A review of power electronics for grid connection of utility-scale battery energy storage systems," *IEEE Transactions on Sustainable Energy*, vol. 7, no. 4, pp. 1778–1790, 2016.

[122] J. G. Nielsen and F. Blaabjerg, "A detailed comparison of system topologies for dynamic voltage restorers," *IEEE Transactions on Industry Applications*, vol. 41, no. 5, pp. 1272–1280, 2005.

[123] D. Somayajula and M. L. Crow, "An integrated dynamic voltage restorer-ultracapacitor design for improving power quality of the distribution grid," *IEEE Transactions on Sustainable Energy*, vol. 6, no. 2, pp. 616–624, 2015.

[124] H. J. Kim, K. C. Seong, J. W. Cho et al., "3 MJ/750 kVA SMES system for improving power quality," *IEEE Transactions on Applied Superconductivity*, vol. 16, no. 2, pp. 574–577, 2006.

[125] J. Shi, Y. Tang, K. Yang et al., "SMES based dynamic voltage restorer for voltage fluctuations compensation," *IEEE Transactions on Applied Superconductivity*, vol. 20, no. 3, pp. 1360–1364, 2010.

[126] X. Jiang, X. Zhu, Z. Cheng, X. Ren, and Y. He, "A 150 kVA/0.3 MJ SMES voltage sag compensation system," *IEEE Transactions on Appiled Superconductivity*, vol. 15, no. 2, pp. 1903–1906, 2005.

[127] S. Nagaya, N. Hirano, H. Moriguchi et al., "Field test results of the 5 MVA SMES system for bridging instantaneous voltage dips," *IEEE Transactions on Applied Superconductivity*, vol. 16, no. 2, pp. 632–635, 2006.

[128] W. Guo, L. Xiao, S. Dai, and L. Lin, "Control strategy of a 0.5 MVA/1 MJ SMES based dynamic voltage restorer," *IEEE Transactions on Applied Superconductivity*, vol. 20, no. 3, pp. 1329–1333, 2010.

[129] M. A. Green and B. P. Strauss, "The cost of superconducting magnets as a function of stored energy and design magnetic induction times the field volume," *IEEE Transactions on Applied Superconductivity*, vol. 18, no. 2, pp. 248–251, 2008.

[130] J. W. Shim, Y. Cho, S.-J. Kim, S. W. Min, and K. Hur, "Synergistic control of SMES and battery energy storage for enabling dispatchability of renewable energy sources," *IEEE Transactions on Applied Superconductivity*, vol. 23, no. 3, Article ID 5701205, 2013.

[131] A. M. Gee, F. Robinson, and W. Yuan, "A superconducting magnetic energy storage-emulator/battery supported dynamic voltage restorer," *IEEE Transactions on Energy Conversion*, vol. 32, no. 1, pp. 55–64, 2017.

[132] Z. Zheng, X. Xiao, C. Huang, and C. Li, "Enhancing transient voltage quality in a distribution power system with SMES-based DVR and SFCL," *IEEE Transactions on Applied Superconductivity*, vol. 29, no. 2, pp. 1–5, 2019.

[133] H. Abdollahzadeh, M. Jazaeri, and A. Tavighi, "A new fast-converged estimation approach for Dynamic Voltage Restorer (DVR) to compensate voltage sags in waveform distortion conditions," *International Journal of Electrical Power & Energy Systems*, vol. 54, pp. 598–609, 2014.

[134] J. G. Nielsen, M. Newman, H. Nielsen, and F. Blaabjerg, "Control and testing of a dynamic voltage restorer (DVR) at medium voltage level," *IEEE Transactions on Power Electronics*, vol. 19, no. 3, pp. 806–813, 2004.

[135] M. H. J. Bollen and I. Gu, *Signal processing of power quality disturbances*, Vol. 30, John Wiley & Sons, , Hoboken, New Jersey, USA, 2006.

[136] P. Li, L. Xie, J. Han, S. Pang, and P. Li, "New decentralized control scheme for a dynamic voltage restorer based on the elliptical trajectory compensation," *IEEE Transactions on Industrial Electronics*, vol. 64, no. 8, pp. 6484–6495, 2017.

[137] H.-Y. Chu, H.-L. Jou, and C.-L. Huang, "Transient response of a peak voltage detector for sinusoidal signals," *IEEE Transactions on Industrial Electronics*, vol. 39, no. 1, pp. 74–79, 1992.

[138] H. Sardar Kamil, D. M. Said, M. W. Mustafa, M. R. Miveh, and N. Ahmad, "Recent advances in phase-locked loop based synchronization methods for inverter-based renewable energy sources," *Indonesian Journal of Electrical Engineering and Computer Science*, vol. 18, no. 1, pp. 1–8, 2020.

[139] M. Reyes, P. Rodriguez, S. Vazquez, A. Luna, R. Teodorescu, and J. M. Carrasco, "Enhanced decoupled double synchronous reference frame current controller for unbalanced grid-voltage conditions," *IEEE Transactions on Power Electronics*, vol. 27, no. 9, pp. 3934–3943, 2012.

[140] F. González-Espín, E. Figueres, and G. Garcerá, "An adaptive synchronous-reference-frame phase-locked loop for power quality improvement in a polluted utility grid," *IEEE Transactions on Industrial Electronics*, vol. 59, no. 6, pp. 2718–2731, 2012.

[141] R. Teodorescu, M. Liserre, and P. Rodriguez, *Grid converters for photovoltaic and wind power systems*, Vol. 29, John Wiley & Sons, , Hoboken, New Jersey, USA, 2011.

[142] F. Filipović, B. Banković, M. Petronijević, N. Mitrović, and V. Kostić, "Benchmarking of phase lock loop based synchronization algorithms for grid-tied inverter," *Serbian Journal of Electrical Engineering*, vol. 16, no. 1, pp. 1–19, 2019.

[143] M. Karimi-Ghartemani, M. Mojiri, A. Safaee et al., "A new phase-locked loop system for three-phase applications," *IEEE Transactions on Power Electronics*, vol. 28, no. 3, pp. 1208–1218, 2013.

[144] S. Galeshi and H. Iman-Eini, "Dynamic voltage restorer employing multilevel cascaded H-bridge inverter," *IET Power Electronics*, vol. 9, no. 11, pp. 2196–2204, 2016.

[145] S. S. Choi, J. D. Li, and D. Vilathgamuwa, "A generalized voltage compensation strategy for mitigating the impacts of voltage sags/swells," *IEEE Transactions on Power Delivery*, vol. 20, no. 3, pp. 2289–2297, 2005.

[146] C. Meyer, R. W. De Doncker, Y. W. Li, and F. Blaabjerg, "Optimized control strategy for a medium-voltage DVR-theoretical investigations and experimental results," *IEEE Transactions on Power Electronics*, vol. 23, no. 6, pp. 2746–2754, 2008.
[147] R. Pal and S. Gupta, "Topologies and control strategies implicated in dynamic voltage restorer (DVR) for power quality improvement," *Iranian Journal of Science and Technology, Transactions of Electrical Engineering*, vol. 44, no. 2, pp. 581–603, 2020.
[148] M. Gonzalez, V. Cardenas, and G. Espinosa, "Advantages of the passivity based control in dynamic voltage restorers for power quality improvement," *Simulation Modelling Practice and Theory*, vol. 47, pp. 221–235, 2014.
[149] A. P. Torres, P. Roncero-Sanchez, and V. F. Batlle, "A two degrees of freedom resonant control scheme for voltage-sag compensation in dynamic voltage restorers," *IEEE Transactions on Power Electronics*, vol. 33, no. 6, pp. 4852–4867, 2018.
[150] P. Roncero-Sanchez, E. Acha, J. E. Ortega-Calderon, V. Feliu, and A. García-Cerrada, "A versatile control scheme for a dynamic voltage restorer for power-quality improvement," *IEEE Transactions on Power Delivery*, vol. 24, no. 1, pp. 277–284, 2009.
[151] S.-J. Lee, H. Kim, S.-K. Sul, and F. Blaabjerg, "A novel control algorithm for static series compensators by use of PQR instantaneous power theory," *IEEE Transactions on Power Electronics*, vol. 19, no. 3, pp. 814–827, 2004.
[152] Y. W. Li, F. Blaabjerg, D. M. Vilathgamuwa, and P. C. Loh, "Design and comparison of high performance stationary-frame controllers for DVR implementation," *IEEE Transactions on Power Electronics*, vol. 22, no. 2, pp. 602–612, 2007.
[153] F. Jurado and F. P. Hidalgo, "Neural network control for dynamic voltage restorer," in *Proceedings of the IEEE 2002 28th Annual Conference of the Industrial Electronics Society. IECON 02*, vol. 1, pp. 615–620, IEEE, Seville, Spain, November 2002.
[154] B. Ferdi, C. Benachaiba, S. Dib, and R. Dehini, "Adaptive PI control of dynamic voltage restorer using fuzzy logic," *Journal of Electrical Engineering: Theory and Application*, vol. 1, no. 3, 2010.
[155] D. M. Vilathgamuwa, C. J. Gajanayake, P. C. Loh, and Y. W. Li, "Voltage sag compensation with Z-source inverter based dynamic voltage restorer," in *Proceedings of the Conference Record of the 2006 IEEE Industry Applications Conference Forty-First IAS Annual Meeting*, pp. 2242–2248, IEEE, Tampa, FL, USA, October 2006.
[156] C. K. Sundarabalan and K. Selvi, "Real coded GA optimized fuzzy logic controlled PEMFC based Dynamic Voltage Restorer for reparation of voltage disturbances in distribution system," *International Journal of Hydrogen Energy*, vol. 42, no. 1, pp. 603–613, 2017.
[157] G. Chen, M. Zhu, and X. Cai, "Medium-voltage level dynamic voltage restorer compensation strategy by positive and negative sequence extractions in multiple reference frames," *IET Power Electronics*, vol. 7, no. 7, pp. 1747–1758, 2014.
[158] C. Tu, Q. Guo, F. Jiang, H. Wang, and Z. Shuai, "A comprehensive study to mitigate voltage sags and phase jumps using a dynamic voltage restorer," *IEEE Journal of Emerging and Selected Topics in Power Electronics*, vol. 8, no. 2, pp. 1490–1502, 2020.
[159] J. Wang, Y. Xing, H. Wu, and T. Yang, "A novel dual-DC-port dynamic voltage restorer with reduced-rating integrated DC–DC converter for wide-range voltage sag compensation," *IEEE Transactions on Power Electronics*, vol. 34, no. 8, pp. 7437–7449, 2019.
[160] E. Babaei, M. F. Kangarlu, and M. Sabahi, "Dynamic voltage restorer based on multilevel inverter with adjustable dc-link voltage," *IET Power Electronics*, vol. 7, no. 3, pp. 576–590, 2014.
[161] Y. Zhao, "Design and implementation of inverter in dynamic voltage restorer based on selective harmonic elimination PWM," in *Proceedings of the 2008 Third International Conference on Electric Utility Deregulation and Restructuring and Power Technologies*, pp. 2239–2244, IEEE, Nanjing, China, April 2008.
[162] F. A. L. Jowder, "Modeling and simulation of dynamic voltage restorer (DVR) based on hysteresis voltage control," in *Proceedings of the IECON 2007-33rd Annual Conference of the IEEE Industrial Electronics Society*, pp. 1726–1731, IEEE, Taipei, Taiwan, November 2007.
[163] P. Boonchiam and N. Mithulananthan, "Diode-clamped multilevel voltage source converter based on medium voltage DVR," *International Journal of Electrical Power and Energy Systems Engineering*, vol. 1, no. 2, pp. 62–67, 2008.
[164] P. Roncero-Sanchez and E. Acha, "Dynamic voltage restorer based on flying capacitor multilevel converters operated by repetitive control," *IEEE Transactions on Power Delivery*, vol. 24, no. 2, pp. 951–960, 2009.
[165] G. A. de Almeida Carlos, E. C. dos Santos, C. B. Jacobina, and J. P. R. A. Mello, "Dynamic voltage restorer based on three-phase inverters cascaded through an open-end winding transformer," *IEEE Transactions on Power Electronics*, vol. 31, no. 1, pp. 188–199, 2016.
[166] V. Ansal, K. Ravikumar, and P. Parthiban, "Transformerless dynamic voltage restorer for voltage sag mitigation," in *Proceedings of the 2016 Biennial International Conference on Power and Energy Systems: Towards Sustainable Energy (PESTSE)*, pp. 1–4, IEEE, Bengaluru, India, January 2016.
[167] H. K. Al-Hadidi, A. M. Gole, and D. A. Jacobson, "Minimum power operation of cascade inverter-based dynamic voltage restorer," *IEEE Transactions on Power Delivery*, vol. 23, no. 2, pp. 889–898, 2008.
[168] A. M. Massoud, S. Ahmed, P. N. Enjeti, and B. W. Williams, "Evaluation of a multilevel cascaded-type dynamic voltage restorer employing discontinuous space vector modulation," *IEEE Transactions on Industrial Electronics*, vol. 57, no. 7, pp. 2398–2410, 2010.
[169] M. Hosseinpour, M. Mohamadian, and A. Yazdian Varjani, "Design and analysis of the droop-controlled parallel four-leg inverters to share unbalanced and nonlinear loads," *Przeglad Elektrotechniczny*, vol. 90, no. 1, pp. 105–110, 2014.
[170] R. Cárdenas, R. Peña, J. Clare, P. Wheeler, and P. Zanchetta, "A repetitive control system for four-leg matrix converters feeding non-linear loads," *Electric Power Systems Research*, vol. 104, pp. 18–27, 2013.
[171] X. Zhang, J. Wang, and C. Li, "Three-phase four-leg inverter based on voltage hysteresis control," in *Proceedings of the 2010 International Conference on Electrical and Control Engineering*, pp. 4482–4485, IEEE, Wuhan, China, June 2010.
[172] E. Demirkutlu and A. M. Hava, "A scalar resonant-filter-bank-based output-voltage control method and a scalar minimum-switching-loss discontinuous PWM method for the four-leg-inverter-based three-phase four-wire power

supply," *IEEE Transactions on Industry Applications*, vol. 45, no. 3, pp. 982–991, 2009.

[173] E. Demirkutlu, S. Cetinkaya, and A. M. Hava, "Output voltage control of a four-leg inverter based three-phase UPS by means of stationary frame resonant filter banks,"vol. 1, pp. 880–885, in *Proceedings of the 2007 IEEE International Electric Machines & Drives Conference*, vol. 1, pp. 880–885, IEEE, Antalya, Turkey, May 2007.

[174] P. Cortés, G. Ortiz, J. I. Yuz, J. Rodríguez, S. Vazquez, and L. Franquelo, "Model predictive control of an inverter with output $ LC $ filter for UPS applications," *IEEE Transactions on Industrial Electronics*, vol. 56, no. 6, pp. 1875–1883, 2009.

[175] V. Yaramasu, M. Rivera, M. Narimani, B. Wu, and J. Rodriguez, "Model predictive approach for a simple and effective load voltage control of four-leg inverter with an output *LC* filter," *IEEE Transactions on Industrial Electronics*, vol. 61, no. 10, pp. 5259–5270, 2014.

[176] V. Yaramasu, M. Rivera, M. Narimani, B. Wu, and J. Rodriguez, "High performance operation for a four-leg NPC inverter with two-sample-ahead predictive control strategy," *Electric Power Systems Research*, vol. 123, pp. 31–39, 2015.

[177] L.-Y. Yang, J.-H. Liu, C.-L. Wang, and G.-F. Du, "Sliding mode control of three-phase four-leg inverters via state feedback," *Journal of Power Electronics*, vol. 14, no. 5, pp. 1028–1037, 2014.

[178] Y. Li, D. M. Vilathgamuwa, and P. C. Loh, "Microgrid power quality enhancement using a three-phase four-wire grid-interfacing compensator," *IEEE Transactions on Industry Applications*, vol. 41, no. 6, pp. 1707–1719, 2005.

[179] F. Wang, J. L. Duarte, and M. A. M. Hendrix, "Grid-interfacing converter systems with enhanced voltage quality for microgrid application—concept and implementation," *IEEE Transactions on Power Electronics*, vol. 26, no. 12, pp. 3501–3513, 2011.

[180] E. Rokrok and M. E. H. Golshan, "Comprehensive control scheme for an inverter-based distributed generation unit," *Iranian Journal of Science and Technology Transaction B: Engineering*, vol. 33, no. 6, pp. 477–490, 2009.

[181] H. Nazifi and R. Ahmad, "Current control assisted and non-ideal proportional-resonant voltage controller for four-leg three-phase inverters with time-variant loads," in *Proceedings of the 4th Annual International Power Electronics, Drive Systems and Technologies Conference*, pp. 355–360, IEEE, Tehran, Iran, February 2013.

[182] H. Lei, L. Fei, J. Xiong, X. Lin, and Y. Kang, "Research on paralleled three-phase four-leg voltage source inverters based on dual-loop control in $\alpha\beta o$ coordinate," in *Proceedings of the 8th International Conference on Power Electronics-ECCE Asia*, pp. 2912–2919, IEEE, Jeju, Korea (South), June 2011.

[183] R. A. Gannett, J. C. Sozio, and D. Boroyevich, "Application of synchronous and stationary frame controllers for unbalanced and nonlinear load compensation in 4-leg inverters,"vol. 2, pp. 1038–1043, in *Proceedings of the APEC. Seventeenth Annual IEEE Applied Power Electronics Conference and Exposition (Cat. No. 02CH37335)*, vol. 2, pp. 1038–1043, IEEE, Dallas, TX, USA, March 2002.

[184] H. Z. Yi and S. Jin, "Study on control strategy for three-phase four-leg inverter power supply,"vol. 1, pp. 805–809, in *Proceedings of the 30th Annual Conference of IEEE Industrial Electronics Society, 2004. IECON 2004*, vol. 1, pp. 805–809, IEEE, Busan, Korea (South), November 2004.

[185] N. A. Ninad, L. Lopes, and L. Lopes, "Per-phase vector control strategy for a four-leg voltage source inverter operating with highly unbalanced loads in stand-alone hybrid systems," *International Journal of Electrical Power & Energy Systems*, vol. 55, pp. 449–459, 2014.

[186] N. A. Ninad and A. C. L. Luiz, "Unbalanced operation of per-phase vector controlled four-leg grid forming inverter for stand-alone hybrid systems," in *Proceedings of the IECON 2012-38th Annual Conference on IEEE Industrial Electronics Society*, pp. 3500–3505, IEEE, Montreal, QC, Canada, October 2012.

[187] C. Liu, F. Wang, and H. Bai, "High performance controller design with PD feedback inner loop for three-phase four-leg inverter," in *Proceedings of the 2009 4th IEEE Conference on Industrial Electronics and Applications*, pp. 1057–1061, IEEE, Xi'an, May 2009.

[188] I. Vechiu, H. Camblong, G. Tapia, B. Dakyo, and O. Curea, "Control of four leg inverter for hybrid power system applications with unbalanced load," *Energy Conversion and Management*, vol. 48, no. 7, pp. 2119–2128, 2007.

[189] I. Vechiu, O. Curea, and H. Camblong, "Transient operation of a four-leg inverter for autonomous applications with unbalanced load," *IEEE Transactions on Power Electronics*, vol. 25, no. 2, pp. 399–407, 2010.

[190] W. Sinsukthavorn, E. Ortjohann, A. Mohd, N. Hamsic, and D. Morton, "Control strategy for three-/four-wire-inverter-based distributed generation," *IEEE Transactions on Industrial Electronics*, vol. 59, no. 10, pp. 3890–3899, 2012.

[191] R. Cárdenas, R. Peña, P. Wheeler, J. Clare, and C. Juri, "Control of a matrix converter for the operation of autonomous systems," *Renewable Energy*, vol. 43, pp. 343–353, 2012.

[192] H. Bai, F. Wang, D. Wang, C. L. Liu, and T. Y. Wang, "A pole assignment of state feedback based on system matrix for three-phase four-leg inverter of high speed pm generator driven by micro-turbine," in *Proceedings of the 2009 4th IEEE Conference on Industrial Electronics and Applications*, pp. 1361–1366, IEEE, Xi'an, China, May 2009.

[193] R. Nasiri and A. Radan, "Adaptive pole-placement control of 4-leg voltage-source inverters for standalone photovoltaic systems," *Renewable Energy*, vol. 36, no. 7, pp. 2032–2042, 2011.

[194] Il-Y. Chung, D.-J. Won, S.-Y. Park, S.-Il Moon, and J. K. Park, "The DC link energy control method in dynamic voltage restorer system," *International Journal of Electrical Power & Energy Systems*, vol. 25, no. 7, pp. 525–531, 2003.

[195] M. Danbumrungtrakul, T. Saengsuwan, and P. Srithorn, "Evaluation of DVR capability enhancement-zero active power tracking technique," *IEEE Access*, vol. 5, pp. 10285–10295, 2017.

[196] A. M. Rauf, V. Khadkikar, and V. Khadkikar, "An enhanced voltage sag compensation scheme for dynamic voltage restorer," *IEEE Transactions on Industrial Electronics*, vol. 62, no. 5, pp. 2683–2692, 2015.

[197] P. Kala and S. Arora, "A comprehensive study of classical and hybrid multilevel inverter topologies for renewable energy applications," *Renewable and Sustainable Energy Reviews*, vol. 76, pp. 905–931, 2017.

[198] J. Rodriguez, J.-S. Lai, and F. Z. Peng, "Multilevel inverters: a survey of topologies, controls, and applications," *IEEE Transactions on Industrial Electronics*, vol. 49, no. 4, pp. 724–738, 2002.

[199] K. K. Gupta, A. Ranjan, P. Bhatnagar, L. K. Sahu, and S. Jain, "Multilevel inverter topologies with reduced device count: a review," *IEEE Transactions on Power Electronics*, vol. 31, no. 1, pp. 135–151, 2016.

[200] S. M. Silva, S. da Silveira, A. S. Reis, and B. J. C. Filho, "Analysis of a dynamic voltage compensator with reduced switch-count and absence of energy storage system," *IEEE Transactions on Industry Applications*, vol. 41, no. 5, pp. 1255–1262, 2005.

[201] M. Fang, A. I. Gardiner, A. MacDougall, and G. A. Mathieson, "A novel series dynamic voltage restorer for distribution systems," in *Proceedings of the POWERCON'98. 1998 International Conference on Power System Technology. Proceedings (Cat. No. 98EX151)*, pp. 38–42, IEEE, Beijing, China, August 1998.

[202] M. R. Banaei and A. R. Dehghanzadeh, "DVR based cascaded multilevel Z-source inverter," in *Proceedings of the 2010 IEEE International Conference on Power and Energy*, pp. 51–56, IEEE, Kuala Lumpur, Malaysia, December 2010.

[203] S. Jothibasu and M. K. Mishra, "An improved direct AC–AC converter for voltage sag mitigation," *IEEE Transactions on Industrial Electronics*, vol. 62, no. 1, pp. 21–29, 2015.

[204] M. Balamurugan, T. S. Sivakumaran, and M. Aishwariya, "Voltage sag/swell compensation using Z-source inverter DVR based on FUZZY controller," in *Proceedings of the 2013 IEEE International Conference ON Emerging Trends in Computing, Communication and Nanotechnology (ICECCN)*, pp. 648–653, IEEE, Tirunelveli, India, March 2013.

[205] C. Zhan, V. Ramachandaramurthy, A. Arulampalam et al., "Dynamic voltage restorer based on voltage-space-vector PWM control," *IEEE Transactions on Industry Applications*, vol. 37, no. 6, pp. 1855–1863, 2001.

[206] D. A. Fernandes, S. R. Naidu, and A. M. N. Lima, "A four leg voltage source converter based dynamic voltage restorer," in *Proceedings of the 2008 IEEE Power Electronics Specialists Conference*, pp. 3760–3766, IEEE, Rhodes, Greece, June 2008.

[207] P. Kanjiya, B. Singh, A. Chandra, and K. Al-Haddad, "SRF theory revisited" to control self-supported dynamic voltage restorer (DVR) for unbalanced and nonlinear loads," *IEEE Transactions on Industry Applications*, vol. 49, no. 5, pp. 2330–2340, 2013.

[208] C. Zhan, A. Arulampalam, and N. Jenkins, "Four-wire dynamic voltage restorer based on a three-dimensional voltage space vector PWM algorithm," *IEEE Transactions on Power Electronics*, vol. 18, no. 4, pp. 1093–1102, 2003.

[209] A. Campbell and R. McHattie, "Backfilling the sinewave. A dynamic voltage restorer case study," *Power Engineering Journal*, vol. 13, no. 3, pp. 153–158, 1999.

[210] M. Vilathgamuwa, A. Ranjith Perera, and S. S. Choi, "Performance improvement of the dynamic voltage restorer with closed-loop load voltage and current-mode control," *IEEE Transactions on Power Electronics*, vol. 17, no. 5, pp. 824–834, 2002.

[211] V. K. Ramachandaramurthy, C. Fitzer, A. Arulampalam, C. Zhan, M. Barnes, and N. Jenkins, "Control of a battery supported dynamic voltage restorer," *IEE Proceedings - Generation, Transmission and Distribution*, vol. 149, no. 5, pp. 533–542, 2002.

[212] C.-J. Huang, S.-J. Huang, and F.-S. Pai, "Design of dynamic voltage restorer with disturbance-filtering enhancement," *IEEE Transactions on Power Electronics*, vol. 18, no. 5, pp. 1202–1210, 2003.

[213] V. K. Ramachandaramurthy, A. Arulampalam, C. Fitzer, C. Zhan, M. Barnes, and N. Jenkins, "Supervisory control of dynamic voltage restorers," *IEE Proceedings - Generation, Transmission and Distribution*, vol. 151, no. 4, pp. 509–516, 2004.

[214] C. Dhanamjayulu and S. Meikandasivam, "Implementation and comparison of symmetric and asymmetric multilevel inverters for dynamic loads," *IEEE Access*, vol. 6, pp. 738–746, 2018.

[215] Y. Suresh, J. Venkataramanaiah, A. K. Panda, C. Dhanamjayulu, and P. Venugopal, "Investigation on cascade multilevel inverter with symmetric, asymmetric, hybrid and multi-cell configurations," *Ain Shams Engineering Journal*, vol. 8, no. 2, pp. 263–276, 2017.

[216] C. Dhanamjayulu, G. Arunkumar, B. Jaganatha Pandian, and S. Padmanaban, "Design and implementation of a novel asymmetrical multilevel inverter optimal hardware components," *International Transactions on Electrical Energy Systems*, vol. 30, no. 2, Article ID e12201, 2020.

[217] D. Prasad, C. Dhanamjayulu, S. Padmanaban, J. B. Holm-Nielsen, F. Blaabjerg, and S. R. Khasim, "Design and implementation of 31-level asymmetrical inverter with reduced components," *IEEE Access*, vol. 9, pp. 22788–22803, 2021.

[218] C. Dhanamjayulu, G. Arunkumar, B. Jaganatha Pandian et al., "Real-time implementation of a 31-level asymmetrical cascaded multilevel inverter for dynamic loads," *IEEE Access*, vol. 7, pp. 51254–51266, 2019.

[219] C. Dhanamjayulu, S. R. Khasim, S. Padmanaban, G. Arunkumar, J. B. Holm-Nielsen, and F. Blaabjerg, "Design and implementation of multilevel inverters for fuel cell energy conversion system," *IEEE Access*, vol. 8, pp. 183690–183707, 2020.

[220] C. Dhanamjayulu, D. Prasad, S. Padmanaban, P. K. Maroti, J. B. Holm-Nielsen, and F. Blaabjerg, "Design and implementation of seventeen level inverter with reduced components," *IEEE Access*, vol. 9, pp. 16746–16760, 2021.

[221] S. S. Lee, M. Sidorov, C. S. Lim, N. R. N. Idris, and Y. E. Heng, "Hybrid cascaded multilevel inverter (HCMLI) with improved symmetrical 4-level submodule," *IEEE Transactions on Power Electronics*, vol. 33, no. 2, pp. 932–935, 2018.

[222] Z.-G. Lu, L.-L. Zhao, W.-P. Zhu, C.-J. Wu, and Y.-S. Qin, "Research on cascaded three-phase-bridge multilevel converter based on CPS-PWM," *IET Power Electronics*, vol. 6, no. 6, pp. 1088–1099, 2013.

[223] R. Rabinovici, D. Baimel, J. Tomasik, and A. Zuckerberger, "Thirteen-level cascaded H-bridge inverter operated by generic phase shifted pulse-width modulation," *IET Power Electronics*, vol. 6, no. 8, pp. 1516–1529, 2013.

[224] S. K. Sahoo and T. Bhattacharya, "Phase-shifted carrier-based synchronized sinusoidal PWM techniques for a cascaded H-bridge multilevel inverter," *IEEE Transactions on Power Electronics*, vol. 33, no. 1, pp. 513–524, 2018.

[225] P. Devalraju and C. Dhanamjayulu, "A novel 19-level asymmetrical multilevel inverter for dynamic voltage restorer applications," in *Proceedings of the 2021 Innovations in Power and Advanced Computing Technologies (i-PACT)*, pp. 1–7, Kuala Lumpur, Malaysia, November 2021.

[226] E. Babaei, M. Farhadi Kangarlu, and M. Sabahi, "Extended multilevel converters: an attempt to reduce the number of independent DC voltage sources in cascaded multilevel converters," *IET Power Electronics*, vol. 7, no. 1, pp. 157–166, 2014.

[227] M. Toupchi Khosroshahi, "Crisscross cascade multilevel inverter with reduction in number of components," *IET Power Electronics*, vol. 7, no. 12, pp. 2914–2924, 2014.

[228] E. Babaei, S. Laali, and S. Alilu, "Cascaded multilevel inverter with series connection of novel H-bridge basic units," *IEEE Transactions on Industrial Electronics*, vol. 61, no. 12, pp. 6664–6671, 2014.

[229] M. R. Jannati Oskuee, E. Salary, S. Najafi-Ravadanegh, and S. Najafi-Ravadanegh, "Creative design of symmetric multilevel converter to enhance the circuit's performance," *IET Power Electronics*, vol. 8, no. 1, pp. 96–102, 2015.

[230] L. Wang, Q. H. Wu, and W. Tang, "Novel cascaded switched-diode multilevel inverter for renewable energy integration," *IEEE Transactions on Energy Conversion*, vol. 32, no. 4, pp. 1574–1582, 2017.

[231] L. He and C. Cheng, "A bridge modular switched-capacitor-based multilevel inverter with optimized SPWM control method and enhanced power-decoupling ability," *IEEE Transactions on Industrial Electronics*, vol. 65, no. 8, pp. 6140–6149, 2018.

[232] K. P. Panda and G. Panda, "Application of swarm optimisation-based modified algorithm for selective harmonic elimination in reduced switch count multilevel inverter," *IET Power Electronics*, vol. 11, no. 8, pp. 1472–1482, 2018.

[233] M. D. Manjrekar, P. K. Steimer, and T. A. Lipo, "Hybrid multilevel power conversion system: a competitive solution for high-power applications," *IEEE Transactions on Industry Applications*, vol. 36, no. 3, pp. 834–841, 2000.

[234] N. Prabaharan and K. Palanisamy, "Comparative analysis of symmetric and asymmetric reduced switch MLI topologies using unipolar pulse width modulation strategies," *IET Power Electronics*, vol. 9, no. 15, pp. 2808–2823, 2016.

[235] R. Shalchi Alishah, D. Nazarpour, S. H. Hosseini, and M. Sabahi, "Novel topologies for symmetric, asymmetric, and cascade switched-diode multilevel converter with minimum number of power electronic components," *IEEE Transactions on Industrial Electronics*, vol. 61, no. 10, pp. 5300–5310, 2014.

[236] D. Prasad and C. Dhanamjayulu, "Reduced voltage stress asymmetrical multilevel inverter with optimal components," *IEEE Access*, vol. 10, pp. 53546–53559, 2022.

[237] E. Babaei, S. Laali, and Z. Bayat, "A single-phase cascaded multilevel inverter based on a new basic unit with reduced number of power switches," *IEEE Transactions on Industrial Electronics*, vol. 62, no. 2, pp. 922–929, 2015.

[238] J. Liu, K. W. E. Cheng, and Y. Ye, "A cascaded multilevel inverter based on switched-capacitor for high-frequency AC power distribution system," *IEEE Transactions on Power Electronics*, vol. 29, no. 8, pp. 4219–4230, 2014.

[239] K. K. Gupta and S. Jain, "A novel multilevel inverter based on switched DC sources," *IEEE Transactions on Industrial Electronics*, vol. 61, no. 7, pp. 3269–3278, 2014.

[240] A. Mokhberdoran and A. Ajami, "Symmetric and asymmetric design and implementation of new cascaded multilevel inverter topology," *IEEE Transactions on Power Electronics*, vol. 29, no. 12, pp. 6712–6724, 2014.

[241] C. I. Odeh, E. S. Obe, and O. Ojo, "Topology for cascaded multilevel inverter," *IET Power Electronics*, vol. 9, no. 5, pp. 921–929, 2016.

[242] M. R. J. Oskuee and A. Mokhberdoran, "Developed cascaded multilevel inverter topology to minimise the number of circuit devices and voltage stresses of switches," pp. 459–466, 2014.

[243] E. Samadaei, S. A. Gholamian, A. Sheikholeslami, and J. Adabi, "An envelope type (E-type) module: asymmetric multilevel inverters with reduced components," *IEEE Transactions on Industrial Electronics*, vol. 63, no. 11, pp. 7148–7156, 2016.

[244] E. Samadaei, A. Sheikholeslami, S. A. Gholamian, and J. Adabi, "A square T-type (ST-type) module for asymmetrical multilevel inverters," *IEEE Transactions on Power Electronics*, vol. 33, no. 2, pp. 987–996, 2018.

[245] N. Arun and M. M. Noel, "Crisscross switched multilevel inverter using cascaded semi-half-bridge cells," *IET Power Electronics*, vol. 11, no. 1, pp. 23–32, 2018.

[246] M. R. Banaei, M. R. Jannati Oskuee, and H. Khounjahan, "Reconfiguration of semi-cascaded multilevel inverter to improve systems performance parameters," *IET Power Electronics*, vol. 7, no. 5, pp. 1106–1112, 2014.

[247] S. Xu, J. Zhang, X. Hu, and Y. Jiang, "A novel hybrid five-level voltage-source converter based on T-type topology for high-efficiency applications," *IEEE Transactions on Industry Applications*, vol. 53, no. 5, pp. 4730–4743, 2017.

[248] C. Dhanamjayulu, S. Padmanaban, V. K. Ramachandaramurthy, J. B. Holm-Nielsen, and F. Blaabjerg, "Design and implementation of multilevel inverters for electric vehicles," *IEEE Access*, vol. 9, pp. 317–338, 2021.

[249] M. S. B. Arif, U. Mustafa, S. B. M. Ayob, J. Rodriguez, A. Nadeem, and M. Abdelrahem, "Asymmetrical 17-level inverter topology with reduced total standing voltage and device count," *IEEE Access*, vol. 9, pp. 69710–69723, 2021.

[250] K. P. Panda, P. Bana, O. Kiselychnyk, J. Wang, and G. Panda, "A single-source switched-capacitor based step-up multilevel inverter with reduced components," *IEEE Transactions on Industry Applications*, vol. 57, no. 4, pp. 3801–3811, 2021.

[251] A. Chappa, S. Gupta, L. K. Sahu, S. P. Gautam, and K. K. Gupta, "Symmetrical and asymmetrical reduced device multilevel inverter topology," *IEEE Journal of Emerging and Selected Topics in Power Electronics*, vol. 9, no. 1, pp. 885–896, 2021.

[252] L. Tan, B. Wu, M. Narimani et al., "A space virtual-vector modulation with voltage balance control for nested neutral-point clamped converter under low output frequency conditions," *IEEE Transactions on Power Electronics*, vol. 32, no. 5, pp. 3458–3466, 2017.

[253] K. Wang, Z. Zheng, Y. Li, K. Liu, and J. Shang, "Neutral-point potential balancing of a five-level active neutral-point-clamped inverter," *IEEE Transactions on Industrial Electronics*, vol. 60, no. 5, pp. 1907–1918, 2013.

[254] C. Dhanamjayulu and S. Meikandasivam, "Fuzzy controller based design of 125 level asymmetric cascaded multilevel inverter for power quality improvement," *Analog Integrated Circuits and Signal Processing*, vol. 101, no. 3, pp. 533–542, 2019.

[255] S. R. Pulikanti and V. G. Agelidis, "Hybrid flying-capacitor-based active-neutral-point-clamped five-level converter operated with SHE-PWM," *IEEE Transactions on Industrial Electronics*, vol. 58, no. 10, pp. 4643–4653, 2011.

[256] S. R. Khasim, C. Dhanamjayulu, S. Padmanaban, J. B. Holm-Nielsen, and M. Mitolo, "A novel asymmetrical 21-level inverter for solar PV energy system with reduced switch count," *IEEE Access*, vol. 9, pp. 11761–11775, 2021.

[257] E. Esfandiari and N. B. Mariun, "Experimental results of 47-level switch-ladder multilevel inverter," *IEEE Transactions on Industrial Electronics*, vol. 60, no. 11, pp. 4960–4967, 2013.

[258] F. S. Kang, S. J. Park, S. Cho, C. U. Kim, and T. Ise, "Multilevel PWM inverters suitable for the use of stand-alone photovoltaic power systems," *IEEE Transactions on Energy Conversion*, vol. 20, no. 4, pp. 906–915, 2005.

[259] R. J. Satputaley and V. B. Borghate, "Performance analysis of DVR using "new reduced component" multilevel inverter,"

International Transactions on Electrical Energy Systems, vol. 27, no. 4, p. e2288, 2017.
[260] J. Ye, H. B. Gooi, X. Zhang, B. Wang, and J. Pou, "Simplified four-level inverter-based dynamic voltage restorer with single DC power source," *IEEE Access*, vol. 7, pp. 137461–137471, 2019.
[261] M. Shahabadini and H. Iman-Eini, "Improving the performance of a cascaded H-bridge-based interline dynamic voltage restorer," *IEEE Transactions on Power Delivery*, vol. 31, no. 3, pp. 1160–1167, 2016.
[262] G. A. de Almeida Carlos, C. B. Jacobina, J. P. R. A. Mello, and E. C. d Santos, "Cascaded open-end winding transformer based DVR," *IEEE Transactions on Industry Applications*, vol. 54, no. 2, pp. 1490–1501, 2018.
[263] K. Rajkumar, P. Parthiban, and N. Lokesh, "Real-time implementation of transformerless dynamic voltage restorer based on T-type multilevel inverter with reduced switch count," *International Transactions on Electrical Energy Systems*, vol. 30, no. 4, Article ID e12301, 2020.
[264] B. Wang and M. Illindala, "Operation and control of a dynamic voltage restorer using transformer coupled H-bridge converters," *IEEE Transactions on Power Electronics*, vol. 21, no. 4, pp. 1053–1061, 2006.
[265] H. K. Al-Hadidi, A. M. Gole, D. A. Jacobson, and D. A. Jacobson, "A novel configuration for a cascade inverter-based dynamic voltage restorer with reduced energy storage requirements," *IEEE Transactions on Power Delivery*, vol. 23, no. 2, pp. 881–888, 2008.
[266] M. I. Marei, A. B. Eltantawy, and A. A. El-Sattar, "An energy optimized control scheme for a transformerless DVR," *Electric Power Systems Research*, vol. 83, no. 1, pp. 110–118, 2012.
[267] K. Chandrasekaran and V. K. Ramachandaramurthy, "An improved dynamic voltage restorer for power quality improvement," *International Journal of Electrical Power & Energy Systems*, vol. 82, pp. 354–362, 2016.
[268] A. J. Visser, J. Enslin, and H. de T Mouton, "Transformerless series sag compensation with a cascaded multilevel inverter," *IEEE Transactions on Industrial Electronics*, vol. 49, no. 4, pp. 824–831, 2002.
[269] D. Prasad and C. Dhanamjayulu, "Solar PV-fed multilevel inverter with series compensator for power quality improvement in grid-connected systems," *IEEE Access*, vol. 10, pp. 81203–81219, 2022.
[270] E. Babaei and M. F. Kangarlu, "Sensitive load voltage compensation against voltage sags/swells and harmonics in the grid voltage and limit downstream fault currents using DVR," *Electric Power Systems Research*, vol. 83, no. 1, pp. 80–90, 2012.
[271] M. J. Newman, D. G. Holmes, J. G. Nielsen, and F. Blaabjerg, "A dynamic voltage restorer (DVR) with selective harmonic compensation at medium voltage level," in *Proceedings of the 38th IAS Annual Meeting on Conference Record of the Industry Applications Conference, 2003*, vol. 2, pp. 1228–1235, IEEE, Salt Lake City, UT, USA, October 2003.
[272] E. Babaei and M. Farhadi Kangarlu, "Operation and control of dynamic voltage restorer using single-phase direct converter," *Energy Conversion and Management*, vol. 52, no. 8-9, pp. 2965–2972, 2011.
[273] E. Babaei and M. Farhadi Kangarlu, "Voltage quality improvement by a dynamic voltage restorer based on a direct three-phase converter with fictitious DC link," *IET Generation, Transmission & Distribution*, vol. 5, no. 8, pp. 814–823, 2011.
[274] M. I. Marei and M. M. A. Salama, "Advanced techniques for voltage flicker mitigation," in *Proceedings of the 2006 IEEE International Power Electronics Congress*, pp. 1–5, IEEE, Puebla, Mexico, October 2006.
[275] F.-z. Wu and S.-p. Pei, "The research and implementation of dynamic voltage restorer with power factor correction," in *Proceedings of the 2011 3rd International Workshop on Intelligent Systems and Applications*, pp. 1–4, IEEE, Wuhan, China, May 2011.
[276] A. K. Jindal, A. Ghosh, and A. Joshi, "Critical load bus voltage control using DVR under system frequency variation," *Electric Power Systems Research*, vol. 78, no. 2, pp. 255–263, 2008.
[277] T. Axente, M. Basu, M. F. Conlon, and K. Gaughan, "Protection of DVR against short circuit faults at the load side," in *Proceedings of the 2006 3rd IET International Conference on Power Electronics, Machines and Drives-PEMD 2006*, pp. 627–631, IET, Dublin, Ireland, April 2006.
[278] Y. W. Li, D. M. Vilathgamuwa, P. C. Loh, and F. Blaabjerg, "A dual-functional medium voltage level DVR to limit downstream fault currents," *IEEE Transactions on Power Electronics*, vol. 22, no. 4, pp. 1330–1340, 2007.
[279] F. B. Ajaei, S. Afsharnia, A. Kahrobaeian, and S. Farhangi, "A fast and effective control scheme for the dynamic voltage restorer," *IEEE Transactions on Power Delivery*, vol. 26, no. 4, pp. 2398–2406, 2011.
[280] F. Badrkhani Ajaei, S. Farhangi, and R. Iravani, "Fault current interruption by the dynamic voltage restorer," *IEEE Transactions on Power Delivery*, vol. 28, no. 2, pp. 903–910, 2013.
[281] F. Díaz-González, A. Sumper, O. Gomis-Bellmunt, and R. Villafáfila-Robles, "A review of energy storage technologies for wind power applications," *Renewable and Sustainable Energy Reviews*, vol. 16, no. 4, pp. 2154–2171, 2012.